Neural Coding Strategies in Cortico-Striatal Circuits Subserving Interval Timing

by

Ruey-Kuang Cheng

Department of Psychology and Neuroscience
Duke University

Date:_____

Approved:

_____
Warren H. Meck, Supervisor

_____
Jennifer M. Groh

_____
Erich D. Jarvis

_____
Christina L. Williams

_____
Henry H. Yin

Dissertation submitted in partial fulfillment of the
requirements for the degree of Doctor of Philosophy
in the Department of Psychology and Neuroscience
in the Graduate School of
Duke University

2010

ABSTRACT

Neural Coding Strategies in Cortico-Striatal Circuits Subserving Interval Timing

by

Ruey-Kuang Cheng

Department of Psychology and Neuroscience
Duke University

Date:_____

Approved:

_____
Warren H. Meck, Supervisor

_____
Jennifer M. Groh

_____
Erich D. Jarvis

_____
Christina L. Williams

_____
Henry H. Yin

An abstract of a dissertation submitted in partial fulfillment of the requirements for the degree of Doctor of Philosophy in the Department of Psychology and Neuroscience in the Graduate School of Duke University

2010

Abstract

Interval timing, defined as timing and time perception in the seconds-to-minutes range, is a higher-order cognitive function that has been shown to be critically dependent upon cortico-striatal circuits in the brain. However, our understanding of how different neuronal subtypes within these circuits cooperate to subserve interval timing remains elusive. The present study was designed to investigate this issue by focusing on the spike waveforms of neurons and their synchronous firing patterns with local field potentials (LFPs) recorded from cortico-striatal circuits while rats were performing two standard interval-timing tasks. Experiment 1 demonstrated that neurons in cortico-striatal circuits can be classified into 4 different clusters based on their distinct spike waveforms and behavioral correlates. These distinct neuronal populations were shown to be differentially involved in timing and reward processing. More importantly, the LFP-spike synchrony data suggested that neurons in 1 particular cluster were putative fast-spiking interneurons (FSIs) in the striatum and these neurons responded to both timing and reward processing. Experiment 2 reported electrophysiological data that were similar with previous findings, but identified a different cluster of striatal neurons – putative tonically-active neurons (TANs), revealed by their distinct spike waveforms and special firing patterns during the acquisition of the task. These firing patterns of FSIs and TANs were in contrast with potential striatal medium-spiny neurons (MSNs) that preferentially responded to temporal processing in the current study. Experiment 3 further

investigated the proposal that interval timing is subserved by cortico-striatal circuits by using microstimulation. The findings revealed a stimulation frequency-dependent ”stop” or “reset” response pattern in rats receiving microstimulation in either the cortex or the striatum during the performance of the timing task. Taken together, the current findings further support that interval timing is represented in cortico-striatal networks that involve multiple types of interneurons (e.g., FSIs and TANs) functionally connected with the principal projection neurons (i.e., MSNs) in the dorsal striatum. When specific components of these complex networks are electrically stimulated, the ongoing timing processes are temporarily “stopped” or “reset” depending on the properties of the stimulation.

Table of Contents

List of Tables

List of Figures

1. Introduction

1.1 Interval Timing as a Critical Cognitive Function

Time is the essential fourth dimension of our physical world along with the three-dimensional space. The ability to measure the passage of time is as vital to survival as the ability to measure position change in space for animals living in the physical world. We, human beings, are no exception. Just as there are different scales in measuring space, such as miles, feet, and inches, there are also different scales in stamping the passage of time, such as days, hours, and seconds. Interval timing, defined as timing and time perception in the seconds-to-minutes range is a crucial ability for spatiotemporal foraging, computational learning, and decision-making in humans and other animals. In the wild, foraging and food protection behaviors in species as diverse as bumble bees, rats, hummingbirds, starlings, and monkeys have been shown to rely on a precise interval-timing system (e.g., Bateson, 2003; Boisvert & Sherry, 2006; Henderson et al., 2006; Hills, 2003; Wallace et al., 2006). In humans, the importance of interval timing has been recognized in the field of psychology since the time of William James (James, 1890) and later clarified by Fraisse (1963). Nevertheless, it is still a major challenge for neuroscientists to identify the precise neural mechanisms that underlie time perception and timed performance in the seconds-to-minutes range given the ability of animals to accurately and precisely track time across scales spanning 15 orders of magnitude (Buonomano, 2007)

Recent evidence suggests that cortico-striatal circuits that utilize dopamine (DA) and glutamate are critically involved in time perception and timed

performance in animals (Buhusi & Meck, 2005; Cheng et al., 2007a, b; Meck 2006a, b) and humans (Coull et al., 2004; 2008). Despite the above evidence that can tell us what brain regions are important for interval timing, it still isn't fully understood how these brain regions interact with each other as functional units and contribute to interval timing. To investigate the underlying neural mechanisms for interval timing, one reasonable approach is to utilize electrophysiological recordings in behaving animals tested under standard timing tasks in order to better understand how neural responses correlate with timing behaviors in a real-time manner. Once the neural correlates of timing have been identified, the next step is to determine if electrical microstimulation in specific brain areas can "interfere" or "facilitate" the animal's ability to measure time. Hence, the goal of the current thesis is to **1) describe how neural signals in the cortex and striatum change dynamically as a function of the rat's timing performance** and **2) if timing and time perception can be altered by electrical microstimulation**. These experiments are an attempt to provide a direct causal relationship between neural responses and interval timing. In order to achieve these goals, two standard and commonly-used behavioral tasks that can measure an animals' ability to time durations in the seconds-to-minutes range will be introduced. These two tasks will provide the primary behavioral data from the rats while they are being electrophysiologically recorded and stimulated.

Temporal Bisection Procedure

One widely used timing task is the temporal bisection procedure (see Allan & Gibbon, 1991; Cheng et al, 2008; Church & Deluty, 1977; Lustig & Meck, 2001; Meck, 1983, 1991; Penney et al., 2000). In this procedure, subjects are initially trained to classify two anchor durations, one being designated as the "short" anchor (e.g., 2 s) and the other as the "long" anchor (e.g., 8 s). During training, one of these signal durations is randomly presented and two response options are offered – the "short" and "long" response alternatives. Subjects are required to select one of two response options and feedback/reinforcement is given based upon whether the correct choice is selected (illustrated in Figure 1). Once subjects are able to reliably classify these two anchor durations, they are presented with a range of intermediate signal durations (e.g., 2.6, 3.2, 4.0, 5.0, and 6.4 s) for which no feedback is given following a choice response. A sigmoidal-shaped response function is usually obtained after averaging over many trials from well-trained subjects. In the function, the probability of a "long" response is plotted as a function of signal duration – which typically ranges from near 0% for the "short" signal to near 100% for the "long" signal (see Figure 2). The signal duration that subjects classify as "long" 50% of the time is referred to as the **point of subjective equality (PSE)** or bisection point and reflects the duration that subjects consider equidistant from the "short" and "long" anchor durations. Evidence has shown that under normal conditions, the PSE is typically located near the geometric mean of the 2 anchor durations (e.g., Allan & Gibbon, 1991; Church & Deluty, 1977) and reflects the subjects' **temporal**

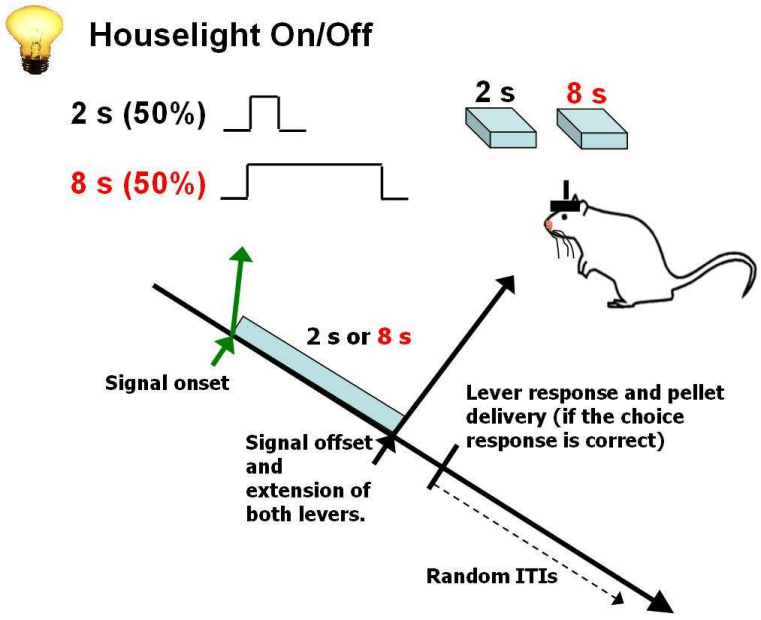

Figure 1: Illustration of the temporal bisection task. During anchor-duration training, the signal is turned on for either 2 s or 8 s. Once the signal is turned off, two response levers are presented. The rat has to decide if the signal presented before was 2 s or 8 s by pressing the associated lever. Correct choice response will be reinforced immediately by a 45 mg food pellet. Once well trained, the rat is presented randomly with a range of 5 intermediate signal durations (e.g., 2.6, 3.2, 4.0, 5.0, and 6.4 s) for which no reinforcement is given following a choice response.

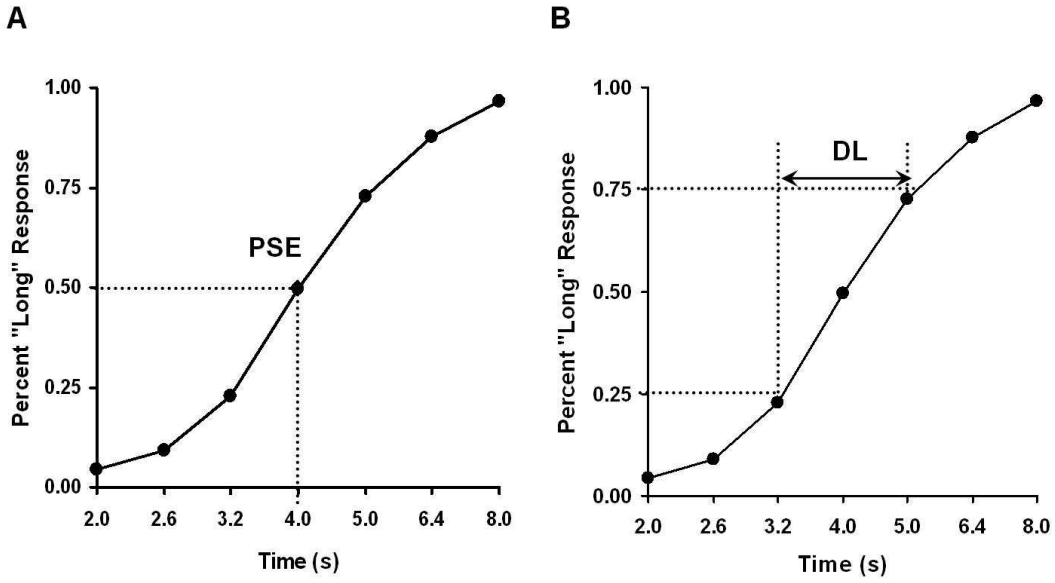

Figure 2: Psychophysical function obtained in a temporal bisection procedure in which 2 s and 8 s served as 2 anchor durations. (A) Point of subjective equality (PSE) reflects the time point with half of the probability (50%) the subject would judge it similar to the anchor "long" duration. In this case, the PSE value is 4 s. (B) Difference limen (DL) represents half of the distance between the signal durations that the psychophysical function intersect with 25% and 75% of the anchor "long" duration. In this case, the DL is 0.9 s (1.8 s /2).

accuracy. The slope or **difference limen** (**DL** – defined as half the distance between the signal durations that define the 25% and 75% “long” response) of the sigmoidal-shaped response function reflects **temporal precision**.

Peak-Interval (PI) Procedure

Another widely used interval-timing task is the peak-interval (PI) procedure (e.g., Malapani et al., 1998; Meck & Church, 1984; Paule et al., 1999; Roberts, 1981). The PI procedure is a modified version of the fixed-interval (FI) procedure that was originally described by Skinner (1938). In a standard discrete-trials FI procedure, subjects can obtain feedback or reward for a response emitted after a fixed duration (criterion time) has elapsed. Catania (1970) introduced the basics of the PI procedure in which a random portion of trials are still FI trials (e.g., 50%), while the remaining trials are probe trials (e.g., 50%). No feedback (e.g., food reward) is given on probe trials and the length of the probe trial is usually 2 or 3 times longer than the criterion time – after which the trial is terminated independent of responding (Figure 3A). Consequently, during probe trials we can observe how subjects would respond both before and after the criterion time. One advantage of this procedure is that during the onset of each trial, there is no discriminative cue for the subject to determine whether the current trial is an FI trial or a probe trial. Consequently, subjects have no option other than to try their best to control their responses as a function of time in each trial. As such, during individual probe trials, we not only observe how subjects determine when to “start” responding prior to the criterion time, but also how they determine when to “stop” responding following the criterion time. This pattern of responding

suggests that subjects use proportional response thresholds (in terms of the temporal distance to the expected time of reinforcement) to decide when to "start" and "stop" a response sequence and that response sequence is typically centered around the criterion time.

After averaging response data across many probe trials from an individual subject, a Gaussian-shaped response function is typically observed (Figure 3B). Several important behavioral indices can be obtained from this Gaussian-shaped peak function. For example, the maximal rate of responding displayed at the peak of the Gaussian-shaped response function is defined as the **peak rate** and its value (high or low) is reflective of the motivational state of the subject. The location of the peak rate on the time-axis is defined as the **peak time**, which is indicative of the psychological time that the subject is expecting to receive feedback during the probe trials. Previous evidence has shown that peak rate and peak time are independent measures of performance, meaning that one can be manipulated without changing the other (e.g., Cheng & Meck, 2007; Roberts, 1981). Changing peak time implies a change of the subjective perception of time while changing peak rate indicates a change in either motivation and/or motor functions (e.g., Cheng & Meck, 2007). Another useful index, **peak spread**, is defined as the distance between the two time points at which the normalized response curve exceeds some level (e.g., 50% of the peak rate) in its ascent prior to the criterion time and in its descent following the criterion time. As one can imagine, the narrower the spread, the more precise the response sequence is on probe trials (e.g., Cheng et al., 2006; Meck & Williams, 1997a).

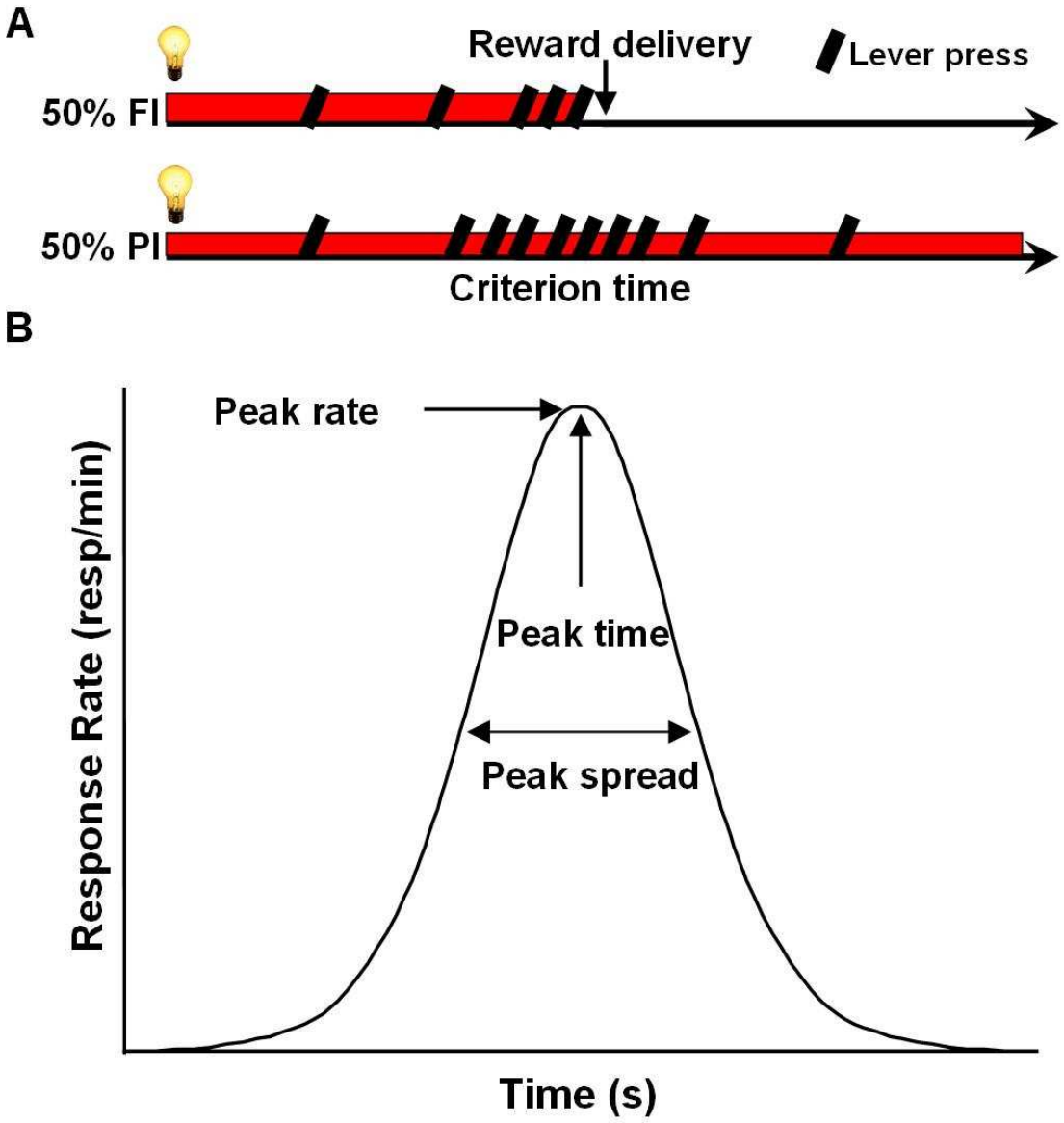

Figure 3: Schematic diagrams of the peak-interval (PI) procedure. (A) Half of the trials are fixed-interval (FI) trials meaning that the first response after criterion time will be reinforced. The other half of the trials are probe trials (PI) meaning that no reward is given and the signal remains on for up to 2 or 3 times of the criterion time. (B) A Gaussian-shaped response function derived by averaging individual data across all probe trials. *Peak rate* is defined as the highest responding rate of the function located at the expected time of reinforcement, which is defined as *peak time*. *Peak spread* is a measure of the distance between the two points at which the responding curve ascends and descends through 50% of the peak rate.

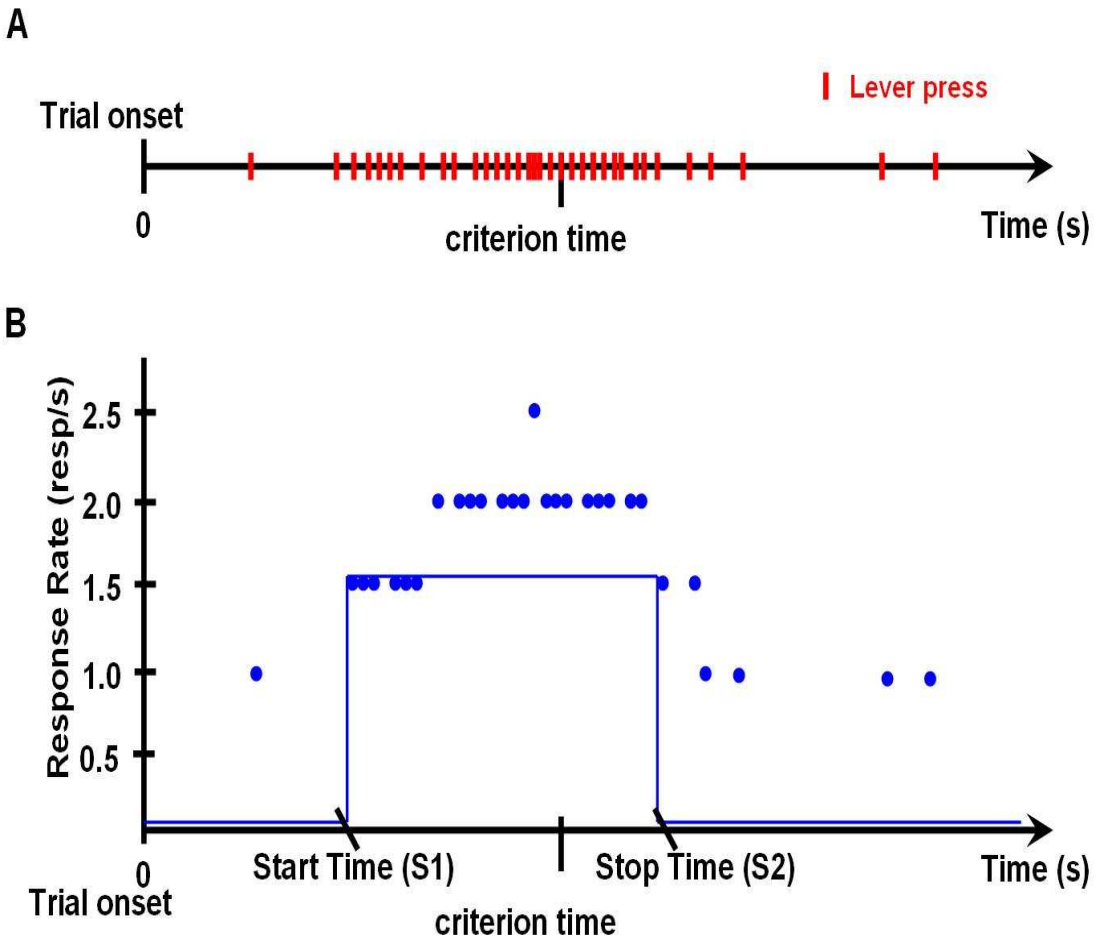

Figure 4: Schematic diagram of single-trials analyses in the PI procedure. (A) represents lever press data in a probe trial. On the x-axis, each red tick means one lever press. (B) converts data in (A) into response rate as a function of time. Each blue dot represents the response rate at a time bin. The blue lines represent the step functions that best fit the current responding patterns in this trial. Start time (S1) and stop time (S2) are derived by the time points that the subject abruptly transitions into a high state of responding before the criterion time and into a low state of responding following the criterion time.

The last two indices that are relevant to the topics of this report are the ones that are indicative of when subjects "**start" (S1)** or "**stop" (S2)** their response sequence on a particular probe trial. The indices of S1 and S2 are usually obtained from single-trials analyses conducted on the response sequence produced during individual probe trials (Figure 4A). This analysis is conducted by fitting a step function to the data so that 2 break points in the

response sequence are identified. The first index (S1) is the time at which subjects abruptly transition from a low rate into a high rate of responding, and the second index (S2) is the time when the subjects transition into a low rate of responding from the high rate (Church et al., 1994). S1 and S2 measures obtained from single-trial analyses provide another useful measures for the evaluation of clock, memory, and decision making involved in timing and time perception (e.g., Church et al., 1994; Gibbon & Church, 1992; Matell et al., 2006; Rakitin et al., 1998).

In comparison of the 2 standard timing tasks, the PI procedure is considered as a production-based task, while the temporal bisection procedure is considered as a perception-based task. A production-based task means that a subject is producing the time in a real-time fashion such that when the subject's response occurs on the time-axis will determine if the response is reinforced or not. For instance, in the PI procedure, a rat is producing the estimated criterion time during the probe trials based on what it was reinforced during the FI trials (Figure 3). A perception-based timing task means that a subject is classifying a signal as "short" or "long" after the subject has perceived the presented stimulus. Hence, the subject is not required to produce any duration, but to perceive the time during the presentation of a stimulus (Figure 1).

1.2 Cortico-Striatal Circuits Subserving Interval Timing

By using the above 2 standard timing tasks, the field has accumulated enough evidence that suggests cortico-striatal circuits are the **loci** for interval timing in the brain. In one recent study, Meck (2006b) demonstrated that lesions

of the substantia nigra pars compacta (SNC) or the caudate-putamen (CPu) in rats that were pre-operatively trained in the PI procedure disrupted their Gaussian-shaped response functions, suggesting a loss of temporal control of their behavior. In other words, both lesioned groups displayed flat response functions, unlike the Gaussian-shaped functions centered at the criterion before lesion, such as the example in Figure 3B. When injected with $_{L}$-DOPA, the precursor of DA, the drug temporarily restored temporal control of the response functions in the SNC-lesioned rats from flat to Gaussian-shaped, but this restoration was not observed in the CPu-lesioned rats. Therefore, an intact CPu and normal DA neurotransmission is critical to maintain normal timing in the PI procedure. In a related study, rats given frontal cortex lesions lost their sensitivity to dopaminergic drugs (e.g., methamphetamine or haloperidol) indicating that they were able to maintain the precision of their baseline timing functions, but were unable to display the typical horizontal shifts following administration of DA drugs (Meck, 2006a). In summary, the above findings elucidate the role of intact DA neurotransmission in cortico-striatal circuits for interval timing.

If interval timing critically depends upon intact cortico-striatal circuits as suggested by the lesion studies described above, one would expect that neural activity in any part of the cortico-striatal circuits should reflect the passage of time when subjects are performing interval-timing tasks. Indeed, electrophysiological recordings have revealed that ensembles of striatal neurons and neurons in the cingulate cortex display neural firing rates that increase around the expected time of reward and decrease after the expected time of reward has passed (Matell et

al., 2003ab). Similar neural response patterns that change as a function of time are also reported in monkeys in recent studies (e.g., supplementary motor area in Mita et al., 2009; prefrontal cortex in Jin et al., 2009). Together, these findings support the striatal-beat frequency (SBF) model for interval timing (Matell & Meck, 2004), a neurobiological model that highlights the input-output relationship between the dorsal striatum and other brain regions. In essence, the SBF model states that striatal projection neurons receive numerous cortical inputs, and then integrate and fire action potentials if the input signals pass a predetermined threshold or reach a specific ensemble firing pattern. Once the neural computation is complete, the dorsal striatum sends the timing signals to the basal ganglia, which, in turn, sends the timing signals back to the frontal cortex (e.g., primary motor cortex, supplementary motor cortex, and the prefrontal cortex) via the thalamus. This cortico-striato-thalamo-cortical circuit has been shown to be critical for various tasks that involve timing, such as temporal integration tasks (e.g., Dale et al., 2010), time-based motor planning tasks (e.g., Mita et al., 2009), as well as temporal judgment tasks (e.g., Harrington et al., 2010; Lustig et al., 2005). Therefore, neurons in any part of this circuit may convey a copy of the temporal information that is being integrated in the striatum. Exactly how the timing signals are generated, maintained, and transmitted in this cortico-striato-thalamo-cortical loop is still under investigation. Given that the striatum is the pivotal region in this loop as evidenced by previous lesion and recording studies (e.g., Matell et al., 2003b; Meck 2006a), our proposal is to examine different populations of neurons in the striatum and to determine how those neurons

represent interval timing, necessary for the performance of two standard timing tasks in the seconds-to-minutes range.

1.3 Electrophysiological Properties of Neurons in the Striatum

In the striatum, the most common type of neurons is the medium-spiny neurons (MSNs) that take up to 90-95% in the whole area according to recent reviews (Kreitzer, 2009; Kreitzer & Malenka, 2008). Each striatal MSN receives about 10,000 to 30,000 cortical inputs (Wilson, 1995), thus making each MSN an ideal locus for the temporal integration of patterns of cortical oscillations due to this high-degree of convergence. MSNs display a bi-modal distribution of their resting membrane potential, or the so-called “Up state” and “Down state,” determined by how close the resting membrane potential is to the threshold potential (Calabresi et al., 1990). During the “Down state”, MSNs display more negative resting membrane potential, due to intrinsic channel properties on the membrane and perhaps due to local inhibition from nearby interneurons. This negativity makes it difficult for MSNs to generate action potentials because a higher voltage change is required to reach the threshold potential. In contrast, when MSNs are in the “Up state,” it is easier to generate action potentials because the resting membrane potential is now closer to the threshold potential. Hence, factors that determine the “Up state” and the “Down state” of MSNs will also determine their output probability, which, in turn, will determine their functions, such as interval timing and other motor functions.

Despite MSNs are the principal neurons in the dorsal striatum, the importance of interneurons in the same region should not be overlooked as

interneurons make synaptic contacts with MSNs and thus regulating the firing probabilities of MSNs. Among these interneurons, 3 major types of interneurons have recently received attention. According to electrophysiological properties, interneurons that display tonic activity (constant firing) are referred to as tonically-active neurons (TANs) and TANs release acetylcholine (ACh) when they fire action potentials. Other interneurons that release GABA can be further classified into fast-spiking interneurons (FSIs) and low-threshold spiking (LTS) interneurons. Together, these interneurons help “modulate” the firing probabilities of their downstream MSNs, perhaps by modifying their “Up” and “Down” states thereby dictating information processing in the striatum.

TANs have a larger cell body than all other types of neurons in the striatum, a feature that allows them to be easily identified (Izzo & Bolam, 1988). Another feature of TANs is the aspiny structures on their dendrites, implying a lack of point-to-point communication between them and upstream neurons. Hence, these TANs are thought to function like sensors that can monitor the concentration gradient of the neurotransmitters that they respond to. Recent *in vivo* studies have shown that TANs respond to salient signals by showing a brief decrease in their neural firing rate upon the onset of a reward or salient stimulus, compared to a brief increase in the neural firing rate of DA neurons to the same event (Apicella, 2006, 2007; Morris et al., 2004). This distinct activity pattern of TANs can be observed in the case of natural rewards, or a salient stimulus that reliably predicts a natural reward, in rodents (Reynolds & Wickens, 2004) and primates (Aosaki et al., 1995). Together with the increased activity of midbrain

DA neurons following a reward or salient stimulus, one can infer that TANs and DA neural terminals are cooperating with one another in the striatum, although they show different change in firing rate when presented with the delivery or omission of an expected reward (Apicella et al., 2009). Exactly how the coordination between MSNs and TANs within striatal circuits regulates the clock, memory, and decision making involved in interval timing is an important question that remains to be addressed (Kubota et al., 2009).

On the other hand, although both FSIs and LTS interneurons are quite similar in their electrophysiological properties (high baseline firing rate and GABA-releasing), one can still distinguish them by the type of receptors that are expressed on their dendrites. While both FSIs and LTS interneurons have DA D1/D5 receptors expressed on their cell bodies (Centonze et al., 2003), nicotinic cholinergic receptors (nAChRs, see Zhou et al., 2002) are expressed only on FSIs that makes FSIs unique because this enables the FSIs to be a fast responder to the cholinergic inputs provided by nearby TANs. When TANs are releasing ACh onto the FSIs, the FSIs will be excited and continue to inhibit their targeting MSNs. Thus, TANs can also control MSNs by their direct influence (i.e., nAChRs) on FSIs, composing a local TAN-FSI-MSN circuit that may contribute to interval timing.

Another measure to distinguish FSIs and LTS interneurons is to increase DA neurotransmission by using stimulant drugs, such as cocaine and methamphetamine as recently reported by Centonze et al. (2002a; 2002b). In these two studies, cocaine and methamphetamine can increase the firing rate of

LTS interneurons by activating to DA D1-like receptors, while the same drugs decrease the firing rate of FSIs. Interestingly, low doses of cocaine and methamphetamine are also commonly used in interval-timing studies, in which these two drugs can increase the speed of the internal clock, thus contributing to the perception that time is passing faster (e.g., Buhusi, 2003; Buhusi & Meck, 2002; Cheng, et al., 2006; 2007; MacDonald & Meck, 2005; Matell et al., 2004, 2006; Meck, 1983, 1986, 2006a). It will be important to determine if the clock-speed accelerating effect of cocaine and methamphetamine is produced by their combined effects on the FSIs and LTS interneurons (or on MSNs) in the striatum.

1.4 Experimental Rationale

As reviewed above, the dorsal striatum in cortico-striatal circuits is found to be the most critical region for interval timing (Meck, 2006b). Hence, it is reasonable to focus on how the neurons in the dorsal striatum, especially subtypes of striatal neurons, represent the passage of time by integrating their neural firing patterns with the cortex as well as by sending their output signals (i.e., spike trains) to the downstream basal ganglia nuclei. While other components of this circuit are implicated in certain types of learning and memory (e.g., Kubikova et al., 2007; Yin & Knowlton, 2006), the present study is focused on the timing functions of this circuit. In order to achieve this goal, recording from cortico-striatal circuits and distinguishing subtypes of neurons in the dorsal striatum while rats are engaging in timing tasks is the first step in understanding the neural mechanisms subserving interval timing. In the first part of the dissertation, two experiments are designed to address the question as to how

interval timing is being represented by different subtypes of striatal neurons (i.e., MSNs and interneurons). In Experiment 1, rats were pre-trained on a PI procedure with two criterion times (12 and 36 s) **before** the recording electrodes were implanted into their dorsal striatum and sensorimotor cortex. In this way, we can observe how cortico-striatal neurons respond as a function of time for two target durations (e.g., 12 and 36 s) in a given trial after rats have been well-trained (Cheng et al., 2007b). In Experiment 2, a separate group of rats were implanted with recording electrodes in their dorsal striatum **before** they started training on a temporal bisection procedure using 4 s and 16 s as anchor durations. Thus, we are able to observe how striatal neurons initially respond to the task early in training and how their firing patterns evolve as a function of training. For example, a specific cell subtype (e.g., TANs) may respond more early in learning and some other cell subtype (e.g., FSIs) may be more important in maintaining the performance after the rats become well trained.

In Experiment 3, the goal is to determine if the rat's temporal processing can be altered by delivering electrical microstimulation to each part of cortico-striatal circuits. This is an approach that has been used to establish a strong causal relationship between brain and behavior. By stimulating the neural circuits directly, one can determine if certain behaviors can be induced or perceptions modified. The same approach has been applied to the study of neural mechanisms involved in singing and the songbird's motor pathway (Arfin et al., 2009; Long & Fee, 2008), microstimulation-induced perception and integration across sensory modalities (e.g., Fitzsimmons et al., 2007; Wickersham & Groh,

1998), as well as motor control in Parkinson's Disease (Fuentes et al., 2009; Gradinaru et al., 2009). In the field of interval timing, however, this type of circuit mapping technique has not been systematically used before. Consequently, a brief summary of all possible scenarios following microstimulation of putative interval-timing circuits is discussed below.

To what extent and how does the delivery of electrical microstimulation to cortico-striatal circuits change interval timing in rats, if any? In other stimulation paradigms, stimulation in specific neural circuits could artificially generate perception (Fitzsimmons et al., 2007), initiate behaviors (Fuentes et al., 2009), or stop on-going behaviors (Arfin et al., 2009; Gradinaru et al., 2009). In the context of interval timing, the current proposal speculates that it could either facilitate or disrupt timing in a manner that we can distinguish by testing rats in a PI procedure following and/or during microstimulation. If microstimulation to cortico-striatal circuits is facilitative to time perception, it could either accelerate the perception of time (i.e., it makes the internal clock run faster), or immediately bring about the maximally responding rate to the expected criterion at the time when microstimulation is delivered (i.e., it moves the **peak time** that normally centers at the criterion time to the delivery time of microstimulation). In contrast, if the same treatment is disruptive to timing, it could induce either one of the following 3 results: 1) it keeps the rats from timing the signal during the period of microstimulation (i.e., it stops the internal clock during stimulation), 2) it makes the rats to time the signal from the starting point again (i.e., it resets the internal clock and the rats begin timing from zero after stimulation), or 3) it slows down

the perception of time (i.e., it makes the internal clock run slower). Finally, another potential disruption to timing is that the stimulated rats may fail to display scalar property in their timing functions. Scalar property states that the variance of timing is proportional to the estimated duration being timed, and this is a hallmark of interval timing, or a form of Weber's Law in perception (Church, 2003). It has been shown that Parkinson's disease patients off medication failed to show scalar property in their timing functions (Malapani et al., 1998). Therefore, it is possible that any disturbance or imbalance in cortico-striatal circuits may contribute to the disruption of scalar property in interval timing. In summary, there are six potential changes of timing and time perception that we could possibly observe following and/or during the delivery of microstimulation to cortico-striatal circuits in rats.

1.5 General Methods

Subjects

Sprague–Dawley male rats were used, obtained from Charles River in Raleigh, N.C. Rats were initially housed in pairs and allowed continuous access to water and food in their home cages. Two weeks before the start of experiments, they were restricted to food consumption so that their body weights were maintained at approximately 85% of ad lib weights. Following surgery, all the rats became individually housed to prevent interference of the headstage from their cage mates. A light–dark (LD) cycle of 12:12 was maintained in the vivarium with fluorescent lights on at 7:00 A.M. Rats were approximately 17 mo

(Experiment 1), 3 mo (Experiment 2), and 24 mo (Experiment 3) of age at the start of the experiment.

Electrodes

Stainless steel (SS) wire arrays were used in the current study (including the microstimulation experiment), obtained from MicroProbes for Life Sciences (Gaithersburg, MD). Each SS array had 1 dedicated reference electrode next to the 8 recording electrodes (with 0.5 mm spacing between each electrode) and all were implanted into target brain areas. All electrodes were 50 µm in diameter and coated with Teflon for insulation. The impedance was between 0.4 and 0.6 mega ohms (MΩ). Each array also had a silver ground wire that was attached to a skull screw right above and in contact with the cerebellum to provide a better ground control.

Surgery

Surgical instruments were autoclaved before the first surgery in a given day. On the same day, the same tools were sterilized between rats using a bead sterilizer. Rats were anesthetized with ketamine (100 mg/kg) and xylazine (10 mg/kg). To begin, the rat was weighed, anesthetized, the top of its head shaved and scrubbed with chlorhexidine or betadine followed by 70% Isopropyl alcohol - alternated 3 times. Anesthesia during surgery was maintained with supplemental injections of only ketamine every 1-2 h as necessary. A scalp incision was made, and the skin was retracted. The skull surface was cleaned for the drilling of holes and the implantation of electrodes by hands slowly and gently into the dorsal striatum and the sensorimotor cortex. Following the dental acrylic became dry,

antibiotic was applied all around the head cap (topical ointment: bacitracin (400 units/g), and neomycin sulfate (5 mg/g), and the skin be sutured rostrally and caudally to the implant, as needed. The Bregma coordinates (Paxinos and Watson, 1998) for the dorsal striatum is: Anterior: +1.2 mm to −1.0 mm, Lateral: +2.0 mm to +4.0 mm, and Ventral: −3.5 mm to −4.0 mm. The Bregma coordinates for the sensorimotor cortex is: Anterior: +1.2 mm to −1.0 mm, Lateral: +2.0 mm to +4.0 mm, and Ventral: −1.8 mm to −2.8 mm. Rats were allowed at least 7 days of post-surgery recovery, followed by 3 days of habituation to the recording lever box or several sessions of retraining.

Lever Boxes

All behavioral data were obtained in 2 identical lever boxes (MED Associates, St. Albans, VT) housed in light and sound attenuating cubicles (MED Associates, Model ENV-019). Each lever box had inside dimensions of approximately 24 cm × 31 cm × 31 cm. The top, sidewalls, and door were constructed of clear acrylic plastic. The front and back walls were constructed of aluminum, and the floor was comprised of 19 parallel stainless steel bars. Each lever box was equipped with two retractable response levers (MED Associates, Model ENV-112) situated on the front wall of the lever box, with 1 stationary lever in between the 2 retractable levers and right above the food cup. Precision food pellets (45 mg; Bio-Serv, Frenchtown, NJ) could be delivered by a pellet dispenser (MED Associates, Model ENV-203) to a food cup on the front wall 1 cm above the floor. A 28 V, 80 mA, 2,500 lx houselight was mounted at the center-top of the front wall and could be used to illuminate the lever box as well

as the signal light for the PI procedure and the temporal bisection procedure. A white noise amplifier/speaker system (MED Associates, Model ENV- 225) was mounted on the opposite wall from the levers, but was not used in the current study. An IBM-PC compatible computer attached to an electronic interface (MED Associates, Model DIG-700 and SG-215) was used to control the lever box and record the behavioral data.

Recording Apparatus

Neural activity was recorded using the Multi-Neuron Acquisition Processor system (MAP; Plexon, Dallas, TX). LFPs were pre-amplified, filtered (0.5–400 Hz), and digitized at 1,000 Hz using a Digital Acquisition card (National Instruments, Austin, TX). All electrophysiological recordings were grounded to one silver ground wire attached to the skull screw right above and in contact with the cerebellum. A dedicated reference electrode right besides 8 recording electrodes was also used in each target brain area. Recording segments demonstrating LFP saturation resulting from movement artifacts or mechanical noise were excluded from analysis. An IBM-PC compatible computer was used to control the Plexon MAP and record the neural data. Please note that the Plexon MAP is connected with the Med Associates interface by receiving TTL events from the Med Associates programs. This connection allows the temporal coordination between the behavioral events recorded in the lever box and the electrophysiological data.

Stimulation Apparatus

Electrical microstimulation was provided by a STG4008 stimulator (Multi Channel Systems MCS GmbH, Reutlingen Germany). The stimulator is controlled by the same computer that controls the Med Associate lever box. This allows synchronization between the behavioral events recorded in the lever box and the simulator. The stimulator provides 8 independent channels that can be programmed to deliver charge-balanced biphasic pulses with the temporal resolution at 20 μs and the current output resolution at 100 nA.

Spike-Sorting Procedures

Individual units were initially judged on the basis of visual inspection of waveform shape, size, and discriminability in a real-time manner during recording sessions. After a recording session, the data were further examined by using Offline Sorter (v2.8; Plexon). In the Offline Sorter, several more steps were conducted to maximize the distinction and quality of each unit clusters from each electrode. First, the Offline Sorter provides a tool to invalidate cross-channel artifacts. This could invalidate artifacts that were present on 75% of the channels (i.e., 6 out of 8 channels from a brain region) at the same time – i.e., the artifacts were identified only by their time-coincidence across all 8 channels. Next, the Offline Sorter can remove short inter-spike-interval (ISI) waveforms, which is defined by any spike that its ISI is shorter than 1 ms in the current study. The idea here is that an action potential that was shorter than 1 ms should be non-biological due to the violation of a hypothesized absolute refractory period. Hence, the software is able to remove those short ISI waveforms for each unit

such that the remaining waveforms in each unit are more reasonable and worth for further analysis. If the clusters of each unit in each channel are too close to one another, the Offline Sorter can also rule out the spikes that are outliers to their parent clusters. This could make sure that all the clusters we obtained were separated enough for further functional analysis. Once all the units were sorted, the data were transferred to NeuroExplorer (v.3x; Plexon) to create peri-event histograms and raster plots.

Statistical Analyses

Throughout the 3 experiments, statistical analyses were conducted by using repeated measures of analysis of variance (ANOVA) or T-test for dependent samples by using a commercial software – STATISTICA (Tulsa, OK), unless specified otherwise. If the main effect of ANOVA reached significance, appropriate post-hoc comparison method (e.g. Fisher least significant different, LSD or unequal N honestly significant difference, HSD) was used to determine the real difference among conditions.

2. Experiment 1: Ensemble Responding Patterns in a Peak-Interval Procedure with Two Criterion Times

2.1 Methods

Subjects

Six (n=6) male Sprague-Dawley rats were used in this experiment when they were approximately 17 months of age. All the rats were well-trained in a PI procedure with two criterion times **before** implanting electrodes into the dorsal striatum and the sensorimotor cortex. Following at least 1 week of post-surgery recovery, they were once again maintained on a 85% free-feeding body weight by a daily ration of regular rodent diet given shortly after training sessions.

Training History

Pre-training (Session 1-5)

All rats received 5 sessions of combined magazine and lever response training. During these sessions, a food pellet (45 mg) was delivered every 60 s for 60 min, regardless of lever response. Also, 1 side lever was primed until 10 reinforced responses were made on that lever in a fixed-ratio 1 schedule (FR-1), at which point, another side lever was primed for another 10 reinforced responses. This procedure was repeated until the rats receive 60 food pellets combined from both sources. By the end of 5 sessions, all rats typically finished the daily session within 20 min.

Discrete-Trial Fixed-Interval (FI) Training (Session 6-15)

During these sessions, each of the 2 side levers was paired with either 12 or 36 s (the 2 criterion times) and the pairing was counterbalanced across rats. In a given trial, only one lever was extended into the lever box for the rats to respond. The first lever response after the criterion times was reinforced with a food pellet and then followed by an inter-trial interval (ITI) of 40 s plus a geometrically distributed duration with a minimum of 0.1 s and a mean of 20 s. During the ITI, the houselight was off and the lever was retracted. In a given session that lasted for 2 h, there were 50% of 12-s FI trials and 50% of 36-s FI trials, randomly determined by the computer program. By the end of this training phase, all rats displayed the typical scallop-shaped FI responding curve meaning that their lever response rate was low early in a trial, but gradually ramped up to the criterion times late in a trial.

PI Training (Session 16-90)

Once the rats acquired the FI task, a non-reinforced probe trial was randomly introduced in a session. In a given session that lasted for 2 h, there were 50% of reinforced FI trials (25% 12 s and 25% 36 s) and 50% of probe trials, randomly determined by the computer program. The probe trials for the 12-s lever were at least 30 s plus another random duration from 1.1 s to 35.2 s with a mean of 11.6 s. The probe trials for the 36-s lever were at least 90 s plus another random duration from 1.1 s to 35.2 s with a mean of 11.6 s. The lever pressing data obtained from these probe trials were analyzed to determine how well the rats could center their responses around the 2 different criterion times (e.g., 12

and 36 s). By the end of this training phase, all rats displayed the Gaussian-shaped responding curve meaning that their lever response rate peaked around the criterion times.

Self-Initiated PI Training (Session 91-120)

To better align the neural firing data and the start the subject's timing, rats were required to press the middle stationary lever to initiate all the trials during this phase of training. The idea here is that if the beginning of a trial was controlled by the computer program, the rats may sometimes ignore the onset of the trial, and then begin timing the signal some time after the trial has begun, but not exactly at the programmed onset of the signal. By requiring the rats to press the middle lever in order to initiate a trial, we can assume that they were prepared to start timing. All the rats quickly learned the requirement of pressing the middle lever in the first session when they were required to do so, even though the middle lever was constantly present in the lever box and had been inactive during the previous 90 sessions of training.

In addition to the "self-initiated" trial requirement, a "free" pellet was also given following the end of half of the probe trials. The purpose of this unearned pellet was to provide a comparison to an earned pellet that the rats obtained by pressing the reward-primed side levers in the FI trials.

Post-Surgery PI retraining (Session 121-130)

After post-surgery recovery, all the rats received at least 10 retraining sessions to make sure that the surgical procedures did not disrupt their timing performance.

PI Testing with Recording (Session 131-137)

The recording sessions were no different from the previous training sessions, except that the recording cables were connected to their headstage. After 5 recording sessions, the rats became accustomed to the situation that they were comfortable performing the timing task while being connected to the recording cables. Following that, 2 electrophysiological recording sessions were conducted for which the data were pooled, analyzed and presented in the Results section.

Unit Classification Based on Spike Waveforms

One major idea of this experiment is to correlate neural firing data to timing performance simultaneously. The idea is based on the assumption that different subtypes of neurons (e.g., projection neurons and local interneurons) may have distinct spike waveforms. Hence, it will be important to determine if neurons with distinct waveforms have different behavioral correlates in the current study. In order to achieve this goal, the following 3 features of averaged waveforms of each neuron were measured – 1) sodium peak amplitude, 2) potassium peak amplitude, and 3) capacitive peak amplitude, as shown in Figure 5 (Gold et al., 2007). The idea of dissecting spike waveforms based on their distinct features has been utilized in studying the functions of different neuronal subtypes in various brain regions, such as the cortex (Constantinidis & Goldman-Rakic, 2002), the hippocampus (Gold et al., 2006; Viskontas et al., 2007), the amygdala (Likhtik et al., 2006), and the striatum (Wiltschko et al., 2010). Although there are many features that can be used to characterize the spike

waveforms as outlined in Gold et al. (2007), we found that the adopted 3 features together can satisfy the current need to classify neurons into different clusters for further behavioral analysis.

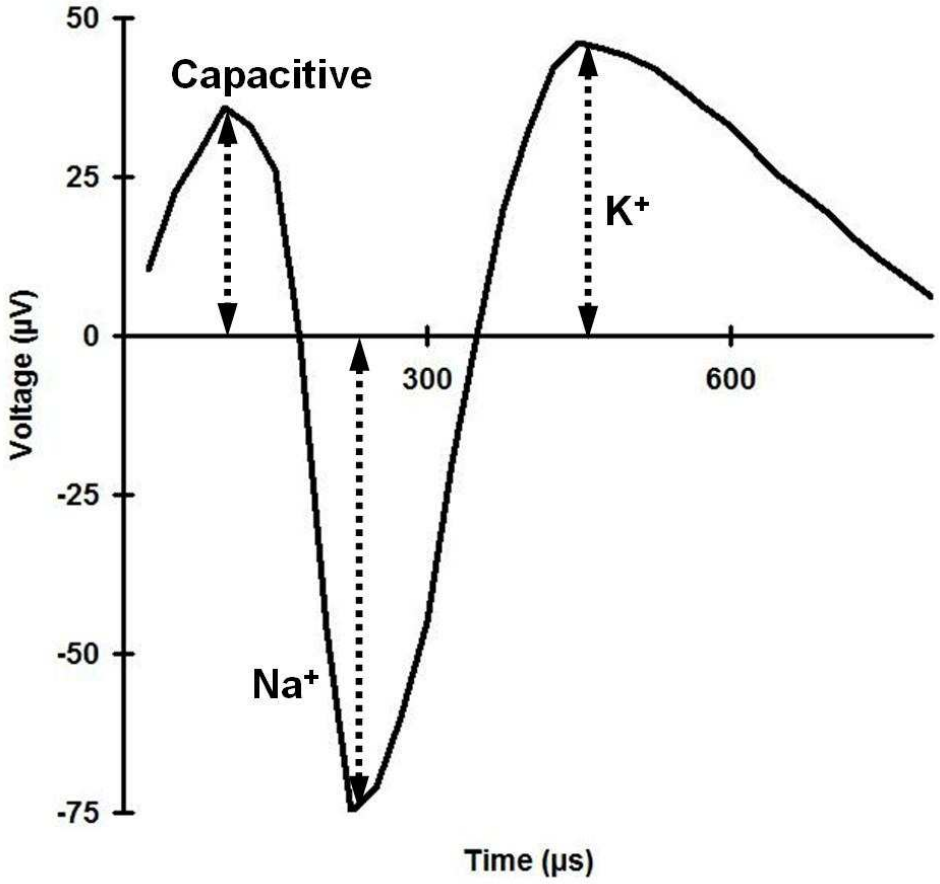

Figure 5: Schematic diagram of the 3 features of averaged spike waveforms – 1) sodium (Na^+) peak amplitude, 2) potassium (K^+) peak amplitude, and 3) capacitive peak amplitude.

Cortico-Striatal High-Voltage Spindles (HVS)

Other than spike waveforms, another measure that can help us distinguish subtypes of neurons in cortico-striatal circuits is the so-called striatal high-voltage spindles (HVS). HVS is a uniform LFP oscillatory pattern with synchronous firing of neurons in the striatum (Berke et al., 2004). In that study, the striatal LFP displays uniform oscillations in the range of 9-12 Hz when the rats were in a quiet

and immobile state (with their eyes open). During that state, it was observed that only FSIs reliably fired in synchrony with striatal HVS, while MSNs did not show such a strong synchronous firing pattern (i.e., MSNs frequently missed the beat). Despite the exact functions of this HVS are still under investigation ever since it was first reported by Buzsaki (1991), we can nevertheless utilize this intrinsic phenomenon as a useful tool to distinguish striatal MSNs and FSIs in the current study. With this intrinsic phenomenon, the current experiment can determine how striatal MSNs and FSIs respectively correlate with the rat's timing performance.

Location of Recording Electrodes in the Brain

The location of the recording electrodes is depicted in Figure 6.

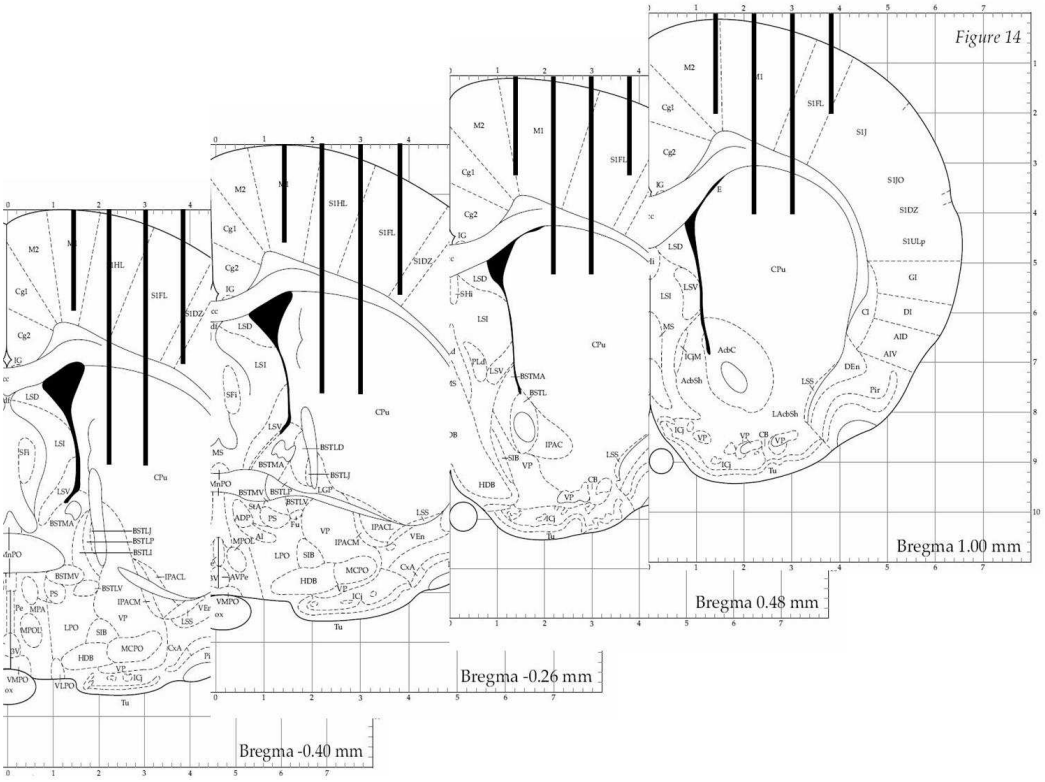

Figure 6: Schematic diagrams of the location of recording electrodes in the rat's brain. Eight electrodes were implanted in each brain region (the dorsal striatum and the sensorimotor cortex). The reference electrode (not shown here) was on a separate section with different A-P coordinate.

2.2 Results

Behavioral Data

The lever response data during the recording session is shown in Figure 7. As can be seen, both timing functions were clearly centered around the criterion (the 36-s function) or slightly after the criterion time (the 12-s function).

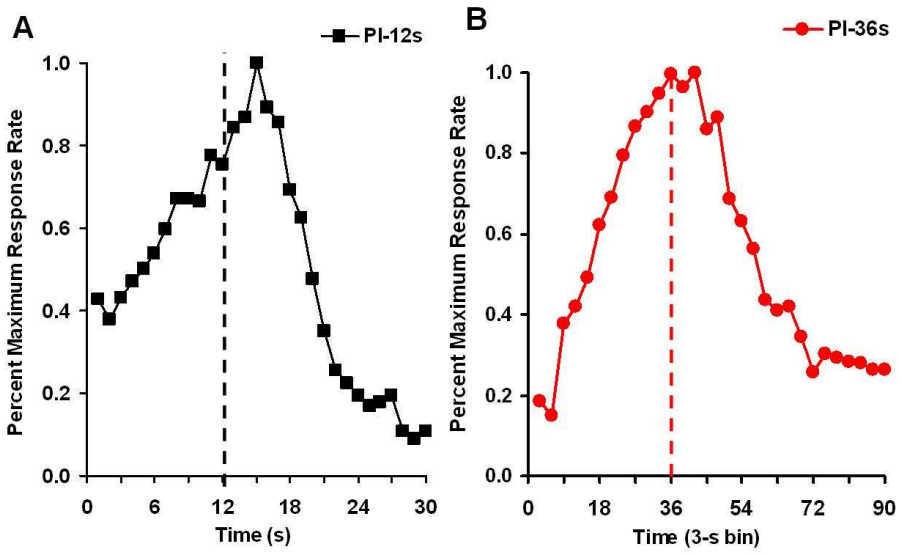

Figure 7: Normalized peak functions by averaging all 6 rats during the recording session. (A) depicts the function from the 12-s probe trials, while (B) depicts the function from the 36-s probe trials.

Recording Data

As mentioned before, the first goal was to distinguish as many units as possible according to their spike waveforms. Initially, 24 different patterns of waveforms were classified. The results are summarized in Table 1 (for the dorsal striatum, DS) and in Table 2 (for the sensorimotor cortex, Cx). Once 24 different patterns of waveforms were classified, we further grouped them together into different clusters according to the similarity of their spike waveforms and behavioral correlates in the PI procedure.

Table 1: Distribution of total observed units from the dorsal striatum (DS) in during the PI recording session. Note that each rat has 8 recording electrodes in the DS.

Brain Region			DS
Number of Rats			n=6
Total Observed Units			161
Average Units per Rat			26.8 ± 1.6
Number of Electrodes			8
Type	Count	%	(spikes/s)
A	5	3.1%	2.771
B	2	1.2%	1.326
C	10	6.2%	1.484
D	5	3.1%	5.571
E	2	1.2%	4.771
F	2	1.2%	9.106
G	1	0.6%	12.871
H	6	3.7%	0.056
I	1	0.6%	0.774
J	1	0.6%	0.423
K	1	0.6%	0.696
L	1	0.6%	10.038
M	8	5.0%	11.393
N	16	9.9%	9.119
O	3	1.9%	6.736
P	27	16.8%	2.772
Q	47	29.2%	8.916
R	9	5.6%	3.421
S	8	5.0%	4.692
T	3	1.9%	1.405
U	1	0.6%	2.376
V	0	0.0%	N/A
W	2	1.2%	5.495
X	0	0.0%	N/A

Table 2: Distribution of total observed units from the sensorimotor cortex (Cx) during the PI recording session. Note that each rat has 8 recording electrodes in the Cx.

Brain Region			Cx
Number of Rats			n=6
Total Observed Units			164
Average Units per Rat			27.3 ± 1.6
Number of Electrodes			8
Type	Count	%	(spikes/s)
A	22	13.4%	2.644
B	4	2.4%	3.373
C	10	6.1%	7.744
D	1	0.6%	0.206
E	0	0.0%	N/A
F	0	0.0%	N/A
G	0	0.0%	N/A
H	4	2.4%	0.019
I	0	0.0%	N/A
J	2	1.2%	0.459
K	0	0.0%	N/A
L	1	0.6%	0.878
M	2	1.2%	3.617
N	4	2.4%	2.685
O	2	1.2%	0.617
P	33	20.1%	1.674
Q	24	14.6%	4.108
R	12	7.3%	1.110
S	10	6.1%	1.885
T	4	2.4%	0.060
U	0	0.0%	N/A
V	5	3.0%	0.646
W	20	12.2%	4.937
X	4	2.4%	1.365

Unit Classification Based on Spike Waveforms

Among the 325 units reported in Tables 1 and 2, we further classified them into 4 major clusters based on the Na^+ peak amplitude and K^+ peak amplitude of their averaged spike waveforms. As can be seen in Figure 8, neurons in Cluster A displayed high Na^+ peak amplitude and high K^+ peak amplitude in their spike waveforms. Neurons in Cluster D had the lowest K^+ peak amplitude. Neurons in Clusters B and C had intermediate level of Na^+ peak amplitude and low K^+ peak amplitude.

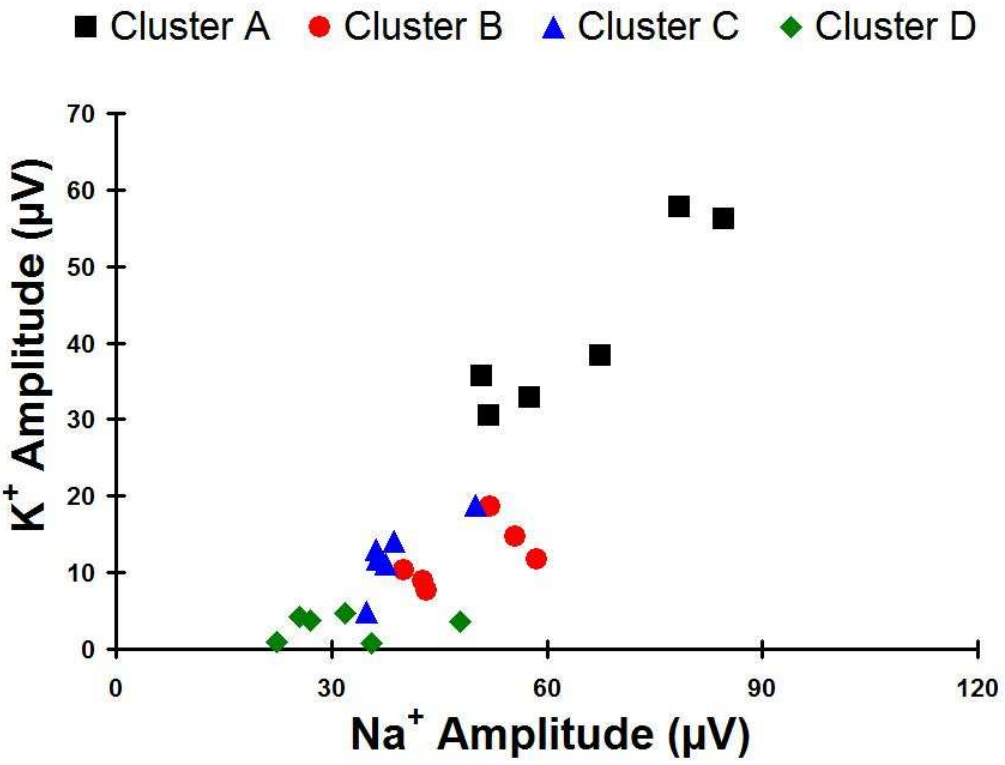

Figure 8: Mean Na^+ peak amplitude ('x') and K^+ peak amplitude ('y') of the neurons in each cluster of individual rats. Each dot represents the mean data from individual rats.

Statistical analyses confirmed that there were significant main effects on the Na^+ peak amplitude ($F_{(3,15)} = 37.4$, $p < 0.001$) and the K^+ peak amplitude ($F_{(3,15)} = 54.6$, $p < 0.001$) among the 4 clusters of neurons. Post-hoc comparisons

(Figure 9) indicated that Cluster A had higher Na^+ peak amplitude than Cluster B ($p < 0.001$), which had higher Na^+ peak amplitude than Cluster C ($p < 0.05$), which had higher Na^+ peak amplitude than Cluster D ($p < 0.05$). On the measure of K^+ peak amplitude, Cluster A had higher ($p < 0.001$) while Cluster D had lower ($p < 0.05$) K^+ peak amplitude than Clusters B and C, which did not differ from each other. Finally, all 4 clusters of neurons did not have high enough capacitive peak amplitude (all below 5 µV on average) for meaningful statistical analyses. Therefore, the measure of capacitive peak amplitude can be ignored when classifying neurons into these 4 clusters.

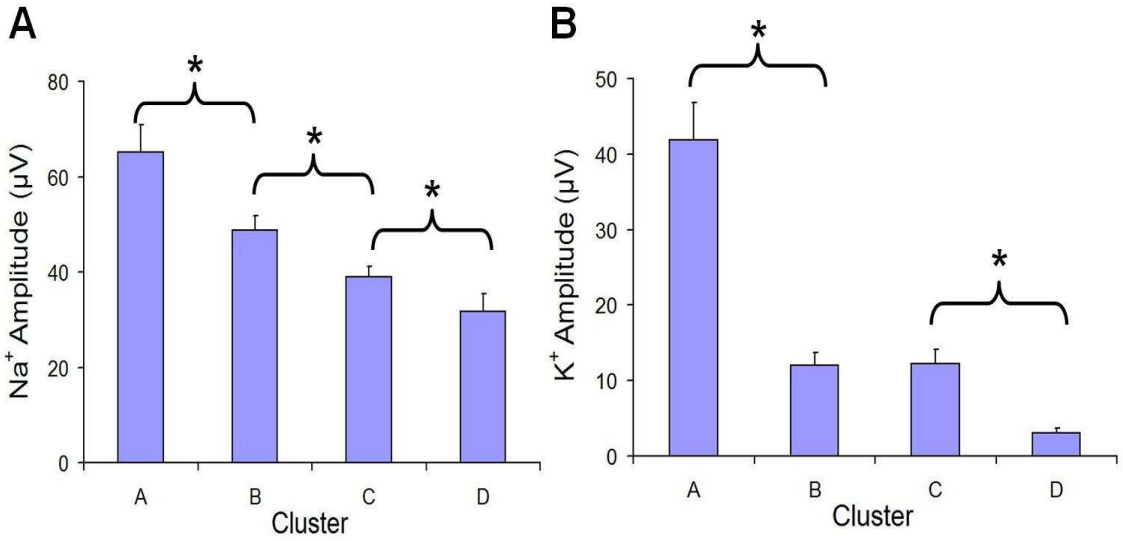

Figure 9: Mean (± SEM) Na^+ peak amplitude in (A) and K^+ peak amplitude in (B) among the 4 clusters of neurons averaged across all 6 rats.

Cluster A

The first cluster includes Type A and Type C units in Table 1 and Table 2 that together constitute 9.3% of total neurons in the DS and 19.5% of total neurons in the Cx. Typical spike waveforms of these 2 types of neurons (Type A and C) in Cluster A are presented in Figure 10. In general, neurons in this Cluster have high Na^+ peak amplitude (mean is 65 μV) and high K^+ peak amplitude (mean is 42 μV) in their spike waveforms. These extracellular recording features relatively correspond to a high peak of an action potential and a deep after-hyperpolarization (AHP).

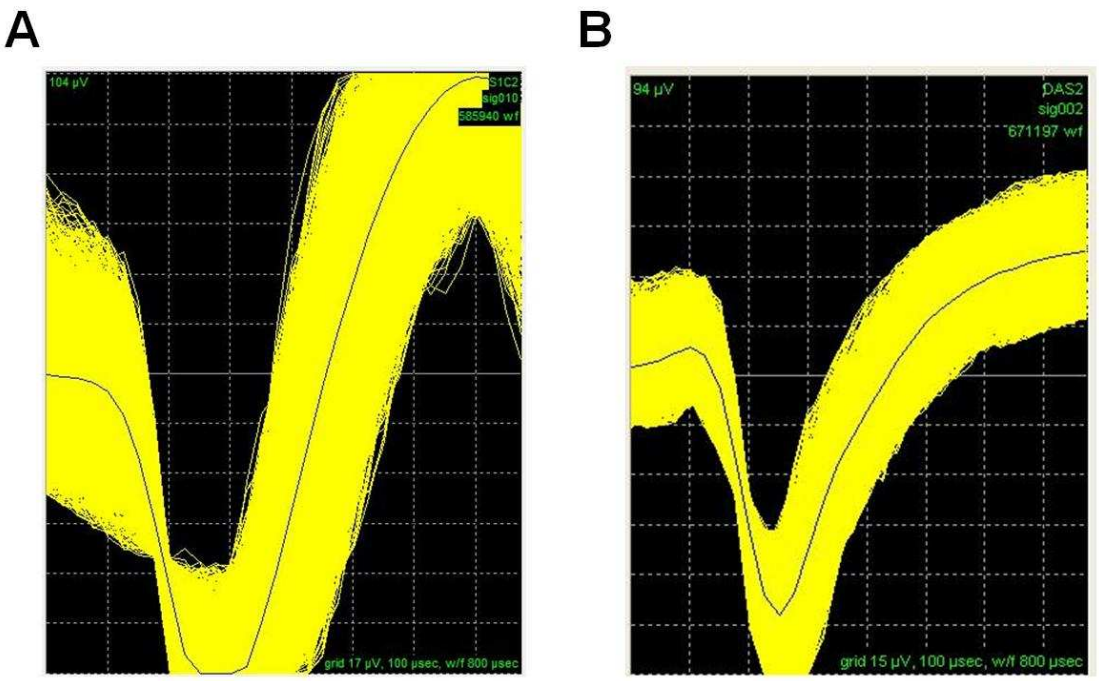

Figure 10: Typical waveforms of neurons in Cluster A. (A) represents the waveforms of neurons in Type A, while (B) represents the waveforms of neurons in Type C. The vertical scale is 17 μV in (A) and 15 μV in (B) per grid and the horizontal scale is 100 μs per grid.

Cluster B

Neurons in this cluster include Type M and Type N that represent 14.9% of total neurons in the DS and only 3.6% of total neurons in the Cx. Spike waveforms of these 2 types of neurons in Cluster B are illustrated in Figure 11. As shown in the figure, neurons in this cluster usually have intermediate Na^+ peak amplitude (mean is 49 μV) and low K^+ peak amplitude (mean is 12 μV) in their spike waveforms.

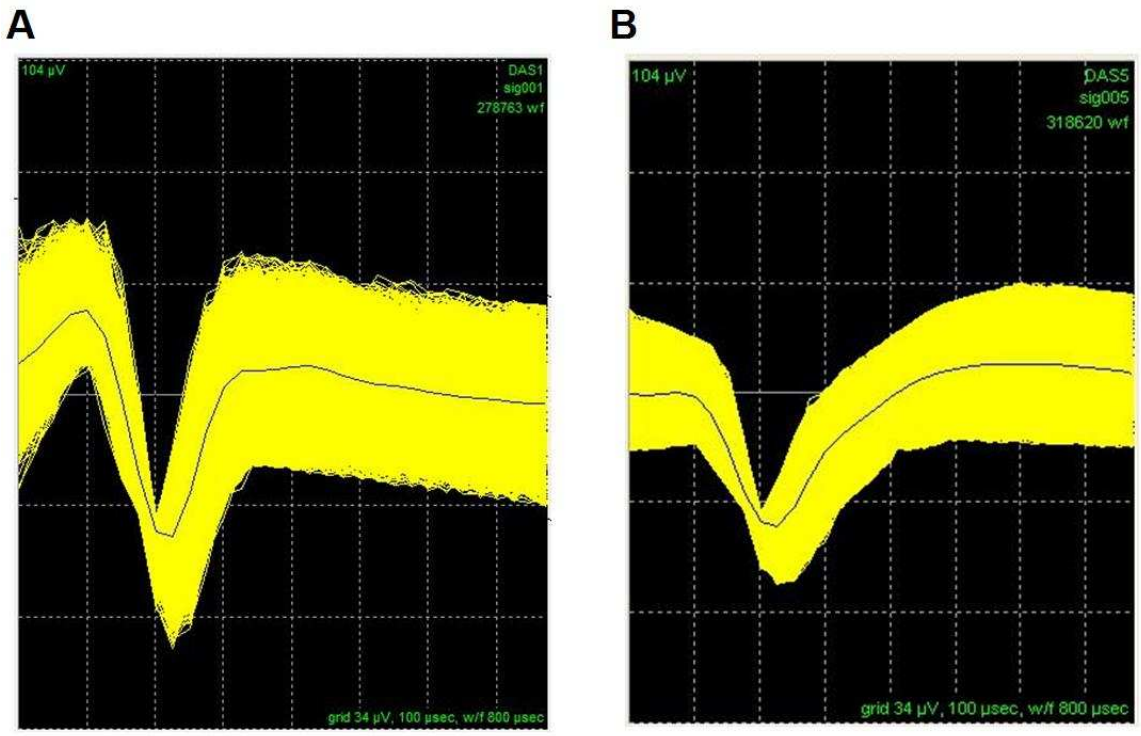

Figure 11: Typical waveforms of neurons in Type M (A) and neurons in Type N (B) in Cluster B. The vertical scale is 34 μV per grid and the horizontal scale is 100 μs per grid.

Cluster C

The third cluster includes Type P, Q, R, and S neurons that represent 56.6% of total neurons in the DS and 48.1% in the Cx. Because this cluster represents almost half of the total neurons, they can be observed easily in almost

every electrode during the recording session. Typical spike waveforms of these 4 types of neurons are shown in Figure 12. As can been seen, neurons in this cluster usually have intermediate Na^+ peak amplitude (mean is 39 μV) and low K^+ peak amplitude (mean is 12 μV) in their spike waveforms.

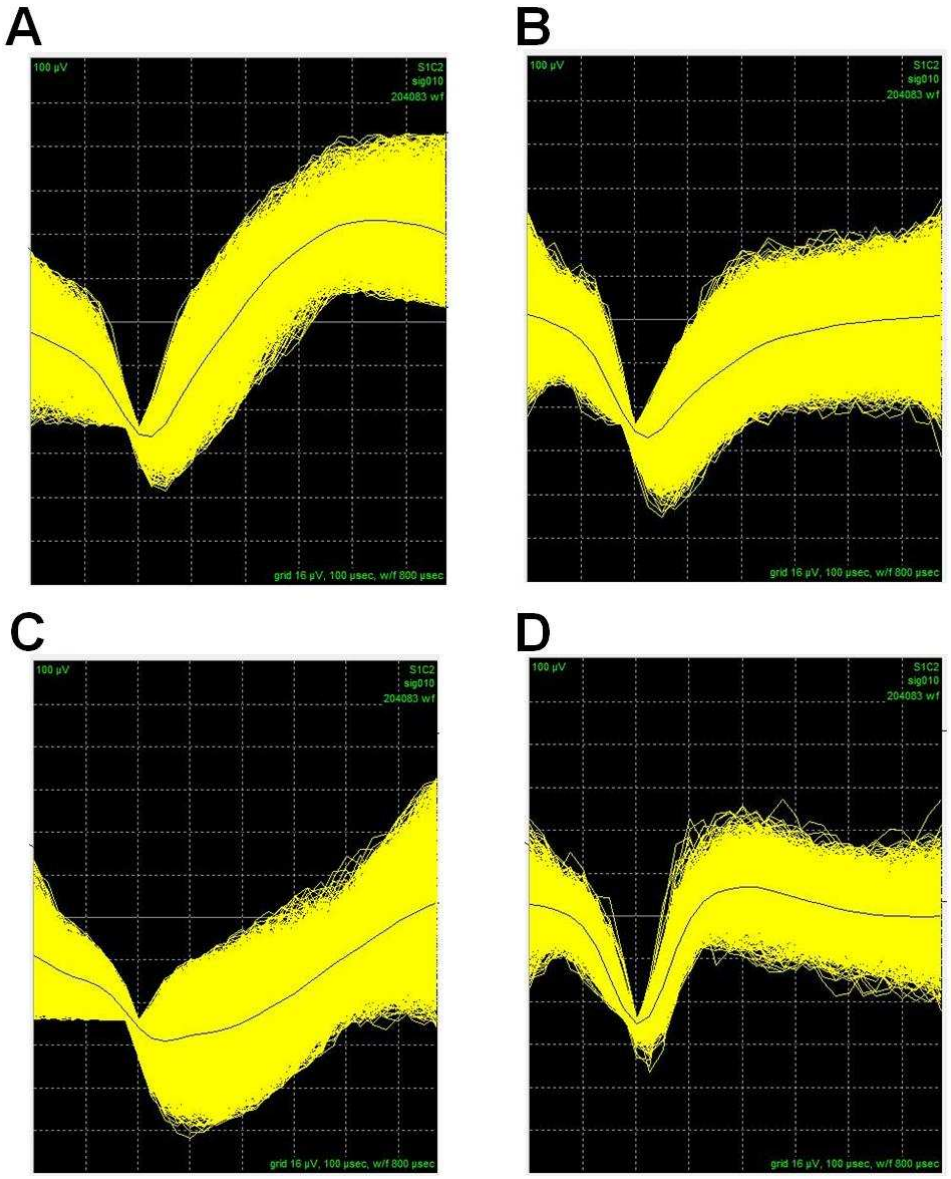

Figure 12: Typical waveforms of neurons in Type P (A), Type Q (B), Type R (C), and Type S (D) in Cluster C. The vertical scale is 16 μV per grid and the horizontal scale is 100 μs per grid.

Cluster D

In this cluster (Type W), there were 20 neurons observed in the Cx (12.2%), while only 2 neurons were observed in the DS (1.2%). Typical spike waveforms of neurons in Type W are illustrated in Figure 13. As shown, neurons in this cluster have the lowest Na^+ peak amplitude (mean is 32 μV) and the lowest K^+ peak amplitude (mean is 3 μV) in their spike waveforms.

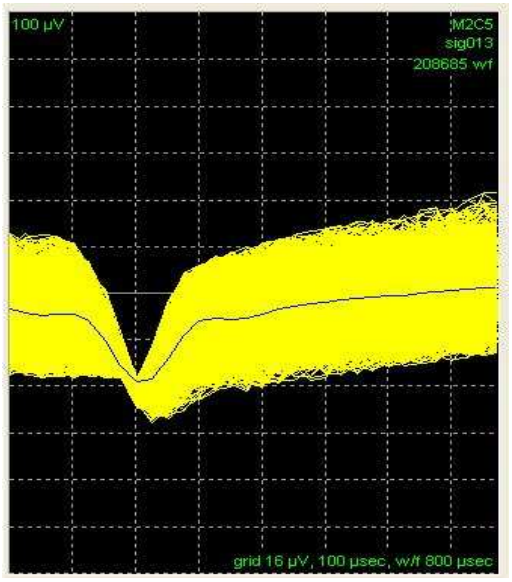

Figure 13: Typical waveforms of neurons in Type W in Cluster D. The vertical scale is 16 μV per grid and the horizontal scale is 100 μs per grid.

Behavioral Correlates of Each Unit Clusters

One major goal of the current experiment is to identify the behavioral correlates of all the neurons that we now have classified into 4 different clusters.

Indeed, they seemed to correlate with different behavioral components in the PI procedure that are summarized below.

Objective Measures of Behavioral Correlates

To determine if a neuron is responding to specific behavioral events (e.g., timing the target durations or receiving the food pellets), the neuron's firing rate during specific time of interest (TOI) was calculated and compared with its own baseline firing rate. The baseline firing rate is determined by averaging the firing rate during the entire probe trials (i.e., 0 to 30 s in 12-s probe trials and 0 s to 90 s in 36-s probe trials). The TOI for determining a timing-related neuron is set at the range from 6 to 18 s in 12-s probe trials and from 18 to 54 s in 36-s probe trials. Thus, a timing neuron is defined as having firing rate in any of the 2 TOI that is 10% higher or lower than its own baseline firing rate (Figure 14A and 14B).

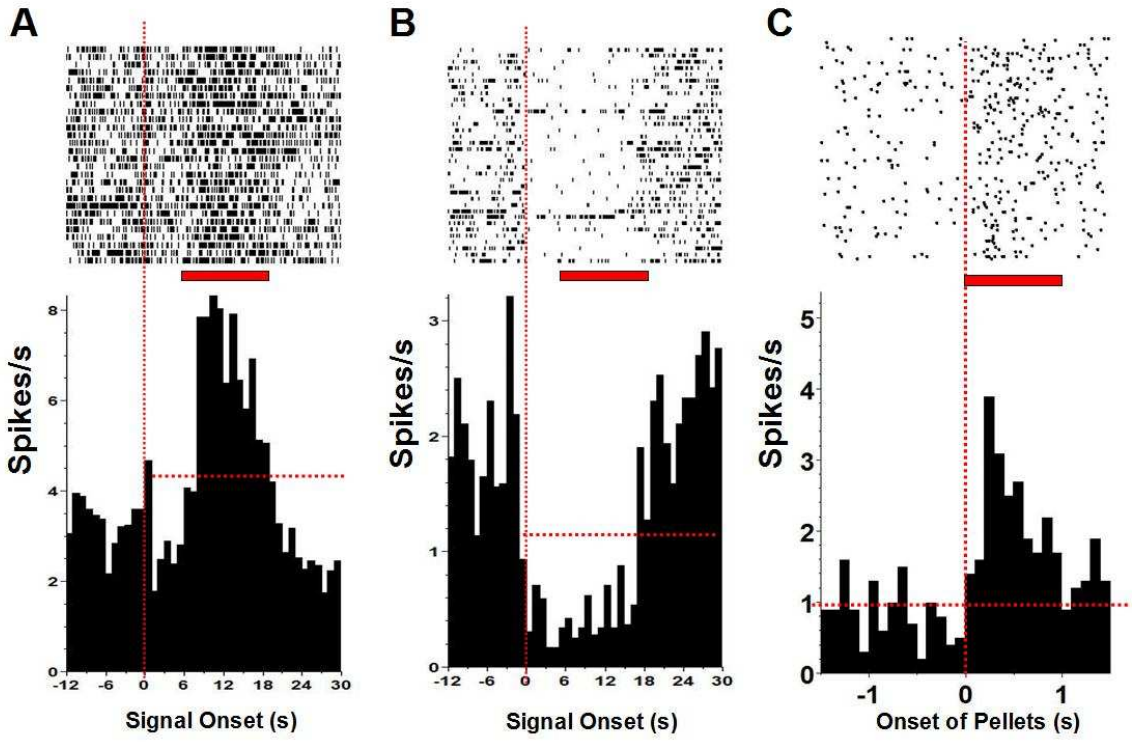

Figure 14: Peri-event time histograms and raster plots of 2 timing neurons and 1 reward neuron. In (A), this timing neuron has a 4.4 spikes/s baseline firing rate (the horizontal dashed line) while having a 6.6 spikes/s firing rate in the TOI (the horizontal bar). In (B), this timing neuron has a 1.2 spikes/s baseline firing rate with a 0.6 spikes/s firing rate in the TOI. In (C), this reward neuron has a 1.0 spikes/s baseline firing rate with a 2.3 spikes/s firing rate in the TOI.

The TOI for determining a reward-related neuron is set at the range from 0 to 1 s right after the delivery of food pellets by averaging the firing rate following 12-s pellets, 36-s pellets, and free pellets. Thus, a reward-related neuron is defined as having firing rate in the TOI region that is at least 50% higher than its own baseline firing rate (Figure 14C).

By applying the above objective measures to all neurons in 4 clusters, we observed that neurons in Clusters A and B appeared to be more correlated with the temporal dimensions than the reward dimensions in the PI procedure, while neurons in Clusters C and D were related to both reward processing and temporal processing, but in general both were more related to reward processing

(as summarized in Table 3). Another interesting observation is that the timing neurons in Clusters A and B had a greater percentage in showing an inhibitory firing pattern during TOI than the neurons in Clusters C and D.

Table 3: Distribution of timing-related and reward-related neurons in each of the 4 clusters. The excitatory timing neuron is defined as having 10% higher firing rate during TOI, while the inhibitory timing neuron is defined as having 10% lower firing rate during TOI.

	Cluster A 44 neurons	Cluster B 31 neurons	Cluster C 147 neurons	Cluster D 22 neurons
Timing-Related	59.1% 26 neurons	61.3% 19 neurons	68.7% 101 neurons	72.7% 16 neurons
Excitatory	38.5% 10 neurons	36.8% 7 neurons	86.2% 87 neurons	93.8% 15 neurons
Inhibitory	61.5% 16 neurons	63.2% 12 neurons	13.8% 14 neurons	6.2% 1 neuron
Reward-Related	40.9% 18 neurons	51.6% 16 neurons	81.0% 119 neurons	81.8% 18 neuron

In addition to the behavioral correlates observed above, we also observed quantitative differences among the 4 clusters between the DS and Cx as summarized in Table 4. Statistical analyses confirmed that the percentage of observed neurons in Cluster B in the DS was significantly higher than the percentage of observed neurons in Cluster B in the Cx ($t_{.05\ (6\text{-}1)} = 3.633$, $p < 0.05$). A trend of difference ($p = 0.059$) was observed in the percentage of neurons in Cluster D between the 2 regions. However, we only observed 2 neurons in Cluster D in the DS in a single rat, so the trend can be considered as significant in that the Cx had a significantly higher percentage of neurons in Cluster D compared to the percentage of neurons in Cluster D in the DS.

Table 4: Mean (± SEM) observed neurons in all clusters and the percentage of each cluster between the DS and the Cx.

	DS (n=6)	Cx (n=6)
Mean observed neurons in all 4 clusters	22.5 ± 2.7	23.3 ± 1.1
Percentage (%) of observed neurons in Cluster A	9.6 ± 4.3	23.1 ± 5.1
Percentage (%) of observed neurons in Cluster B	20.7 ± 3.8 *	4.8 ± 1.8
Percentage (%) of observed neurons in Cluster C	66.7 ± 7.3	57.2 ± 4.2
Percentage (%) of observed neurons in Cluster D	3.0 ± 3.0 *	14.9 ± 2.8

*** Indicates a significant difference between the DS and the Cx**

Cortico-Striatal High-Voltage Spindles (HVS)

As mentioned before, striatal HVS (9 -12 Hz) is a uniform LFP oscillatory pattern with synchronous firing of striatal neurons while the rats are in a quiet and immobile state (Berke et al., 2004). In an earlier study, it was observed that this is a unique phenomenon that only occurs in cortico-striato-thalamo-cortical circuits, not in cortico-hippocampal circuits and cerebellar circuits (Buzsaki, 1991). During the recording sessions, we indeed observed this unique striatal HVS across all the recording channels, especially during ITIs (see one example in Figure 15).

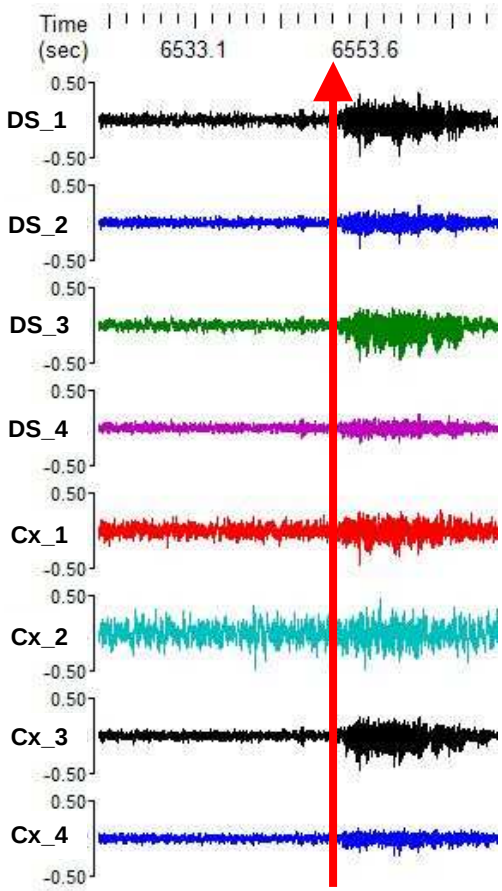

Figure 15: A sample segment of cortico-striatal HVS obtained during one of the baseline training sessions in a rat. Note that all the LFP channels (upper 4 channels in the DS and lower 4 channels in the Cx) displayed this HVS oscillatory patterns after 6549.6 s (the red arrow) simultaneously.

When the power density between the two segments of LFP (before and after the red arrow in Figure 15) was analyzed, it is observed that the observed HVS was composed of strong 9-12 Hz oscillations (above 85% in power density) compared to the non-HVS segment (as shown below in Figure 16). This is consistent with previous studies (Berke et al., 2004; Buszaki, 1991) and also proves that our recording electrodes were indeed in cortico-striatal circuits because this is a signature LFP pattern in this circuit.

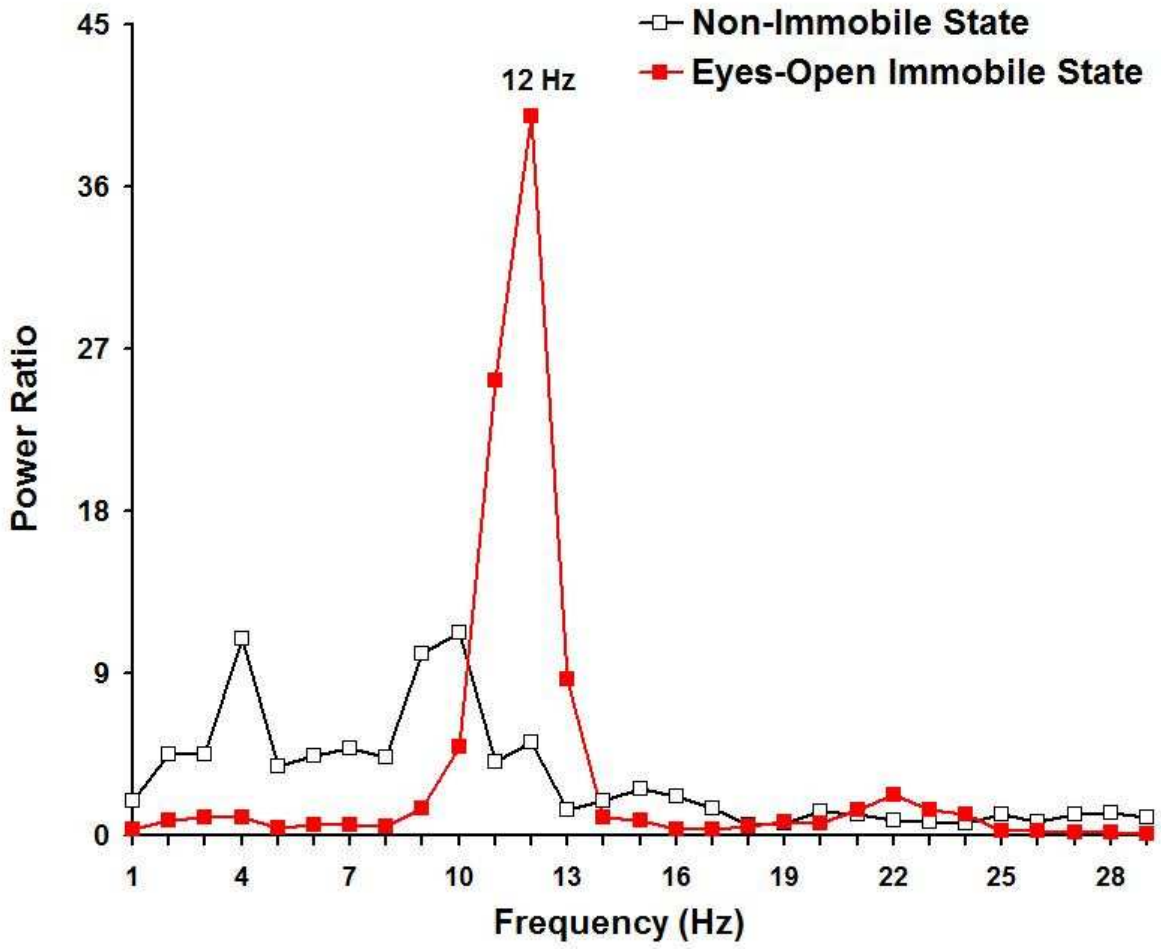

Figure 16: Power density distribution of the observed HVS during eyes-open immobile state (the red function) and the non-HVS during eyes-open non-immobile state (the black function).

Synchrony between Cortico-Striatal HVS and Each Unit Clusters

One hallmark of cortico-striatal HVS is that only FSIs reliably fire in synchrony with HVS, while MSNs do not show such a strong synchronous firing pattern (i.e., MSNs frequently miss the beat). When examining our recording data in a finer time scale, we indeed observed the pattern that some neurons fired in synchrony with HVS, while others did not. A sample segment of unit spike data and LFP data is shown in Figure 17.

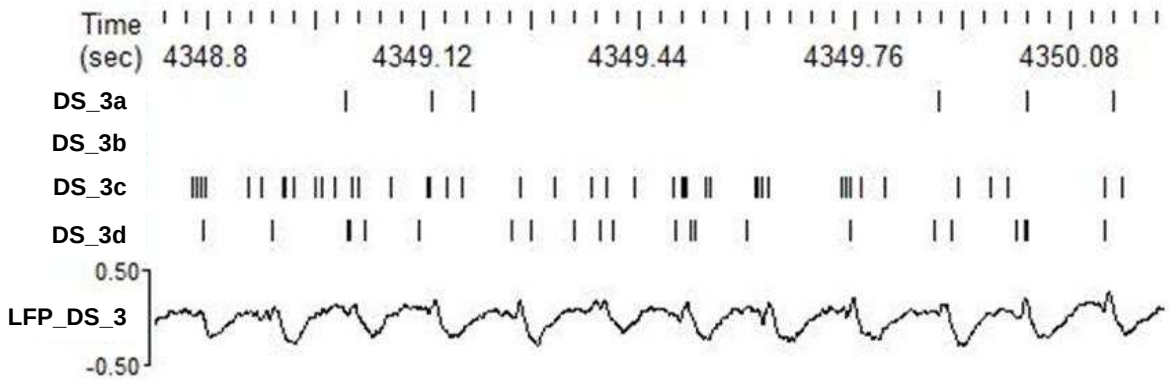

Figure 17: A sample segment (1.2 s) that exemplifies the synchrony between a raw striatal LFP and striatal neurons recorded from the same electrode. Note that neuron DA_3c fired in burst in almost every cycle of HVS, while neuron DA_3a sporadically fired in single spikes in some cycles of HVS.

As such, we can calculate the degree of synchrony between striatal HVS and the neurons that we have classified into the 4 clusters. The calculation is made based on the percentage of a neuron's spikes that co-occurred with the cycles of HVS. For instance, if there were 100 cycles of HVS, and a neuron's spikes co-occurred in 60 cycles out of the 100 cycles, that unit was identified as showing 60% of synchrony with HVS. A higher degree of synchrony suggests that a neuron is more likely to be an FSI than an MSN. The results of synchrony for the neurons in each cluster are summarized in Table 5.

Table 5: Levels of synchrony with HVS of all the units in cortico-striatal circuits. Note that Cluster A is highlighted with a green background color, Cluster B with a blue background color, Cluster C with a yellow background color, and Cluster D with a turquoise background color.

Brain Region			DS
Number of Rats			n=6
Total Observed Units			161
Average Units per Rat			26.8 ± 1.6
Number of Electrodes			8
Type	Count	%	HVS synchrony
A	5	3.1%	15.2%
	10	6.2%	
B	8	5.0%	
	16	9.9%	12.2%
C	27	16.8%	16.8%
	47	29.2%	28.2%
	9	5.6%	
	8	5.0%	
D	2	1.2%	

Brain Region			Cx
Number of Rats			n=6
Total Observed Units			164
Average Units per Rat			27.3 ± 1.6
Number of Electrodes			8
Type	Count	%	HVS synchrony
A	22	13.4%	8.41%
	10	6.1%	6.67%
B	2	1.2%	
	4	2.4%	6.00%
C	33	20.1%	32.58%
	24	14.6%	14.32%
	12	7.3%	66.93%
	10	6.1%	29.24%
D	20	12.2%	3.75%

As shown in Table 5, some neurons in Cluster C showed the strongest degree of synchrony with HVS, while neurons in other 3 clusters did not show such a higher level of synchrony. Consequently, preliminary data analysis suggests that neurons in Cluster C (at least some of them) were more likely to be the FSIs in cortico-striatal circuits, while neurons in other clusters were more likely to be non-FSIs.

2.3 Discussion

In summary, the data from this experiment showed that neurons with distinct waveforms in cortico-striatal circuits have different functional correlates when the rats were performing in the PI procedure. Among the 24 different patterns of waveforms, it was further discovered that they can be grouped into 4 different clusters based on the similarity of their functional correlates. Neurons in Clusters A and B both showed stronger temporal correlates than reward correlates in the PI procedure, although the two clusters have distinct features in their spike waveforms (Figure 9). Neurons in both Clusters C and D appeared to respond to timing and more to reward processing in the PI procedure. Therefore, we conclude that neurons in the 4 clusters (up to 80% of total observed neurons) had similar functional correlates in the PI procedure (either temporal or reward dimensions, or both) in both the DS and the Cx. This observation is consistent with previous studies (e.g., Matell et al., 2003b) and provides additional support for the proposal that interval timing is subserved by the functional connections in cortico-striatal circuits.

Another goal of the current experiment was to determine if different subtypes of neurons in cortico-striatal circuits can be identified and if each of the subtypes differentially contributes to interval timing. In order to achieve this goal, we utilized the phenomenon of striatal HVS in the LFP data to help us distinguish different subtypes of striatal neurons. Striatal HVS is a unique LFP pattern in rats when they are in a quiet immobile state with their eyes open. During this “drowsy” state, HVS is only observed in cortico-striato-thalamo-cortical circuits, but not in

cortico-hippocampal circuits and local circuits in the cerebellum according to a previous study (Buzsaki, 1991). The same phenomenon was also confirmed in a different lab (Burke et al., 2004) and was further discovered that different striatal neuronal subtypes (e.g., FSIs vs. MSNs) fire in different levels of synchrony with striatal HVS. Although the exact functions of HVS in cortico-striatal circuits are still unknown, this unique phenomenon was utilized in the current study as a tool. As shown in Table 5, some neurons in Cluster C in both the DS and Cx displayed a higher level of synchrony with HVS, compared to neurons in other three clusters. This suggests that neurons (at least some neurons) in Cluster C were more likely to be the GABA-releasing FSIs in cortico-striatal circuits according to the findings in Berke et al. (2004). All the other neurons should be non-FSIs, such as MSNs, TANs, or LTS interneurons. How to distinguish the neurons of MSNs, TANs, and LTS interneurons will require further experiments.

3. Experiment 2: Ensemble Responding Patterns in the Acquisition of a Temporal Bisection Procedure

3.1 Methods

Subjects

Ten (n=10) male Sprague-Dawley rats were initially used in this experiment when they were about 3 mo of age. Because this experiment was designed to reveal the neural response change while the rats were acquiring the temporal bisection procedure, all the rats received surgery for implanting recording electrodes into the DS (same coordinates and surgical procedures as described in the previous experiment) **before** they started learning the procedure. While they were acquiring the procedure, recording cables were connected to their headstages in every training session. During the process of training, some of the rats were dropped out of the study as their headstage became loose and came off. At the end of the experiment, 5 rats (n=5) still had intact headstage, so all the recording data reported here were taken from these 5 rats.

Training History

Pre-training (Session 1-5)

All rats received 5 sessions of combined magazine and lever training. During these sessions, a food pellet (45 mg) was delivered every 60 s for 60 min, regardless of lever response. In addition, 1 of the side levers was primed until 10 reinforced responses were made on that lever in a fixed-ratio 1 schedule (FR-1), at which point, another side lever was primed for another 10 reinforced response. This procedure repeated until the rats received a total of 60 food pellets. By the end of 5 sessions, all rats typically finished the daily session within 20 min.

Surgery

Surgery took place after all the rats completed the pre-training phase. Please see the General Methods in the Introduction for more details about the surgical procedures. Following at least 1 week of post-surgery recovery, the rats were once again maintained at 85% free-feeding weight by a daily ration of regular rodent diet given shortly after daily training session.

Two-Signal Training (Session 1-20)

During this phase of training, rats were trained to press the left lever following a “short” (4 s) signal, and to press the right lever following a “long” (16 s) signal (counterbalanced between left and right lever across subjects). A pair of 4 s and 16 s anchor durations is commonly used in the temporal bisection procedure (another common pair is 2 s vs. 8 s). If rats pressed the correct lever following a signal, a 45 mg food pellet was immediately delivered. No reinforcement was given following incorrect responses. The house light (170 mA lamp) in the lever box served as the signal in this experiment. The 2 anchor durations (4 s vs. 16 s) were presented with equal probability and in random order. When either lever was pressed, both levers were retracted and a random ITI that ranged from 4 to 32 s with a mean of 16 s was presented. A record was kept for the number of left and right responses following each of the 2 anchor durations. Sessions lasted approximately 2 h long with sufficient time allowed to complete the current trial in progress. Throughout this stage of training, all rats were connected to the recording cables and being recorded in every session. Behavioral and electrophysiological recording data from 3 separate sessions

were selected to represent Early in training (Session 1), Intermediate in training (Session 7), and Late in training (Session 20).

Two-Signal Training with Long Probe Trials (Session 21-30)

In this phase of training, all the trial conditions were identical to the ones in the previous phase, except that about one-third of the trials were non-reinforced probe trials that last for 32 s long and followed by the delivery of a “free” pellet without any behavioral requirement. The purpose of this design was to see how the rats and the neurons would respond during these unexpected probe trials. Throughout this stage of training, all rats were connected to the recording cables and being recorded in every session. Behavioral and electrophysiological recording data from the first session in this training phase were further analyzed and presented in the Results.

Seven-Signal Training (Session 31-39)

In this phase of training, the conditions of two-signal training were maintained except (a) each of the 2 anchor durations (4 s vs. 16 s) was presented with a probability of 0.25 on each trial, and (b) on the remaining trials, 1 of 5 intermediate durations (between 4 s and 16 s) was presented, each with equal probability. The intermediate signal durations were 5, 6, 8, 10, and 13 s, a series of integer numbers to better fit with the recording data analysis. Neither the left nor the right response was followed by food in the case of these intermediate signals.

Curve Fitting and Statistical Analysis

The mean percent “long” response was used to construct psychometric functions. A point of subjective equality (PSE) was obtained for individual subjects by calculating the signal duration that was associated with a “long” response 50% of the time from a linear regression analysis. A difference limen (DL) was also obtained by determining the signal duration that was associated with a “long” response 25% of the time and the signal duration that was associated with a “long” response 75% of the time. One half of the difference between these signal durations was defined as the DL, which served as a measure of sensitivity to time. See Meck (1983) for additional details of these psychophysical measures obtained from the temporal bisection procedure. Statistical analysis on the PSE, DL, and percent correct response was conducted by using repeated measures ANOVA or T-test for dependent samples in a commercial software package – STATISTICA (Tulsa, OK), unless specified otherwise. If the main effect of ANOVA reached significance, appropriate post-hoc comparison method (e.g., Fisher least significant different, LSD or unequal N honestly significant difference, HSD) was used to determine the real difference among conditions.

Unit Classification Based on Spike Waveforms

In this experiment, the following 3 waveform features were also measured as we did in the previous experiment – 1) sodium peak amplitude, 2) potassium peak amplitude, and 3) capacitive peak amplitude to help classify neurons into different clusters.

3.2 Results

Behavioral Data

Two-Signal Training

The acquisition of the temporal bisection procedure for the 10 recording rats is shown in Figure 18. In the first training session, the rats' percent correct was at chance level (50%) for classifying the 4 and 16-s anchor durations. In Session 7, the rats' percent correct improved to 80% for classifying the 4-s and 16-s anchor durations (i.e., with only 20% classifying the 16-s anchor duration as "short" and with more than 80% classifying the 16-s anchor duration as "long"). By Session 20, the rats were able to achieve 90% of correct response for classifying the 4-s and 16-s anchor durations, a performance level that was comparable with our previous study (Cheng et al., 2008).

Repeated measures ANOVA confirmed that the percent correct response on the 4-s and 16-s trials during the 3 training phases reached a significant difference ($F_{(2, 14)} = 25.15$, $p < 0.001$ for the 4-s trials and $F_{(2, 14)} = 35.50$, $p < 0.001$ for the 16-s anchor trials). Post-hoc comparisons revealed that the performance on both anchor trials during the Early phase was significantly lower than the other two training phases ($p < 0.001$ in both Intermediate and Late phases), while the last two training phases did not differ from each other. This suggests that rats could acquire the discrimination between the two anchor durations (4 s and 16 s) after 7 sessions of training.

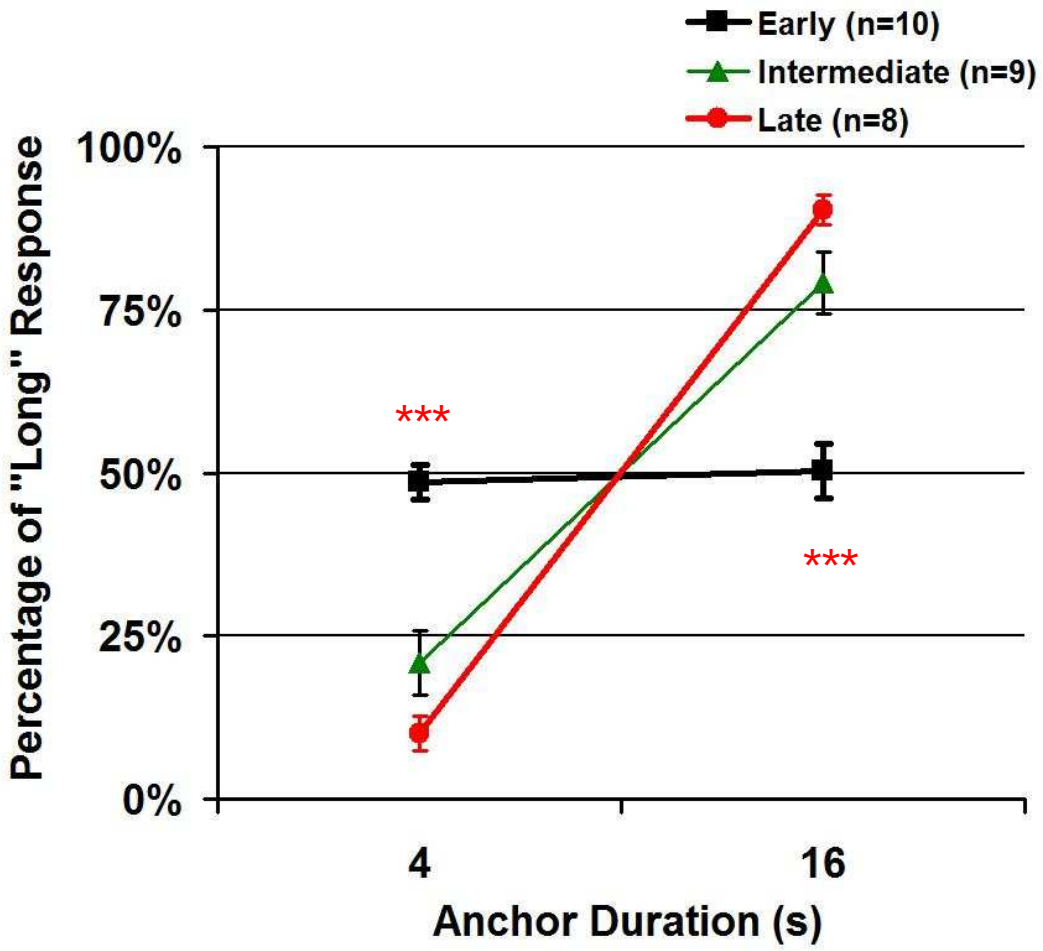

Figure 18: Mean (± SEM) percentage of "long" response plotted as a function of the anchor durations during the 3 learning phases – Early (Session 1), Intermediate (Session 7), and Late (Session 20). Note the poor performance (chance level) during the first session. ***$P < 0.001$

Two-Signal Training with Long Probe Trials

The effects of introducing 32-s probe trials to the rat's performance on anchor durations are plotted in Figure 19. As can be seen, the 32-s probe trials literally had no effect on their performance. Hence, no disruption of discrimination was observed even in the very first session when the 32-s probe trial was introduced. This finding was supported by statistical analyses showing that the percent correct response on both 4-s and 16-s anchor trials during Session 20 and Session 21 was no different ($p > 0.1$).

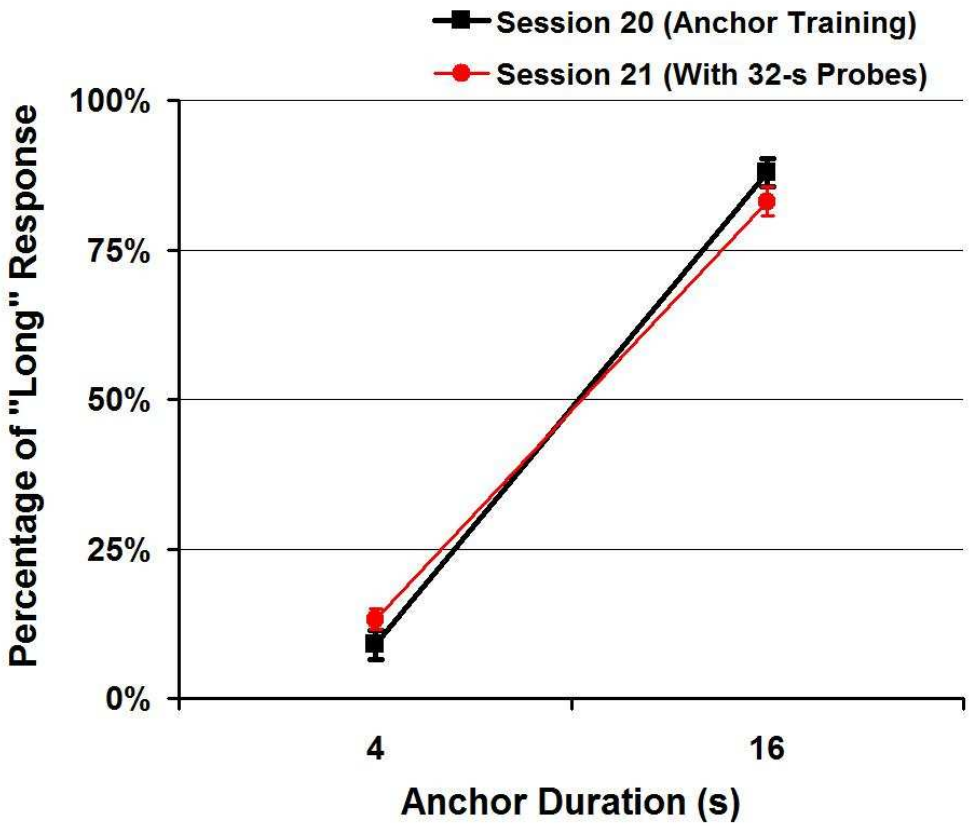

Figure 19: Mean (± SEM, n=6) percentage of "long" response plotted as a function of the anchor durations in comparison between the last anchor training session (Session 20) and the first session with 32-s probes (Session 21).

Seven-Signal Training

Finally, the performance during the session when the 5 intermediate signal durations were first introduced (Session 31) and after 9 sessions of training in the same condition is illustrated in Figure 20. As shown, the introduction of 5 intermediate signal durations had no effects on the discrimination of the 2 anchor durations (two red arrows in Figure 20).

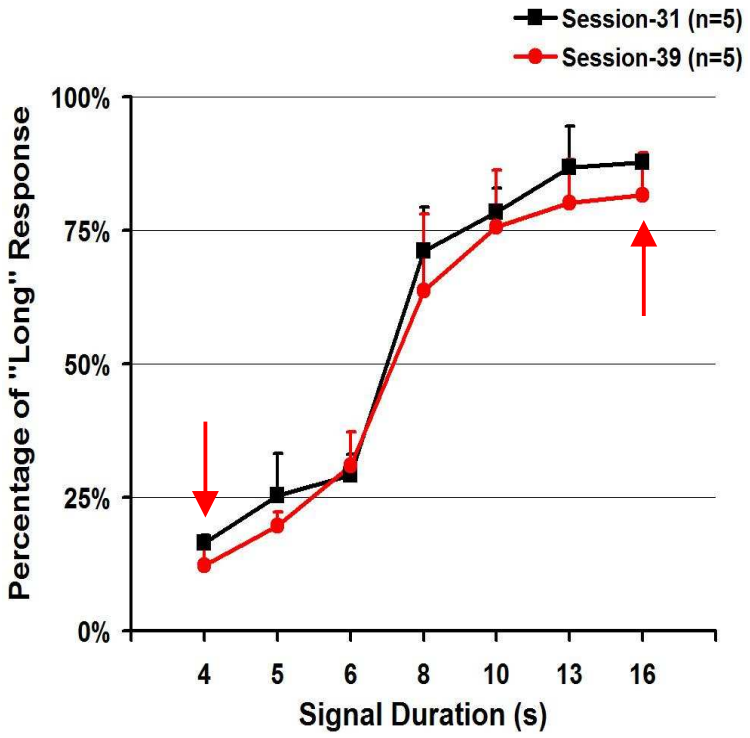

Figure 20: Mean (± SEM) percentage of "long" response plotted as a function of the signal durations in comparison between the first and the last training session (Session 31 vs. 39).

Statistical analyses indeed showed that the percent correct response on both 4-s and 16-s anchor trials during Session 31 and Session 39 were no different ($p > 0.1$). The data of PSE (indicates temporal accuracy) and DL (indicates temporal precision) from Session 31 and Session 39 are summarized in Table 6. There were no significant differences between the two sessions on PSE or DL ($p > 0.1$). Therefore, the statistical results confirmed that the addition of 5 intermediate signal durations had no effects on the discrimination of the 2 anchor durations.

Table 6: Temporal bisection timing measures

	PSE (s)	DL (s)
Session 31	7.31 ± 0.52	4.46 ± 0.86
Session 39	7.16 ± 0.46	3.62 ± 1.24

Numbers = mean (± SEM); PSE = point of subjective equality; DL=difference limen.

Recording Data

In the previous experiment, 4 different clusters of neurons were classified based on their distinct waveform features (i.e., Na^+ and K^+ peak amplitude). The same method was applied in the current experiment to analyze the electrophysiological recording data such that we can directly compare the data between two different sets of experiments and between two different groups of rats. The results of observed neurons in the DS in each of the 24 types from the first 2-signal training session are summarized in Table 7.

As can been seen in Table 7, the total observed neurons (112) in the DS were also distributed into 3 of the 4 major clusters (Clusters A, B and C) that were classified in Experiment 1. Specifically, we observed 23 neurons (20.6%) in Cluster A, 18 neurons (16.1%) in Cluster B, 23 neurons (20.6%) in Cluster C, and 1 neuron (0.9%) in Cluster D. The percentage of Cluster D was also low (1.2% in Table 1) in the same brain region (DS) in Experiment 1. A new cluster (Cluster E) of neurons was noticed in Table 7 that includes the neurons in Type J, K, and L. We observed 20 neurons (17.9%) in this new cluster that we did not observe as a major cluster in Experiment 1 (only 1.8% in the DS and the Cx). Therefore, it will be important to examine the waveforms of the neurons in this new cluster and their functional correlates in the current experiment.

Table 7: Distribution of all the units obtained from the DS during the first 2-signal training session. Please note that each rat has 8 recording electrodes in the DS. A new cluster (Cluster E) was also identified.

Brain Region			DS
Number of Rats			n=5
Total Observed Units			112
Average Units per Rat			22.4 ± 1.3
Number of Electrodes			8
Type	Count	%	(spikes/s)
A	6	5.4%	1.112
B	2	1.8%	4.471
C	17	15.2%	1.934
D	5	4.5%	2.713
E	0	0.0%	N/A
F	2	1.8%	3.158
G	0	0.0%	N/A
H	0	0.0%	N/A
I	5	4.5%	3.635
J	7	6.3%	4.328
K	8	7.1%	11.602
L	5	4.5%	20.663
M	12	10.7%	5.121
N	6	5.4%	2.867
O	3	2.7%	1.976
P	13	11.6%	1.279
Q	4	3.6%	0.875
R	0	0.0%	N/A
S	6	5.4%	3.619
T	0	0.0%	N/A
U	1	0.9%	0.632
V	9	8.0%	0.708
W	1	0.9%	0.478
X	0	0.0%	N/A
	0	0.0%	N/A
	0	0.0%	N/A

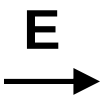

Waveform Features of Neurons in Cluster E

Typical waveforms of the neurons in Cluster E are depicted in Figure 21. As shown, neurons in this cluster displayed high Na^+ peak amplitude (mean is 80 µV and high K^+ peak amplitude (mean is 36 µV) in their waveforms. In addition, we also observed high capacitive peak amplitude (mean is 29 µV). The distinct waveforms of these neurons deserve special attention and it will be important to determine if these neurons have any behavioral correlates in the temporal bisection procedure.

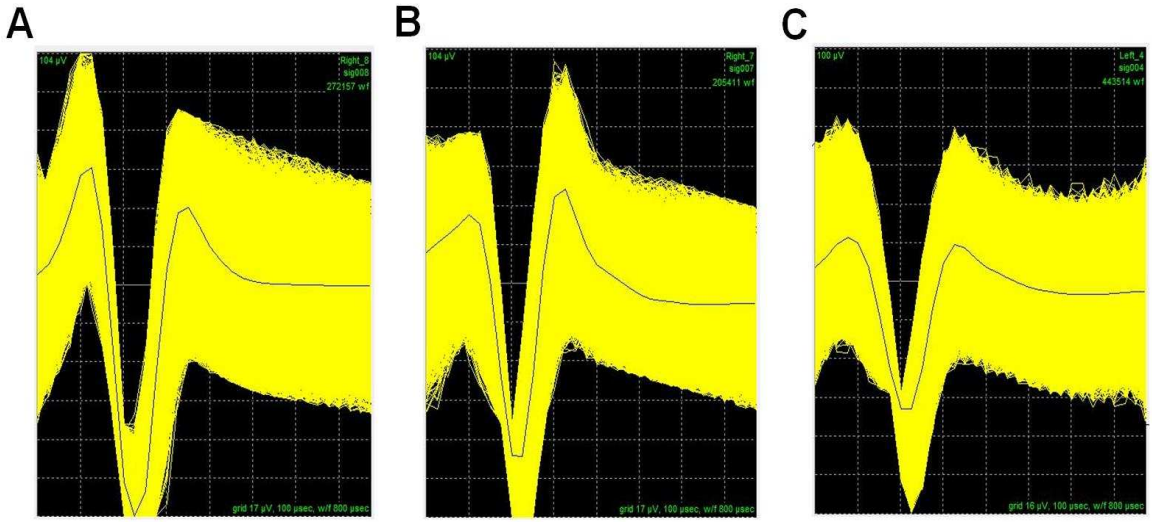

Figure 21: Typical waveforms of neurons in Type J (A), Type K (B), and Type L (C) in Cluster E. The vertical scale is 208 µV and the horizontal scale is 800 µs.

Statistical analyses confirmed that there were significant main effects on the Na^+ peak amplitude ($F_{(3,12)} = 9.4$, $p < 0.01$), the K^+ peak amplitude ($F_{(3,12)} = 20.3$, $p < 0.001$), and the capacitive peak amplitude ($F_{(3,12)} = 23.5$, $p < 0.001$) among the 4 clusters of neurons. Post-hoc comparisons indicated that Clusters A and E had higher Na^+ peak amplitude than Clusters B and C ($p < 0.001$), which did not differ from each other. On the measure of K^+ peak amplitude, both

Clusters A and E had higher K^+ peak amplitude than Clusters B ($p < 0.001$) and C ($p < 0.001$), which did not differ from each other. Finally, on the measure of capacitive peak amplitude, only Cluster E had the highest level of capacitive peak amplitude compared to other clusters ($p < 0.001$). The comparisons from the K^+ peak amplitude and capacitive peak amplitude are depicted in Figure 22.

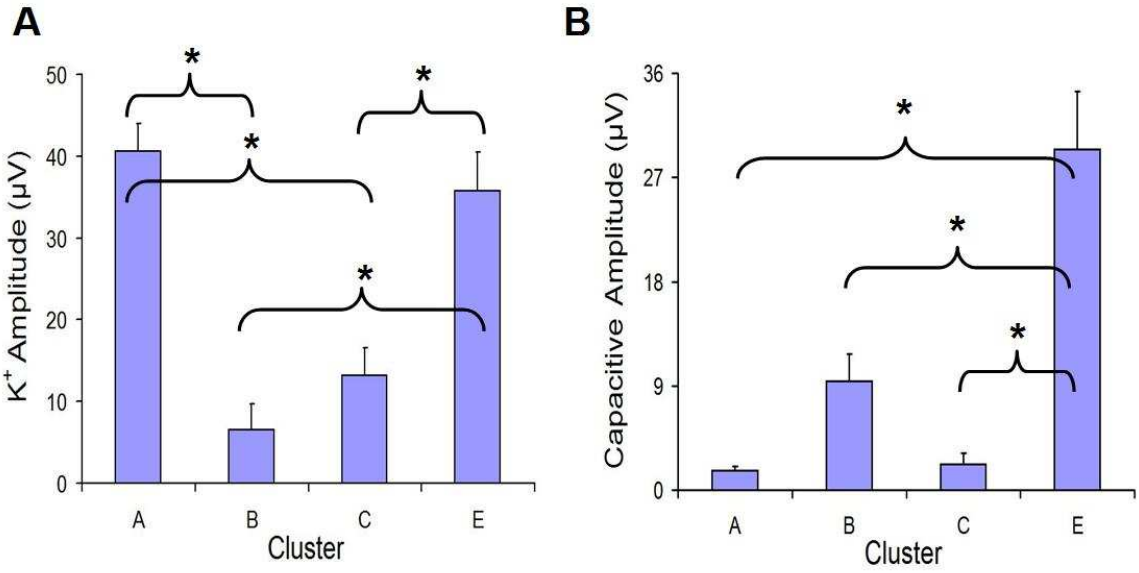

Figure 22: Mean (± SEM) K^+ peak amplitude in (A) and capacitive peak amplitude in (B) among the 4 clusters of neurons averaged across all 5 rats.

Behavioral Correlates of Each Unit Clusters

The change of total observed neurons and the change of percentage in each unit clusters as a function of training are illustrated in Figure 23. The number of neurons in Cluster A and B were pooled together in Figure 23 because according to the data in Experiment 1, both clusters share similar behavioral correlates.

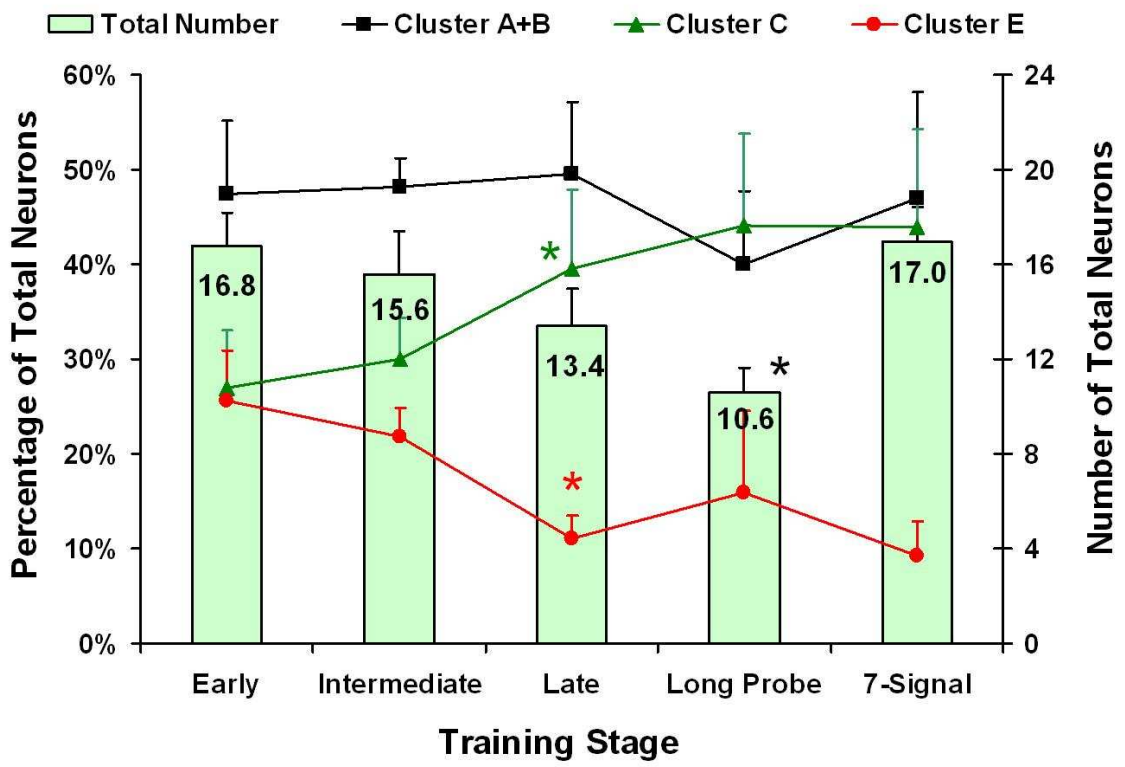

Figure 23: Mean (SEM, n=5) change of total observed neurons (green column) and the percentage of each unit clusters (color lines) as a function of each training stages (Early intermediate, and late in 2-sginal training, 2-signal training with long probe trials, and 7-signal training). The number of total observed neurons here ruled out the neurons that did not belong to Cluster A, B, C, and E.

As shown in Figure 23, Cluster A and B together maintained a similar percentage of total neurons across all training stages (all above 40%). In addition, it was observed that the percentage of neurons in Cluster C showed an increase, while the percentage in Cluster E showed a decrease throughout the training stages. Because the behavioral data demonstrated that the rats acquired the temporal discrimination (4 s vs. 16 s) during the intermediate stage of 2-signal training (Figure 18), and did not improve further (Figure 19 and 20), statistical analyses were conducted on the change of Cluster E and Cluster C as a function of training in the 2-signal training stages (Early, Intermediate, and Late). Two-

way ANOVA (2 cluster types vs. 3 training stages) revealed a significant interaction ($F_{(2, 16)} = 5.78$, $p < 0.05$) between cluster types and training stages. Post-hoc comparisons indicated that the percentage of Cluster E showed the lowest level (11%) in Late anchor training ($p < 0.05$ as denoted by the red star in Figure 23), while the percentage of Cluster C showed the highest level (39.5%) in Late anchor training ($p < 0.05$ as denoted by the green star in Figure 23) compared to Early and Intermediate training stages. When examining the total number of neurons in Figure 23 (green columns) across all 5 training stages, one-way ANOVA indicated that there was a training main effect on the total number of observed neurons ($F_{(4, 16)} = 7.11$, $p < 0.01$). Post-hoc comparisons confirmed that it was the 32-s long probe session that had the lowest number of neurons (10.6) among all other 4 training stages ($p < 0.05$ as denoted by the black star in Figure 23). In conclusion, our observation is that there was a training-dependent change in the percentage of neurons in Cluster C and Cluster E as well a change in the number of total observed neurons as a function of training.

Objective Measures of Behavioral Correlates

Similar to what was done in Experiment 1, a neuron's firing rate during specific TOI was calculated and compared with its own baseline firing rate. The baseline firing rate is determined by the mean firing rate during the 16-s anchor trials. The 3 TOI regions for determining a timing-related neuron is set at the range from 0 to 5 s, from 6 to 10 s, and from 11 to 16 s in 16-s anchor trials.

Thus, a timing neuron is defined as having firing rate in any of the 3 TOI that is 20% higher or lower than its own baseline firing rate (Figure 24).

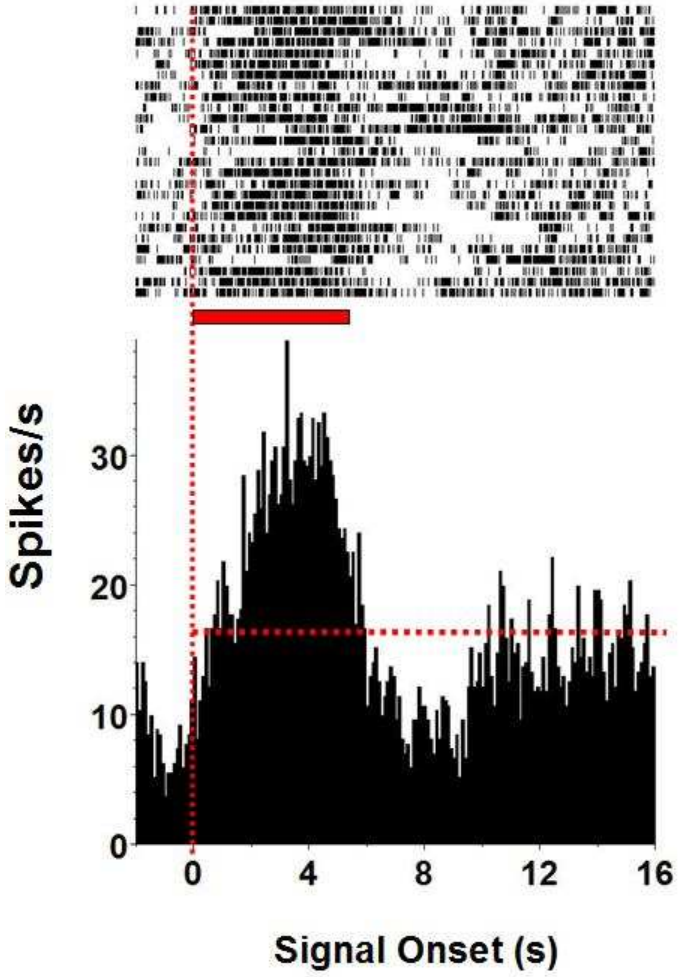

Figure 24: Peri-event time histogram and raster plot of a timing neuron in 16-s anchor trials in the temporal bisection procedure. This timing neuron has a 17.3 spikes/s baseline firing rate (the horizontal dashed line) while having a 24.6 spikes/s firing rate in the first TOI region (during the period from 0 to 5 s as shown by the horizontal bar). This is a 42% increase in firing rate and therefore suggests that this timing neuron is a 4-s specific timing neuron.

The TOI for determining a reward-related neuron is set at the range from 0 to 1 s after the delivery of food pellets by averaging the firing rate following 4-s pellets and 16-s pellets. Thus, a reward-related neuron is defined as having firing rate in the TOI region that is at least 50% higher than its own baseline firing rate.

Behavioral Correlates of Cluster A

In Experiment 1, neurons in Cluster A were more related to the temporal dimensions in the PI procedure. In the current experiment, during the first session of 2-signal training, the rats had poor performance in discriminating the 2 anchor durations (Figure 18). Similarly, it was observed that neurons in Cluster A did not show any correlated firing patterns to any of the 3 TOI regions (as shown in Figure 25A). As the rats received more training, neurons in Cluster A started to show firing patterns that were correlated with the temporal aspects of the task. For example, a neuron can show a decrease in firing rate during the first TOI (Figure 25B and 25C) or an increase in firing rate during the 16-s anchor trials (Figure 25D).

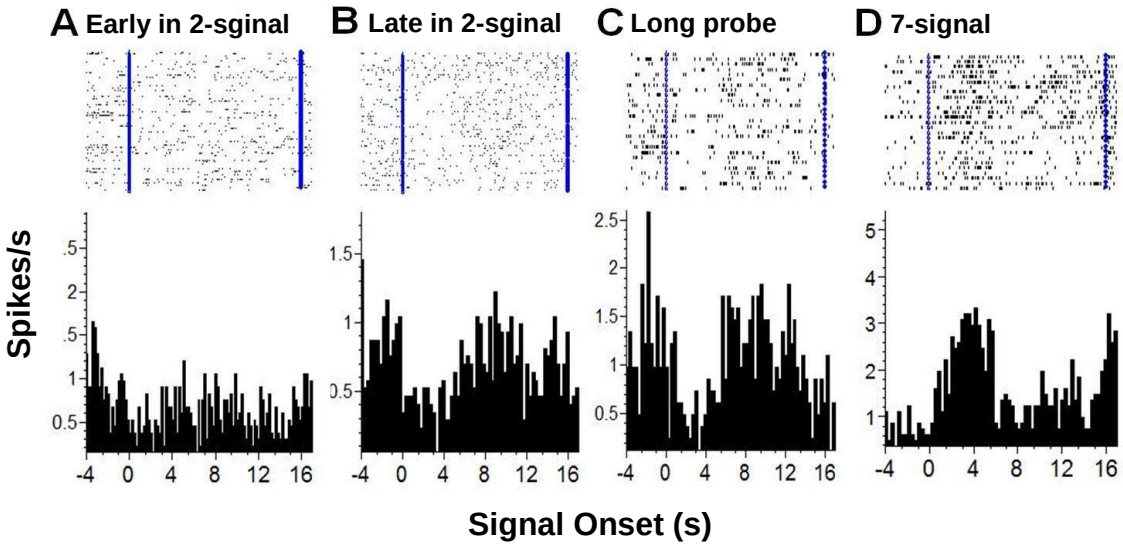

Figure 25: Neurons in Cluster A gradually showed temporal correlates to the task as a function of training - (A) early in the 2-signal training (B) late in the 2-signal training, (C) 2-signal training with long probe trials, and (D) 7-signal training. Bin size is 0.2 s for all figures. The blue dots here represent the signal onset (on the left of the raster plots) and signal offset (on the right of the raster plots) of the 16-s anchor trials. These are 4 different neurons taken from Cluster A.

Behavioral Correlates of Cluster B

In Experiment 1, neurons in Cluster B were also more related to the temporal dimensions in the PI procedure. Here, it was also observed that neurons in Cluster B had similar firing patterns that were more correlated with the temporal dimensions in the temporal bisection procedure, especially after some amount of training (Figure 26). As can be seen, neurons in Cluster B had no clear firing patterns initially during the first session of 2-signal training (Figure 26A). As the rats received more training, neurons in this cluster began to show temporal firing patterns, such as an increase in firing rate when the signal was turned on (Figure 26C). As a result, the amount of training seemed to be correlated with the transition that these neurons started to become sensitive to the timing components in the temporal bisection procedure.

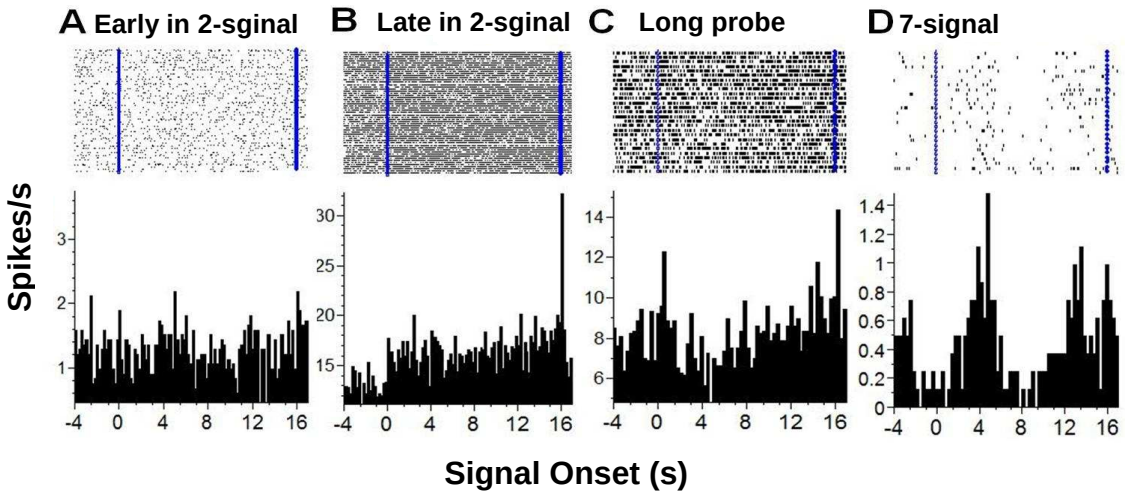

Figure 26: Neurons in Cluster B gradually showed temporal correlates to the task as a function of training - (A) early in the 2-signal training (B) late in the 2-signal training, (C) 2-signal training with long probe trials, and (D) 7-signal training. Figures here are aligned at the signal onset (s) of the 16-s anchor trials. Bin size is 0.2 s for all figures. The blue dots here represent the signal onset (on the left of the raster plots) and signal offset (on the right of the raster plots) of the 16-s anchor trials.

Behavioral Correlates of Cluster C

In Experiment 1, neurons in Cluster C were related to both timing and reward processing in the PI procedure. The same firing patterns were also observed here as shown in Figure 27 from 4 different neurons in 4 different training stages. In Figure 27A, there was no clear firing pattern following the food pellets in the very first 2-signal training session. Once the rats received more training, neurons in this cluster started to show an increase in firing rate to food pellets (Figure 27B, 27C, and 27D) as well as temporal correlates. This suggests that a learning mechanism was involved such that the units in Cluster C gradually responded to the temporal aspects and reward processing of the task as a function of training.

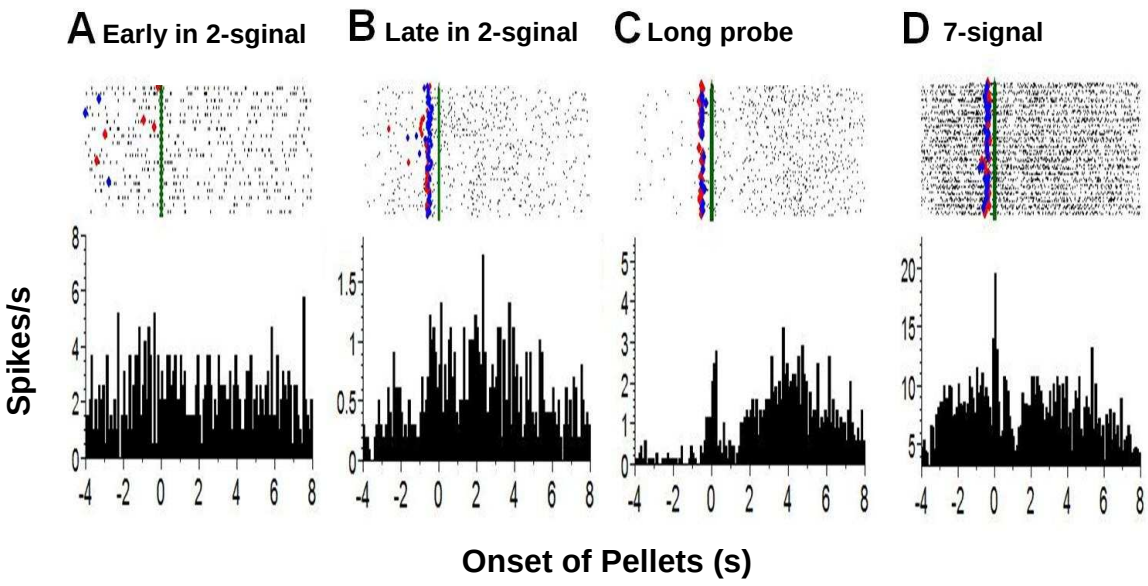

Figure 27: Neurons in Cluster C gradually showed an increase in firing rate following the food pellets as a function of training - (A) early in the 2-signal training (B) late in the 2-signal training, (C) 2-signal training with long probe trials, and (D) 7-signal training. Figures here are all aligned at the delivery of pellets (green dots). Bin size is 0.2 s. The blue dots represent the signal offset of the 16-s anchor trials, while the red dots represent the signal offset of the 4-s anchor trials.

Behavioral Correlates of Cluster E

Cluster E includes neurons in Type J, K and L. These three types of neurons showed a decrease in numbers as a function of training as they became more difficult to be observed during late in training (from 17.9% to 7.8% as shown in Figure 23). As such, it will be important to examine what their behavioral correlates were during early in training. In general, the observation was that most of the neurons in this cluster had no clear behavioral correlates (timing or reward processing) during both early in training (Figure 28) and late in training. However, in between early and late stages of training, a few of these neurons showed firing patterns that were very similar to the ones in Clusters A and B – two clusters that showed temporal correlates after training. Examples of the temporal firing patterns by a neuron in Cluster E are shown in Figure 29.

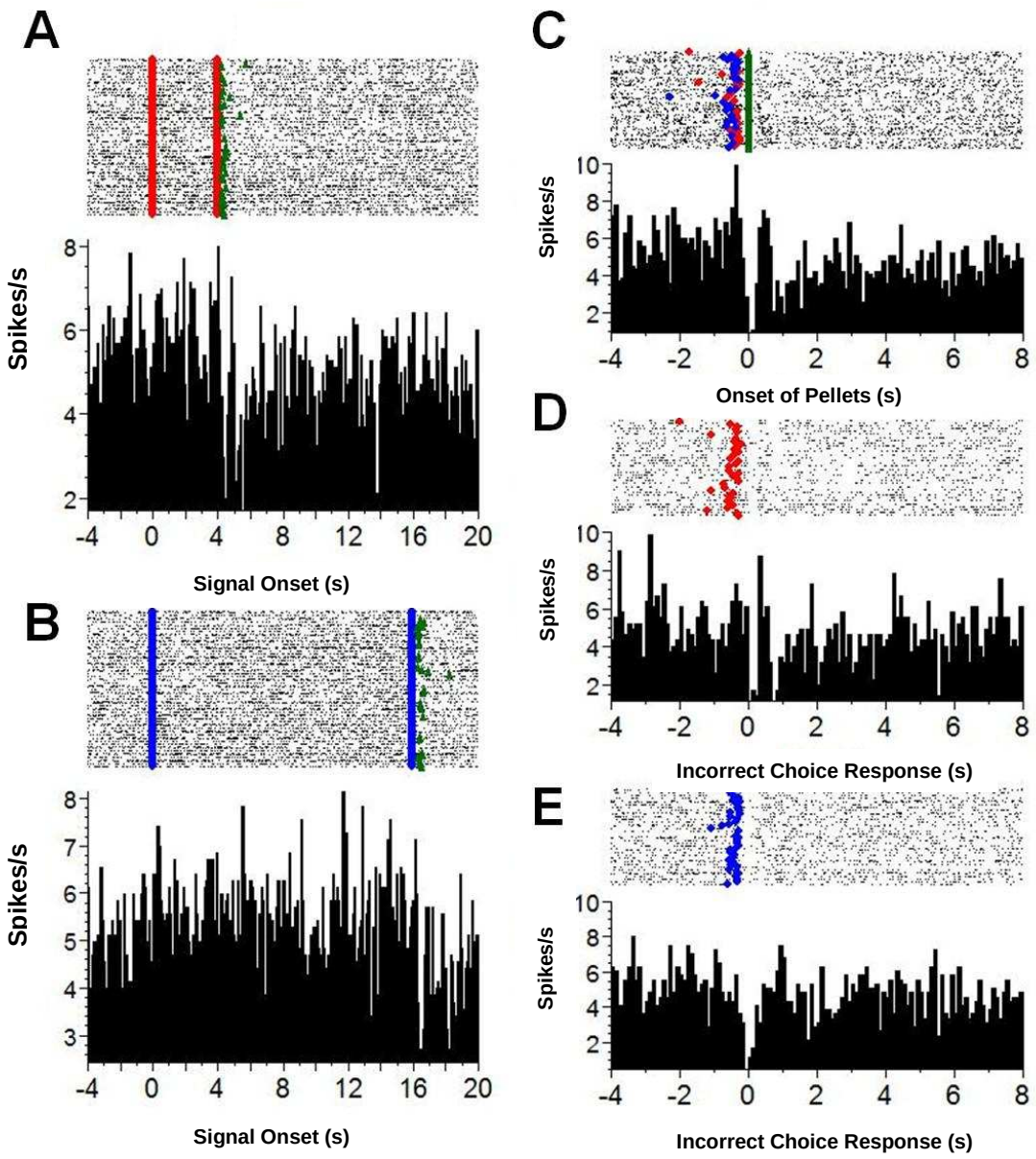

Figure 28: A sample neuron in Cluster E in different conditions from the first 2-signal training session (Early). (A) is aligned at the signal onset (left red dots) of the 4-s anchor trials. (B) is aligned at the signal onset (left blue dots) of the 16-s anchor trials. (C) is aligned at the delivery of pellets (green dots) following correct choice responses. (D) is aligned at the right lever press in the trials that this rat should press the left lever (i.e., incorrect choice response). (E) is aligned at the left lever press in the trials that this rat should press the right lever (i.e., incorrect choice response). Note that there was a transient decrease in firing rate right at the time when this rat made a choice (either correct or incorrect). Bin size is 0.1 s in all figures.

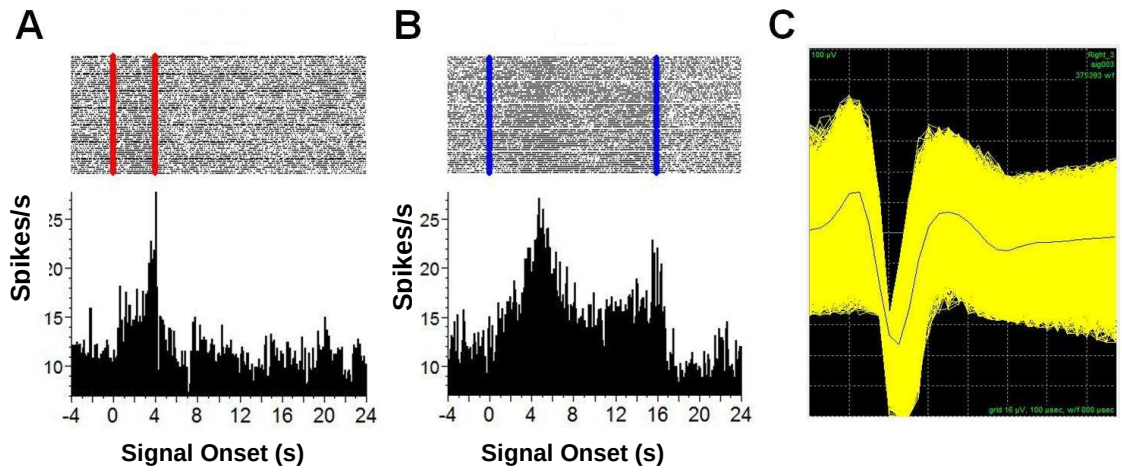

Figure 29: A sample neuron (Type J) taken from the late 2-signal training session (A) is aligned at the signal onset (left red dots) of the 4-s anchor trials. (B) is aligned at the signal onset (left blue dots) of the 16-s anchor trials. (C) represents the waveforms of this neuron. Bin size here is 0.1 s in all figures. In (C), the vertical scale is 200 μV and the horizontal scale is 800 μs.

In conclusion, neurons in Cluster A and Cluster B were both responding to the temporal dimensions in the temporal bisection procedure, same responding patterns that we observed in Experiment 1. Neurons in Cluster C were also responding to the temporal and reward dimensions in the temporal bisection procedure, same as the data in Experiment 1. For the new identified Cluster E, we observed that the percentage of neurons in Cluster E decreased as a function of training (as shown in Figure 23). We also observed that most of the neurons in Cluster E continued to show no behavioral correlates at any point, including the 7-signal training stage. The only two exceptions were 1) these neurons showed a transient decrease in firing rate following choice response during early in training (Figure 28) and 2) some of these neurons started to show behavioral correlates in the late 2-signal training session (Figure 29). Proposals concerning neurons in Cluster E units will be reviewed below.

3.3 Discussion

The data from Experiment 2 support our previous findings showing that neurons in Cluster A and Cluster B responded to the temporal dimensions of the timing task while neurons in Cluster C responded to both the temporal and reward dimensions. This was true even though Experiment 1 and 2 used 2 different timing tasks (PI vs. temporal bisection) requiring different types of responses (e.g., production vs. classification). Despite these procedural differences at the behavioral level, we still observed similar firing patterns among all three clusters of neurons. Hence, the findings from both experiments strongly suggest that the neural firing patterns that we observed were indeed related to temporal processing, but not correlated to any specific behavioral requirement, which are consistent with previous findings (e.g. Matell et al., 2003ab).

Another goal of the current experiment was to determine if the neurons in those clusters showed differential firing patterns as a function of training in rats while they were acquiring the temporal bisection procedure. Indeed, we observed interesting change of neural firing patterns as a function of training in the following two manners. First, from the behavioral data as shown in Figure 18, the rats did acquire the ability to discriminate the 2 anchor durations (4 s vs. 16 s) after 7 sessions of training as their correct response improved to above 80%. During the acquisition of the 2 anchor durations, the average observed neurons per rat decreased from 16.8 (Early) to 13.4 (Late). In the very first session when the 32-s probe trials were introduced (Session 21), the average number of neurons even decreased to 10.6. Taken together, there was a 37% decrease of

observed neurons in the DS (from 16.8 to 10.6 per rat) from early to late in training. Interestingly, after the 5 intermediate durations of probe trials were introduced (i.e., the 7-signal training stage) that presumably increased the variability of trial conditions (i.e., 7 different signal durations) in a given session, the average number of observed neurons per rat increased from 10.6 to 17. Thus, the proposal was made that as rats received more training in the temporal bisection procedure, less striatal neurons were involved in supporting the behavioral performance, unless the variability of the trial conditions was increased. This could be explained by the idea that the neural circuits may become more efficient after training and with less active neurons recruited. Or perhaps there was a location shift in that a different brain area became in charge of supporting the well-trained behaviors (e.g., habit formation; Yin et al, 2009).

The second training-dependent change of neural firing patterns involved the new identified Cluster E that was not observed before in Experiment 1. One reason why Cluster E was not observed in the previous experiment is that the number of neurons in this cluster showed a sustained decrease as a function of training in the current experiment (from 25.5% in Session 1 to 11.0% in Session 20) as shown in Figure 23 (the red function). This may explain why there were only a few of these neurons observed in Experiment 1, in which the rats had received at least 130 training sessions before the recording sessions. In contrast, rats in the current experiment were recorded from beginning with the first training session, so we were able to observe these neurons in Cluster E. This finding leads to important questions about the identity and the functions of the neurons

in Cluster E, such as, what neural subtypes do they belong to and what happened to them during the training process?

According to the waveforms of neurons in Cluster E (as shown in Figure 21), these neurons have short spike durations (within 300 μs), high Na^+ peak amplitude, high K^+ peak amplitude, and high capacitive peak amplitude. This combined waveform features are very different from the features of neurons in other clusters. Hence, the difference in waveforms suggests that neurons in Cluster E belong to a distinct subtype of neurons in the DS compared to the neurons in other clusters. From their behavioral correlates presented in Figure 28, the observation in the first 2-signal training session was that these neurons showed a transient decrease in firing rate when the rats received food pellets as well as when the rats made incorrect responses. That transient decrease of firing rate (a pause) toward salient and significant events (e.g., reward pellet or incorrect response) was the typical firing patterns of TANs that have been observed in the striatum in previous literatures (e.g., a recent review by Apicella, 2007). According to previous reports (Aosaki et al., 1994; Apicella et al., 2009), TANs have a tonic and irregular firing pattern with 2 to 10 spikes/s, which is very similar to our observation in Figures 28. The transient depression in activity is also the signature of TANs in the striatum, compared to phasic firing patterns of projection neurons (e.g., MSNs) and dopaminergic neurons in the same area. Consequently, we infer that neurons in Cluster E were most likely to be the interneuron subtype – TANs in the dorsal striatum.

The last question is what happened to these TANs during the training process? According to our observations reported in Figure 23, the percentage of observed TANs decreased as a function of training. This suggests that these neurons either became less involved in supporting the behavioral performance after training, or they **slightly** changed their waveforms, by some unknown mechanism, such that they became sensitive to certain behavioral correlates in the temporal bisection procedure. Just as an example shown in Figure 29, that neuron (Type J) responded to both 4 s and 16 s signal durations as if it was a neuron from Cluster A or Cluster B. That neuron did not respond to food pellets, so it was not behaving like the neurons in Cluster C. When examining the waveforms of that neuron in Figure 29C, that particular neuron had waveforms that were somewhat in between the waveforms of neurons in Cluster E (Figure 21) and in Cluster B (Figure 11). The slightly changed waveforms of that particular neuron may be the reason why that neuron became sensitive to the temporal processing in the temporal bisection procedure.

4. Experiment 3: Effects of Cortico-Striatal Microstimulation in a Peak-Interval Procedure with Two Criterion Times

4.1 Methods

Subjects

Six (n=6) male Sprague-Dawley rats were used in this experiment when they were approximately 24 mo of age. All the rats were well-trained in the PI procedure with 2 criterion times (the same procedure as described in the previous experiment), **before** implanting electrodes into the dorsal striatum and the sensorimotor cortex (same coordinates and surgical procedures as described in the previous experiment). Following at least 2 weeks of post-surgery recovery, they were once again maintained on a 85% free-feeding weight by a daily ration of regular rodent diet given shortly after training sessions.

Training History

Pre-training (Session 1-5), Fixed-Interval Training (Session 6-15) and PI Training (Session 16-90)

These parts of training were identical with those in Experiment 1.

Post-surgery PI retraining (Session 91-100)

After post-surgery recovery, all the rats received at least 10 retraining sessions to make sure that the surgical procedures did not disrupt their timing performance.

PI Testing with Microstimulation (Session 101-110)

During the testing sessions with microstimulation, the stimulation was delivered only in **half** of the probe trials, randomly determined by the computer program. In those probe trials, stimulation was delivered between the 6th and the

12th second in the 12-s probe trials and between the 18th and the 36th second in the 36-s probe trials. This allows a direct comparison of the stimulation data obtained from the same subject in the same testing session, but just from different probe trials. This design greatly rules out session-to-session variations across different testing days in the same subject.

Stimulation Protocol

In all testing sessions, biphasic rectangular pulses were delivered with a cathodic phase preceding an anodic phase of equal amplitude to all electrodes in a given brain region (DS or Cx). Biphasic stimulation pulses can prevent neuronal damage due to electrode polarization and hydrolysis near the electrode tips. Therefore, in a chronic behavioral study like the current experiment, it is highly recommended to use biphasic stimulation pulses (Tehovnik, 1996). The amplitude of each phase was set at 40 μA (adjusted if needed) that can easily induce observable behavioral effects according to previous pilot studies in the lab and that was also below the estimated amplitude to damage neural tissues (Tehovnik, 1996). Pulse width and pulse delay were kept constant at 0.2 ms. The frequency range was manipulated between 10 Hz to 200 Hz to determine if there is a frequency-dependent effect on interval timing. The temporal arrangement of each pair of stimulation pulses is illustrated in Figure 30.

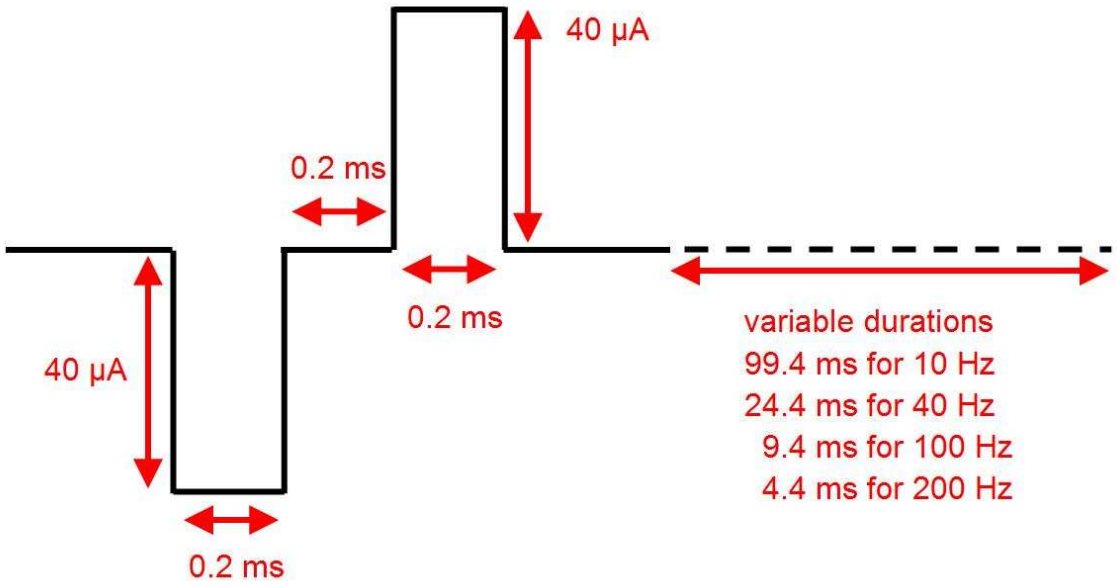

Figure 30: Parameters of the stimulation pulses. Each pair is composed of a cathodic phase preceding an anodic phase with 40 µA in amplitude. The duration of the pulse width and pulse delay were kept constant at 0.2 ms. Hence, a pair of pulses was always 0.6 ms. Each pair of pulses was followed by a variable duration of no pulses, depending on the assigned frequency. For example, trains of stimulation at 100 Hz mean that a pair of pulses was followed by 9.4 ms of no pulses. The computer will repeat this sequence 100 times/s, and thus delivering stimulation at 100 Hz to the target brain region.

Curve Fitting and Statistical Analysis

In the case that fitting the response rate functions was required to determine the peak time, peak rate, and peak spread, the Levenberg-Marquardt algorithm (LMA) was used to optimize the above 3 parameters and to obtain the best fit (square-root minimization) for the timing functions. The following generalized Gaussian + linear model was fit to the individual peak functions:

$$R(t) = a \times \exp\{-.5 \times [(t - to)/b]^2\} + c \times (t - to) + d,$$

where t is the current time bin, and R(t) is the mean number of responses in time bin t. The iterative algorithm provided parameters *a, b, c, d*, and t_0. Parameter t_0

was used as an estimate of the peak time, *a* + *d* was used as an estimate of peak rate, and parameter *b* was used as an estimate of the precision of timing, i.e., peak spread. Statistical analysis was conducted in computer software – STATISTICA (Tulsa, OK) by using repeated measures (ANOVA) or T-test for dependent samples.

4.2 Results

Baseline Performance Before Microstimulation

The baseline performance obtained from the last post-surgery retraining session is shown in Figure 31. As can be seen, rats' timing functions clearly demonstrated that they can center their response curves around the criterion times (12 and 36 s) in a single session.

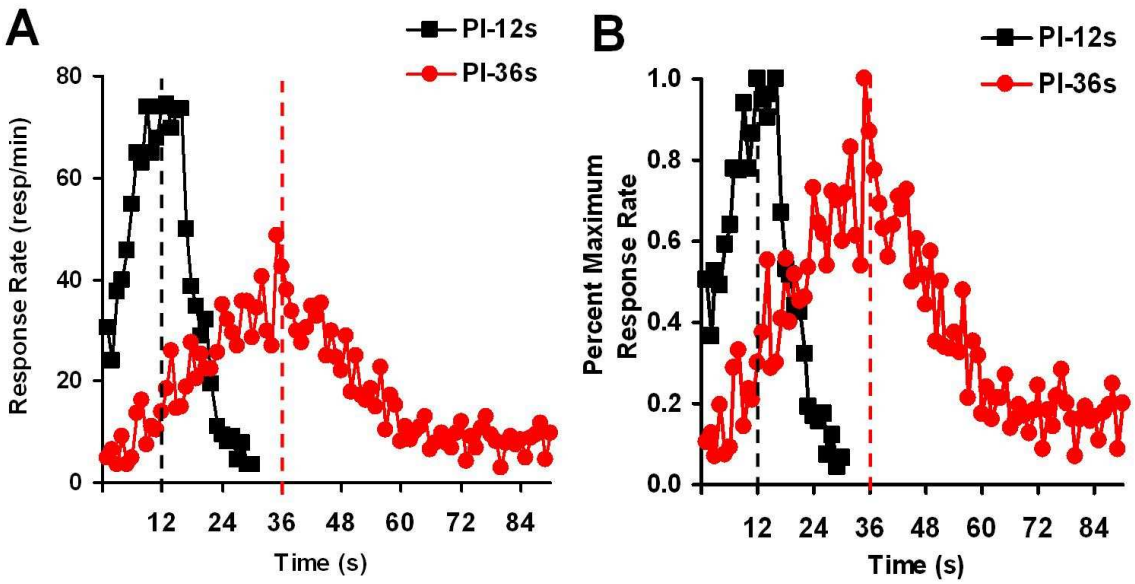

Figure 31: Baseline PI performance for the 12-s and 36-s functions following post-surgery recovery and right before microstimulation. (A) represents the response rate functions, while (B) represents the normalized functions.

Effects of Microstimulation in the Dorsal Striatum

Stimulations with three different frequency ranges (10, 40, and 200 Hz) were delivered into the dorsal striatum in separate sessions. Because the obtained number of stimulated probe trials was small during high-frequency stimulation (40 and 200 Hz), the data from the 2 sessions were pooled together for statistical analysis and plotting functions. The response rate functions under the two stimulation conditions (10 Hz and 40 + 200 Hz) are shown in Figure 32. As can be seen, low-frequency stimulation (10 Hz) had no effects in changing the PI-12s and PI-36-s functions (Figure 32A and 32B), while high-frequency stimulation (combined 40 and 200 Hz) “disrupted” the timing functions in a systematic manner (Figure 32C and 32D). In the 12-s probe trials (Figure 32C), high-frequency stimulation shifted the 12-s function to the right compared to the function obtained in the baseline probe trials. The same shift (although smaller) was also observed in the 36-s probe trials (Figure 32D).

In order to determine what caused the rightward shift in Figure 32C and 32D, peak time, peak rate, and peak spread were determined by using a curve-fitting algorithm (the LMA as described before). The behavioral results are summarized in Table 8 and 9.

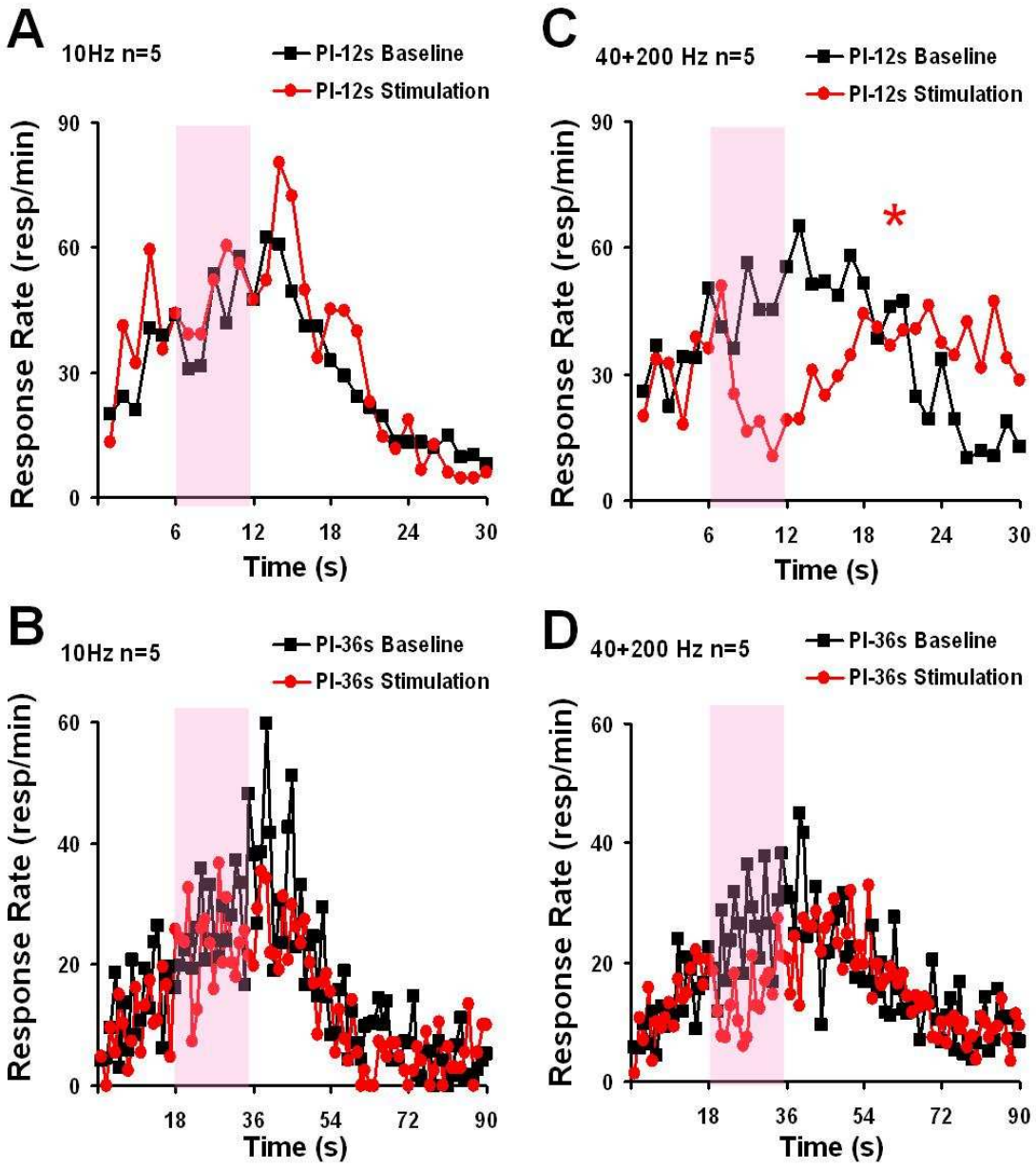

Figure 32: Effects of microstimulation in the DS. (A) represents the PI-12s functions (A) and (B) represents the PI-36s functions from the baseline probe trials (black function) and the probe trials with microstimulation (red function) at 10 Hz. (C) and (D) represent the PI-12s and PI-36s functions from high-frequency stimulation sessions. * *P* < 0.001 in (C) and indicates a significant change in peak time that confirmed a rightward shift of the function with stimulation. The shaded area indicates the period of microstimulation.

Table 8: Peak time, peak rate, and peak spread obtained by using the LMA to fit the response rate functions in the 12-s probe trials with and without stimulation in the DS.

PI-12s	Peak Time (s)	Peak Rate (resp/min)	Peak Spread (s)
10Hz Baseline	13.73 ± 1.31	63.03 ± 9.96	5.62 ± 2.03
10Hz Stimulation	12.51 ± 0.54	64.93 ± 10.11	6.74 ± 0.79
40+200 Hz Baseline	16.89 ± 3.25	58.72 ± 13.26	7.20 ± 1.47
40+200 Hz Stimulation	21.20 ± 3.91	45.79 ± 9.49	9.07 ± 0.99

Numbers = mean (± SEM)

Table 9: Peak time, peak rate, and peak spread obtained by using the LMA to fit the response rate functions in the 36-s probe trials with and without stimulation in the DS.

PI-36s	Peak Time (s)	Peak Rate (resp/min)	Peak Spread (s)
10Hz Baseline	35.89 ± 5.41	43.14 ± 13.82	18.45 ± 6.85
10Hz Stimulation	34.31 ± 4.05	36.14 ± 7.30	9.33 ± 3.42
40+200 Hz Baseline	29.82 ± 3.66	34.38 ± 6.76	17.68 ± 6.32
40+200 Hz Stimulation	40.75 ± 5.48	30.45 ± 6.99	12.16 ± 4.02

Numbers = mean (± SEM)

Statistical analyses were conducted on the measure of peak time in the high-frequency stimulation condition. One of the rats was excluded for all the statistical analyses because it displayed flat response functions during the entire session (i.e., no temporal control of responding). T-test for dependent samples on the comparison of peak time between baseline probe trials and the probe trials with stimulation (40+200 Hz) showed that there was a significant rightward shift on the PI-12s function (from 14 s to 24.9 s, $t_{.05\ (4\text{-}1)} = -3.309$, $p < 0.05$). On the PI-36s function, a trend of rightward shift (from 26.9 s to 42.3 s) was observed ($t_{.05\ (4\text{-}1)} = -2.72$, $p = 0.07$). In summary, the statistical results confirmed that there was a rightward shift on the PI-12s function because the peak time following stimulation was at 24.9 s, a value that suggests a rest response pattern

occurred during stimulation. Following the offset of the stimulation, the rats began timing the signal from the beginning again as if they were timing a new 12-s trial. On the PI-36s functions, however, the result was not strong enough to support a “reset” or “stop” response pattern. A “reset” response pattern predicts that the peak time should be at 72 s, while a stop response pattern predicts that the peak time should be at 54 s. Hence, a peak time at 42.3 s in Figure 32D only suggests a trend ($p = 0.07$) of a partial stop response pattern. On the other hand, low-frequency stimulation did not cause any effects on the timing functions, suggesting that the rats continued to respond during the stimulation. In conclusion, the data support a frequency-dependent “run,” ”stop,” or “reset” response patterns during the microstimulation in the DS.

Examples of “stop” and “reset” response patterns from an individual rat are highlighted in Figure 33. In Figure 33A, the predicted function derived by curve fitting indicates a peak time at 16.3 s for the unstimulated response data as well as a peak time at 24.3 s for the stimulated response data. Given that the peak time is at 24.3 s, we can infer that this rat reset its response pattern, but resumed responding following the stimulation as if a new 12-s trial began. In Figure 33B, the predicted function derived by curve fitting indicates a peak time at 33.6 s for the unstimulated response data as well as a peak time at 48.9 s for the stimulated. Given that the peak time is at 48.9 s, a 12.9 s difference from the 36-s criterion time, we can infer that this rat stopped responding during the stimulation, but was able to continue responding near the end of stimulation, thus showing a peak time at 48.9 s.

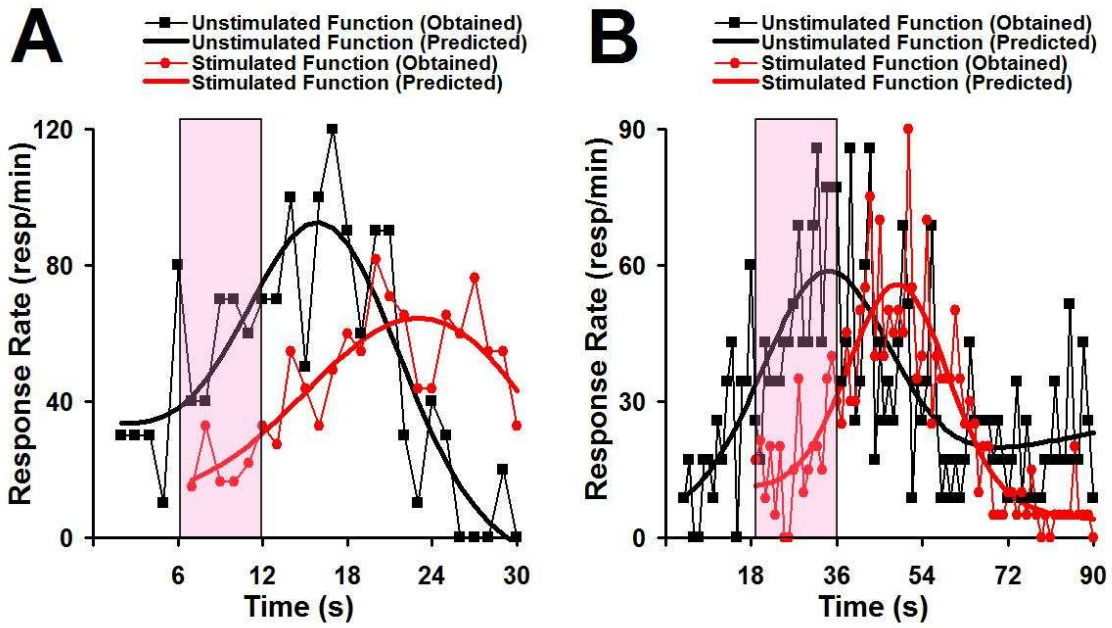

Figure 33: Effects of high-frequency stimulation in the DS on the 12-s functions (A) and 36-s functions (B) from an individual rat. The dots represent the obtained response data from the unstimulated probe trials (black) and the stimulated probe trials (red dots). The smooth lines derived from curve fitting represent the predicted response data from the unstimulated probe trials (the thick black line) and stimulated probe trials (the thick red line). The shaded area indicates the period of microstimulation.

Effects of Microstimulation in the Sensorimotor Cortex

Stimulations with three different frequency ranges (10, 40, and 100 Hz) were delivered into the Cx in separate sessions. The highest frequency range was reduced from 200 Hz in the DS to 100 Hz in the Cx because our pilot data suggest that the cortical areas are more sensitive to electrical stimulation, i.e., a tissue damage might be induced by trains of stimulation at 200 Hz. Also, the data from the two high-frequency stimulation sessions were combined together for statistical analysis and plotting functions. The response rate functions under the two stimulation frequencies (10 Hz and 40 + 100 Hz) are shown in Figure 34.

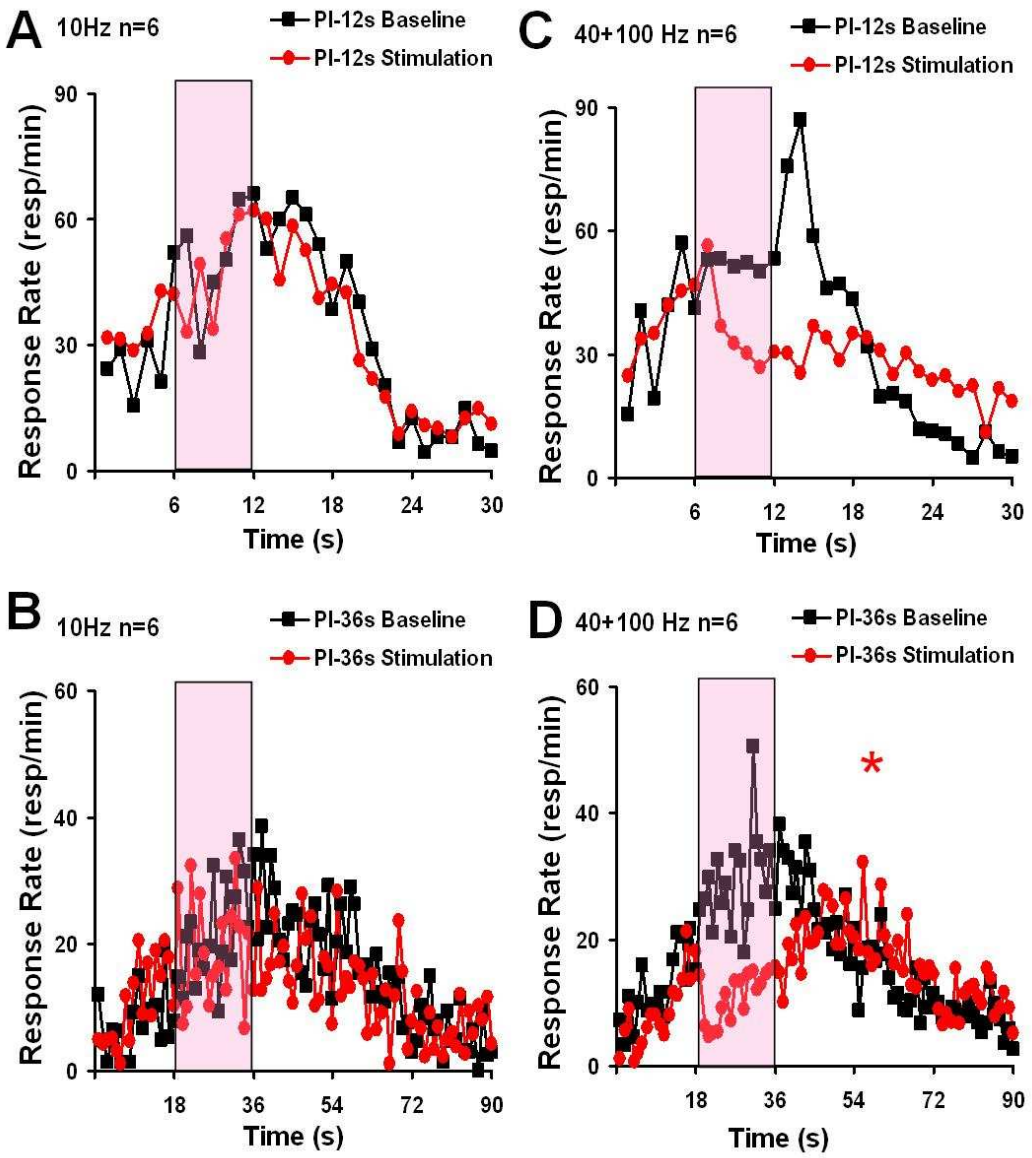

Figure 34: Effects of microstimulation in the Cx. (A) represents the PI-12s functions and (B) represents the PI-36s functions from baseline probe trials (black function) and the probe trials with microstimulation (red function) at 10 Hz. (C) and (D) represent the PI-12s and PI-36s functions from high-frequency stimulation sessions. * *P* < 0.001 in (D) and indicates a significant change in peak time that confirmed a rightward shift of the function with stimulation. The shaded area indicates the period of microstimulation.

As can be seen in Figure 34, low-frequency stimulation had no clear behavioral effects (Figure 34A and 34B), while high-frequency stimulation (40+100 Hz) disrupted the timing functions (Figure 34C and 34D) in a systematic

way. In order to determine what caused the rightward shift of the functions in Figure 34C and 34D, peak time, peak rate, and peak spread were determined by using a curve-fitting algorithm (the LMA as described before). The behavioral results are summarized in Table 10 and 11

Table 10: Peak time, peak rate, and peak spread obtained by using the LMA to fit the response rate functions in the 12-s probe trials with and without stimulation in the Cx.

PI-12s	Peak Time (s)	Peak Rate (resp/min)	Peak Spread (s)
10Hz Baseline	12.25 ± 1.53	69.46 ±15.11	5.44 ± 0.76
10Hz Stimulation	12.81 ± 0.87	64.42 ±14.61	5.07 ± 0.83
40+200 Hz Baseline	11.90 ± 1.28	70.58 ±12.78	7.01 ± 2.06
40+200 Hz Stimulation	9.46 ± 3.49	52.15 ± 8.68	6.52 ± 1.64

Numbers = mean (± SEM)

Table 11: Peak time, peak rate, and peak spread obtained by using the LMA to fit the response rate functions in the 36-s probe trials with and without stimulation in the Cx.

PI-36s	Peak Time (s)	Peak Rate (resp/min)	Peak Spread (s)
10Hz Baseline	39.05 ± 4.10	27.72 ± 8.76	19.62 ± 6.39
10Hz Stimulation	28.43 ± 7.67	20.91 ± 2.48	20.71 ± 7.53
40+200 Hz Baseline	32.31 ± 1.03	32.34 ± 3.89	19.68 ± 3.16
40+200 Hz Stimulation	47.46 ± 4.99	26.05 ± 3.37	12.53 ± 2.59

Numbers = mean (± SEM)

When examining the data on peak time, statistical analysis confirmed that there is a significant rightward shift on the PI-36s function (from 32.3 s to 47.5 s, $t_{.05\ (6\text{-}1)} = -3.333$, $p < 0.05$) in high-frequency stimulation, while no significant effect was observed on the PI-12s functions ($p > 0.5$), due to a general disruption of the timing functions in most of the rats. In the PI-36s functions, a peak time at 47.5 s following stimulation suggests that the rats showed a partial “stop” response pattern during microstimulation.

Response Rate Decrease during Microstimulation

As can be seen from the PI-12s and PI-36s functions during high-frequency stimulation (Figure 32C, 32D, and Figure 34C, 34D), the response rate decreased during microstimulation. Results of this response rate decrease are depicted in Figure 35. Statistical analysis confirmed that there was a significant decrease in response rate during the 6-s period of stimulation in the 12-s probe trials compared to the same 6-s period without stimulation in the DS ($t_{.05\ (4\text{-}1)}$ = - 3.468, $p < 0.05$). In the Cx, the significant effect was observed in the PI-36s trials ($t_{.05\ (6\text{-}1)}$ = - 4.365, $p < 0.01$). Together, during the time of microstimulation, the strongest decrease can be observed if the rats showed a "reset" response pattern (e.g., Figure 32C) or a partial "stop" response pattern (e.g., in Figure 34D).

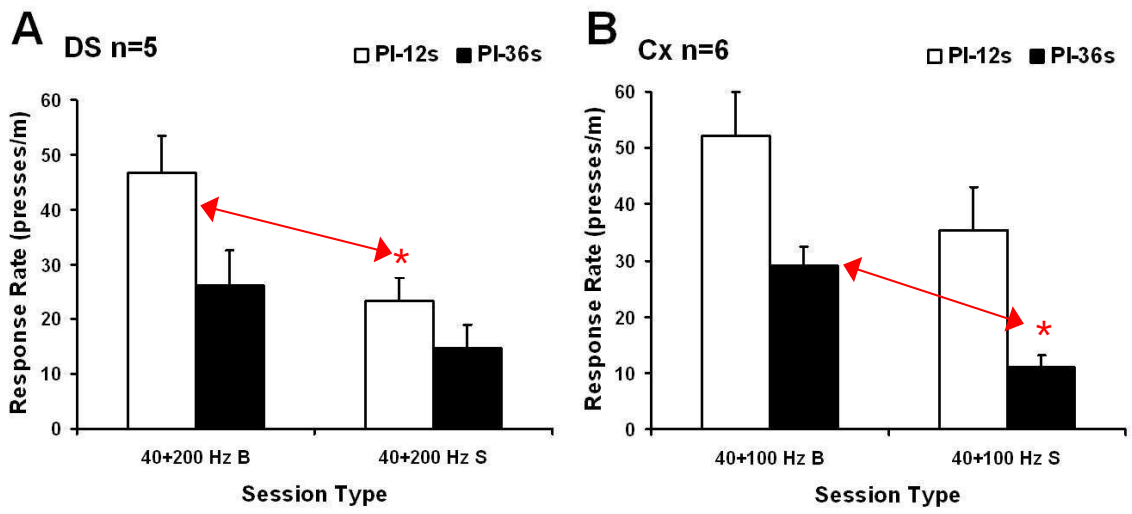

Figure 35: Mean (± SEM) response rate obtained during the 6-s period in the 12-s probe trials and during the 18-s period in the 36-s probe trials with (40+200 Hz S) or without (40+200 Hz B) high-frequency microstimulation in the DS (A) or in the Cx (B).

4.3 Discussion

In the current experiment, a frequency-dependent rightward shift of the timing functions was observed when trains of stimulation at 40 μA were delivered into the DS and the Cx. The stimulation was delivered only in **half** of the probe trials in the same testing session such that we can compare the behavioral effects of stimulation in half of the probe trials with another half of probe trials with no stimulation. Therefore, the current paradigm provides a useful tool to investigate how electrical microstimulation in the brain can change timing and time perception in a much better spatiotemporal resolution (i.e., on a trial by trial basis) compared to any pharmacological tools (systemic or microinjection). The remaining issue is where to stimulate, what the proper stimulation parameters are, and what behavioral changes we expect to see.

We previously outlined 6 possible scenarios of the effects of microstimulation on timing and time perception in that the microstimulation could 1) speed up the internal clock, 2) slow down the internal clock, 3) stop timing during microstimulation, 4) reset the internal clock, 5) create an artificial peak time at the point of stimulation, or 6) disrupt the scalar property. Any change of clock speed (faster or slower) should induce a proportional shift in the response functions, but this is not what we observed in the current data. The microstimulation that we used in the current experiment did not induce an artificial peak time right at the stimulation. Consequently, what we observed in the current study might be a combination of clock “reset” and “stop,” thus violating the scalar property. If the rats reset their response pattern during

microstimulation, their response rate should begin from zero again after the stimulation stops as if this is the beginning of a new trial. An example of this "reset" response pattern is shown in Figure 33. As can be seen in the fitted functions in Figure 33, this rat clearly showed a "reset" response pattern during microstimulation in the 12-s probe trials. Once the microstimulation stopped at the 12th second, this rat resumed timing again as if a new trial just began after the microstimulation. Hence, this rat was generating a separate 12-s function after the microstimulation was turned off, producing a peak time at 24.3 s (Figure 33A). The data from the 36-s functions appeared to be the result of a partial "stop" response pattern, such that the peak time was at 48.9 s (Figure 33B). In conclusion, our data support the scenario that microstimulation in cortico-striatal circuits could induce a "reset" or a "stop" response pattern. There was a trend to suggest that microstimulation of the DS induced a "reset" response pattern in the PI-12s functions (Figure 32C), while microstimulation of the Cx induced a "stop" response pattern in the PI-36s functions (Figure 34D).

5. Final Discussion

5.1 Comparisons of Striatal Neural Response Patterns in the Peak-Interval and Temporal Bisection Procedures

Data from the first two experiments clearly demonstrated that neurons in the DS and the Cx were actively involved in temporal and reward processing in the two timing tasks that were used in the current study. Specifically, neurons with high Na^+ and K^+ peak amplitude (Cluster A, Figure 10) and neurons with intermediate levels of Na^+ and K^+ peak amplitude (Cluster B, Figure 11) were more correlated with the temporal aspects of the two timing tasks (PI and temporal bisection). These two clusters of neurons constituted about 24.2% of the total observed neurons in the DS and 23.1% of the neurons in the Cx. On the other hand, neurons with intermediate levels of Na^+ and K^+ peak amplitude (Cluster C, Figure 12) were the largest group of neurons (up to 50%) in both brain areas and correlated with both temporal and reward dimensions in the two timing tasks. Cluster D (Figure 13) contained the neurons with the lowest Na^+ and K^+ peak amplitude and were mostly observed in the Cx. These neurons shared similar response profiles with the neurons in Cluster C. Finally, an additional Cluster E was observed in the DS (Figure 21) with the most frequent occurrence during early stage of training in a temporal bisection procedure (Figure 23).

Determining which neuronal subtype each of these 5 clusters of units belongs to is the primary goal of our study in order correlate each subtype of neuron to different aspects of timing and time perception. The same research strategy has been applied to the investigation of functional circuits in the

hippocampus (Jinno et al., 2007; Klausberger et al., 2003) and in the cortex (Fee et al., 1996) regarding spatial learning and information processing in cortico-hippocampal circuits. A recent study has reported that there are 12 distinct cell types of interneurons in the hippocampus (Klausberger, 2009) that might respond differently in different brain states. Although the goal of the current study is not *per se* to look for 12 distinct interneuron subtypes in the DS, we can still compare the 5 clusters of observed neurons with the major subtypes of striatal neurons (MSNs and interneurons) that other researchers have identified (e.g., Kreitzer, 2009). By utilizing the idea of different levels of synchronous firing with striatal HVS by different striatal cell subtypes, we found that neurons in Cluster C showed the highest degree of synchronous firing with striatal HVS, suggesting that these neurons are more likely to be the FSIs. GABA-releasing FSIs make synaptic contacts with a large number of MSNs, the major output neurons in the striatum. It is estimated that a single FSI connects to 135 – 541 MSNs, thus making an inhibitory FSI-MSN local circuits (Koos & Tepper, 1999). More importantly, striatal FSIs are mostly expressed in the dorsolateral region (Kita et al., 1990) and they shares similar electrophysiological properties with the FSIs in the hippocampus and in the cortex (Kawaguchi, 1993). This explains our findings that the percentage of the neurons observed in Cluster C was similar in both the DS (56.6%) and the Cx (48.1%). In addition to sharing similar electrophysiological properties in the two brain regions (Kawaguchi, 1993), we also observed that these FSIs share similar firing patterns to both temporal and reward dimensions in the two timing tasks.

Cluster E contains neurons that are most likely to be TANs in the striatum because of their signature baseline firing rate (2-10 spikes/s) and its transient depression in firing rate to stimuli with motivational value (Figure 28). In Experiment 2, we observed that the number of neurons in Cluster E decreased as a function of training in a temporal bisection procedure. This negative correlation (decrease in number with increased training) suggests that neurons in Cluster E were more involved in acquiring a behavioral task, especially during the early stage of training. This is consistent with recent findings that striatal TANs contribute to the processing of positive and negative reward in reinforcement learning (Apicella et al., 2009; Joshua et al., 2008). In the striatum, TANs form synaptic contacts with MSNs (TAN-MSN), but also with FSIs, thus creating TAN-FSI-MSN local networks (Izzo & Bolam, 1988; Koos & Tepper, 2002). During intermediate stage of training, we observed some of the neurons in Cluster E became related to timing. These neurons may become involved by exerting their influence on downstream MSNs directly (TAN-MSN), or through their connections with FSIs (TAN-FSI-MAN).

Together, our findings suggest that neurons (at least some neurons) in Cluster C are striatal FSIs because of their synchronous firing with striatal HVS (Burke et al., 2004) and the neurons in Cluster E are striatal TANs because of their transient decrease in firing to stimuli with motivational value (Apicella et al., 2009). The remaining question is what neuronal subtypes that the neurons in Cluster A, B, and D belong to. The neurons in Cluster D were mostly observed in the Cx (12.2%), but not in the DS (1.2%). Hence, we infer that the neurons in

Cluster D are more likely to be cortical pyramidal cells or interneurons. Consequently, the remaining two clusters (A and B) are more likely to be striatal projection neurons (i.e., MSNs) or other types of striatal interneurons (e.g., LTS interneurons). Neurons in Cluster A and B showed firing patterns that were more correlated with the temporal dimensions of the two timing tasks. In Experiment 1, we observed more neurons in Cluster B in the DS (14.9%) than in the Cx (3.6%). Because the number of neurons in Cluster B was also high in Experiment 2 (19.4% in the final 7-signal training session) in the DS, we can infer that neurons in Cluster B should be the type of neurons that is unique in the DS, such as the projection neurons in the striatum (MSNs). Therefore, the remaining Cluster A should contain the neurons that are more likely to be a type of interneurons (e.g., LTS) that co-exists in the DS and the Cx given that these neurons can be frequently observed in both regions (around 10% or higher). On the other hand, researchers who investigated the spike waveforms of projection neurons in other brain regions have reached the consensus that projection neurons tend to display strong spike waveforms, such as high Na^+ and K^+ peak amplitude (Constantinidis & Goldman-Rakic, 2002; Likhtik et al., 2006; Viskontas et al., 2007; Wiltschko et al., 2010). In this case, neurons in Cluster A should be the major projection neurons in the DS (i.e., MSNs) and in the Cx (i.e., cortical pyramidal cells), while neurons in Cluster B should be local interneurons in the DS. Comparisons of all the clusters and their functional correlates are listed in Table 12.

Table 12: Electrophysiological and functional correlates of all neuron clusters.

	Cluster A	Cluster B	Cluster C	Cluster D	Cluster E
Percentage observed in the DS in Experiment 1	9.3%	14.9%	56.6%	1.2%	1.8%
Percentage observed in the Cx in Experiment 1	19.5%	3.6%	48.1%	12.2%	1.7%
Percentage observed in the DS in Experiment 2 in the first 2-signal training	20.5%	16.1%	20.5%	0.9%	17.9%
Percentage observed in the DS in Experiment 2 in the 7-signal training	21.4%	19.4%	34.0%	3.9%	7.8%
Na^+ peak amplitude	High	Intermediate	Intermediate	Low	High
K^+ peak amplitude	High	Low	Low	Low/None	High
Capacitive peak amplitude	Low	Low	Low	Low/None	High
Levels of synchrony with HVS in Experiment 1	Low	Low	High	Low	N/A
Correlates with temporal processing	High	High	High	High	N/A
Correlates with reward processing	Low	Low	High	High	N/A
Putative cell subtypes in the DS	MSNs	LTS interneurons	FSIs	cortical neurons	TANs

Abbreviation: Cx (sensorimotor cortex), DS (dorsal striatum), FSIs (fast-spike interneurons), HVS (high-voltage spindles), LTS (low-threshold spiking), MSN (medium-spiny neurons), and TAN (tonically-active neurons).

5.2 Differential Response Patterns by Cortico-Striatal Microstimulation

Previous studies have observed that microstimulating the visual area MT biased the perceptual judgements of motion direction (Murasugi et al., 1993). When electrical microstimulation was delivered into the somatosensory cortex, monkeys were able to discriminate the real somatosensation and the different patterns of electrical microstimulation in the somatosensory cortex (Fitzsimmons et al., 2007). Here, electrical microstimulation is used to probe the functions of cortico-striatal circuits and determine if the stimulation can alter the ongoing temporal processing in a real-time manner. The data suggest that indeed the temporal processing can be altered in a systematic way when the electrical microstimulation was delivered either into the DS (Figure 32) or the Cx (Figure 34).

What we observed during/following microstimulation was a frequency-dependent “stop” or “reset” response patterns for rats receiving microstimulation in the PI procedure. That is, when the stimulation frequency was low (10 Hz), the rats ignored the stimulation and therefore their timing functions were not altered. When the stimulation frequency was increased to a higher level (40, 100, and 200 Hz), the response functions showed that the rats’ ongoing temporal processing during the period of microstimulation (6 s in the 12-s probe trials and 18 s in the 36-s probe trials) was altered or biased. The pattern was that the rats seemed to “stop” timing the 12-s or 36-s signals when the stimulation was turned on (“pause”) and they resumed timing the signals after the stimulation was turned off. This frequency-dependent “stop” or “reset” response patterns are similar to

previous studies when using a gap paradigm in the PI procedure (Buhusi et al., 2002). In that particular study, a gap was introduced (i.e., the signal was turned off for a short period of time) in a probe trial such that the rats could either “run” (i.e., ignore the gap), “stop” (i.e., stop timing during the gap), and “reset” (i.e., stop timing during the gap, but restart as if a new trial has begun when the signal resumes). The finding was that when the intensity of the gap was manipulated in a systematic way (from low to high intensity), the rats showed “run,” “stop,” or “reset” response patterns as a function of the gap’s intensity. Our finding was similar in that the frequency of the microstimulation can determine the rats’ response patterns. Specifically, high-frequency microstimulation in cortico-striatal circuits could induce response patterns (“stop” or “reset”) as if there was a gap presented during the stimulated probe trials. In conclusion, our data suggest that delivering electrical microstimulation into cortico-striatal circuits can dynamically alter temporal processing.

5.3 Future Directions

Our findings further support the importance of cortico-striatal circuits subserving interval timing. For example, different subtypes of neurons in the circuits all responded to different dimensions (temporal and/or reward) in the two timing tasks. A distinct neural subtype (TANs) was also found to be involved in the acquisition of a temporal bisection task, a property of TANs that is consistent with previous studies by using other behavioral paradigms (Apicella et al., 2009; Joshua et al., 2008). To further investigate the exact functions of each neuronal subtype in the striatum and their contributions to interval timing, one should adopt tools that can provide cell-type specific stimulation or inhibition, such as optogenetics for future interval-timing studies. Recently, the development of optogenetics (as reviewed by Scanziani and Hausser, 2009) is providing a promising tool for dissecting the functional roles of specific cell subtypes within a neural circuit (e,g, Gradinaru et al, 2009). Optogenetics is a tool that can stimulate or inhibit light-sensitive channels such as channelrhodopsin-2 (ChR2) and halorhodopsin (NpHR) that can be expressed in a target cell by using cell-type specific genetic tools (e.g., Arrenberg et al., 2009; Berdyyeva et al., 2009; Numano et al., 2009). As such, using this tool can selectively activate or inhibit neuronal subtypes in cortico-striatal circuits to study various timing functions (e.g., “stop” or “reset”) or properties (scalar variance or altered clock speed). The remaining issue is to decide what subtype(s) of neurons in cortico-striatal circuits that should receive this optical stimulation or inhibition. According to our findings, neurons in Cluster A (LTS interneurons) and Cluster B (MSNs) are the neurons

that preferentially responded to the temporal aspects in the two timing tasks. Hence, these two clusters of neurons (MSNs and LTS interneurons) should be the first target to investigate by using optogenetics for future interval-timing research. A vertebrate animal species, such as zebrafish may provide an ideal genetic model to combine optogenetics and behavioral studies within a specified neural circuit (e.g., Baier & Scott, 2009; Jesuthasan & Mathuru, 2008).

Another interesting cell-type to investigate is the ACh-releasing TANs in the striatum. In our study, TANs were found to be involved in the acquisition of a temporal bisection procedure as the number of observed TANs decreased as a function of training. One recent study has found that electrically microstimulating the anterior portion of caudate in monkeys could enhance associative learning (Williams & Eskandar, 2006). Although electrical microstimulation is not a cell-type specific stimulation tool, we can infer that the learning-enhancing effect of microstimulation may be due to the activation of TANs. If this is the case, one should adopt optogenetics to selectively stimulate or inhibit TANs during the acquisition of a behavioral task and observe if the acquisition of a timing task is enhanced or impaired. Another method to investigate the potential functions of TANs is to require the rats to switch to a different response strategy or to learn a new response rule after they have become well-trained. Requiring rats to learn a new response rule (e.g., reversal of the response mapping) after being well-trained in a choice task may reactivate the “silent” TANs in cortico-striatal circuits. In Experiment 2, introducing 32-s long probe trials and 5 intermediate-duration probe trials did not involve learning a new response rule because the

reinforcement contingency was still the same (i.e., 4 s to press the “short” lever and 16 s to press the “long” lever). Changing the reinforcement contingency or requiring rats to learn new target durations may revive the “silent” TANs in cortico-striatal circuits in timing tasks. Finally, it was noticed that the TANs that started showing behavioral correlates in Experiment 2 showed lightly modified waveforms. Spike waveforms can be changed by modifying various types of voltage-dependent ion channels (as reviewed by Bean, 2007). It was recently proposed that modifying those channels allows neurons to encode information by generating action potentials with a wide range of shapes, frequencies and patterns (Bean, 2007). Although determining how these TANs could modify their spike waveforms as a function of training is beyond the scope of the current study, this is certainly an important issue to investigate in future studies.

In addition to optogenetics, another plausible approach is to combine microstimulation and *in vivo* recording simultaneously. On example of this combined approach is to use the antidromic neural impulses (from axon to cell body) as a tool to identify upstream neurons that project to the stimulated area. Researchers have used this idea to microstimulate the substantia nigra pars reticulata (SNR) and then record from the striatum to identify the SNR-stimulation responsive MSNs (Ballion et al., 2008). The SNR-stimulation responsive MSNs are presumably the D1-expressed striatonigral MSNs that forms the direct pathway to basal ganglia (Kreitzer & Malenka, 2008). The rest SNR-stimulation non-responsive cells could be the D2-expressed striatopallidal MSNs or interneurons. After distinguishing the two types of MSNs, one can further

determine their functional connections to other brain regions (e.g., cortical regions) and investigate the behavioral functions of D1-MSNs and D2-MSNs (Ballion et al., 2009) in the striatum. As such, this combined approach will be useful to investigate the functions of each MSN subtypes (D1 vs. D2) for future interval-timing research.

References

Allan, L. G., & Gibbon, J. (1991). Human bisection at the geometric mean. *Learning & Motivation, 22,* 39-58.

Aosaki, T., Graybiel, A. M., & Kimura, M. (1994). Effect of nigrostriatal dopamine system on acquired neural responses in the striatum of behaving monkey. *Science, 265,* 412-415.

Aosaki, T., Kimura, M., & Graybiel, A. M. (1995). Temporal and spatial characteristics of tonically active neurons of the primate's striatum. *Journal of Neurophysiology, 73,* 1234-1252.

Apicella, P. (2007). Leading tonically active neurons of the striatum from reward detection to context recognition. *Trends in Neuroscience, 30,* 299-306.

Apicella, P., Legallet, E., & Ravel, S. (2006). A possible role for tonically active neurons of the primate striatum in learning about temporal relationships among salient stimuli. In: Bezard, E (Ed.), *Recent breakthroughs in basal ganglia research.* (pp. 55–63). New York, Nova Science Publishers.

Apicella, P., Deffains, M., Ravel, S., & Legallet, E. (2009). Tonically active neurons in the striatum differentiate between delivery and omission of expected reward in a probabilistic task context. *European Journal of Neuroscience, 30,* 515-526.

Arfin, S. K., Long, M. A., Fee, M. S., & Sarpeshkar, R. (2009). Wireless neural stimulation in freely behaving small animals. *Journal of Neurophysiology, 102,* 598-605.

Arrenberg, A. B., Bene, F. D., & Baier, H. (2009). Optical control of zebrafish behavior with halorhodopsin. *PNAS, 106,* 17968-17973.

Ballion, B., Mallet, N., Bezard, E., Lanciego, J. L., & Gonon, F. (2008). Intratelencephalic corticostriatal neurons equally excite striatonigral and striatopallidal neurons and their discharge activity is selectively reduced un experimental parkinsonism. *European Journal of Neuroscience, 27,* 2313-2321.

Ballion, B., Frenois, F., Zold, C. L., Chetrit, J., Murer, M. G., & Gonon, F. (2009). D2 receptor stimulation, but not D1, restores striatal equilibrium in a rat model of Parkinsonism. *Neurobiology of Disease, 35,* 376-384.

Baier, H., & Scott, E. K. (2009). Genetic and optical targeting of neural circuits and behavior – zebrafish in the spotlight. *Current Opinion in Neurobiology, 19,* 553-560.

Bateson, M. (2003). Interval timing and optimal foraging. In: Meck, W.H. (Ed.), *Functional and neural mechanisms of interval timing.* (pp. 113-141). Boca Raton, FL, CRC Press.

Bean, B. P. (2007). The action potential in mammalian central neurons. *Nature Review of Neuroscience, 8,* 451-465.

Berke, J.D., Okatan, M., Skurski, J., & Eichenbaum, H. B. (2004). Oscillatory entrainment of striatal neurons in freely moving rats. *Neuron, 43,* 886-896.

Berdyyeva, T. K., & Reynolds, J. H. (2009). The dawning of primate optogenetics. *Neuron, 62,* 159-160.

Boisvert, M. J., & Sherry, D. F. (2006). Interval timing by an invertebrate, the bumble bee Bombus impatiens. *Current Biology, 16,* 1636-1640.

Buhusi, C. V., & Meck, W. H. (2002). Differential effects of methamphetamine and haloperidol on the control of an internal clock. *Behavioral Neuroscience, 116,* 291-297.

Buhusi, C. V., & Meck, W. H. (2005). What makes us tick? Functional and neural mechanisms of interval timing. *Natural Review of Neuroscience, 6,* 755-765.

Buhusi, C. V., Sasaki, A., & Meck, W. H. (2002). Temporal integration as a function of signal and gap intensity in rats (*Rattus norvegicus*) and Pigeons (*Columba livia*). *Journal of Comparative Psychology, 116,* 381-390.

Buonomano, D. V. (2007). The biology of time across different scales. *Nature Chemical Biology, 3,* 594-597.

Buzsaki, G. (1991). The thalamic clock: Emergent network properties. *Neuroscience, 41,* 351-364.

Calabresi, P., Mercuri, N. B., Stefani, A., & Bernardi, G. (1990). Synaptic and intrinsic control of membrane excitability of neostriatal neurons. I. an in vivo analysis. *Journal of Neurophysiology, 63,* 651-662.

Catania, A. C. (1970). Reinforcement schedules and psychophysical judgments: a study of some temporal properties of behavior. *The theory of reinforcement schedules*, (Shoenfeld, W. N., Ed.), Appelton Century-Crofts, New York, pp1-42.

Centonze, D., Grande, C., Usiello, A., Gubellini, P., Erbs, E., Martin, A. B., . . . Calabresi, P. (2003). Receptor subtypes involved in the presynaptic and postsynaptic actions of dopamine on striatal interneurons. *Journal of Neuroscience, 23,* 6245-6254.

Centonze, D., Bracci, E., Pisani, A., Gubellini, P., Bernardi, G., & Calabresi, P. (2002). Activation of dopamine D1-like receptors excites LTS interneurons of the striatum. *European Journal of Neuroscience, 15,* 2049-2052.

Centonze, D., Picconi, B., Baunez, C., Borrelli, E., Pisani, A., Bernardi, G., & Calabresi, P. (2002). Cocaine and amphetamine depress striatal GABAergic synaptic transmission through D2 dopamine receptors. *Neuropsychopharmacology, 26,* 164-175.

Cepeda, C., Andre, V. M., Yamazaki, I., Wu, N., Kleiman-Weiner, M., & Levine, M. S. (2008). Differential electrophysiological properties of dopamine D1 and D2 receptor-containing striatal medium-sized spiny neurons. *European Journal of Neuroscience, 27,* 671-682.

Cheng, R. K., & Meck, W. H. (2007). Prenatal choline supplementation increases sensitivity to time by reducing non-scalar sources of variance in adult temporal processing. *Brain Research, 1186,* 242-254.

Cheng, R. K., Ali, Y. M., & Meck, W. H. (2007a). Ketamine “unlocks” the reduced clock-speed effect of cocaine following extended training: Evidence for dopamine-glutamate interactions in timing and time perception. *Neurobiology of Learning and Memory, 88,* 149-159.

Cheng, R. K., Hakak, O., & Meck, W. H. (2007b). Habit formation and the loss of control of an internal clock: Inverse relationship between the level of baseline training and the clock-speed enhancing effects of methamphetamine. *Psychopharmacology, 193,* 351-362.

Cheng, R. K., Meck, W. H., & Williams, C. L. (2006). α7 Nicotinic acetylcholine receptors and temporal memory: Synergistic effects of combining prenatal choline and nicotine on reinforcement-induced resetting of an interval clock. Learning and Memory, 13, 127-134.

Cheng, R. K., Scott, A, C., Penney, T. B., & Meck, W. H. (2008). Prenatal choline supplementation differentially modulates timing of auditory and visual stimuli in aged rats. *Brain Research, 1237,* 167-175.

Church, R. M. (2003). A concise introduction to scalar timing theory. In W.H. Meck (Ed.), *Functional and neural mechanisms of interval timing*. (pp. 3-22). Boca Raton, FL: CRC Press.

Church, R. M., & Deluty, M. Z. (1977). Bisection of temporal intervals. *Journal of Experimental Psychology: Animal Behavior Processes, 3,* 216-228.

Church, R. M., Meck, W. H., & Gibbon, J. (1994). Application of scalar timing theory to individual trials. Journal of Experimental Psychology: Animal *Behavior Processes, 20*, 135-155.

Church, R. M., Miller, K. D., Meck, W. H., & Gibbon, J. (1991). Symmetrical and asymmetrical sources of variance in temporal generalization. Animal *Learning & Behavior, 19*, 207-214.

Cohen, M. R., & Newsome, W. T. (2004). What electrical microstimulation has revealed about the neural basis of cognition. *Current Opinion in Neurobiology, 14,* 169-177.

Constantinidis, C., & Goldman-Rakic P. S. (2002). Correlated discharges among putative pyramidal neurons and interneurons in the primate prefrontal cortex. *Journal of Neurophysiology, 88,* 3487-3497.

Coull, J. T., Nazarian, B., & Vidal, F. (2008a). Timing, storage, and comparison of stimulus duration engage discrete anatomical components of a perceptual timing network. *Journal of Cognitive Neuroscience, 20,* 2185-2197.

Coull, J. T., Vidal, F., Nazarian, B., & Macar, F. (2004). Functional anatomy of the attentional modulation of time estimation. *Science, 303,* 1506-1508.

Dale, C. L., Findlay, A. M., Adcock, R. A., Vertinski, M., Fisher, M., Genevsky, A., . . . Vinogradov, S. (2010). Timing is everything: Neural response dynamics during syllable processing and its relation to higher-order cognition in schizophrenia and healthy comparison subjects. *International Journal of Psychophysiology, 75,* 183-193.

Fee, M. S., Mitra, P. P., & Kleinfeld, D. (1996). Variability of extracellular spike waveforms of cortical neurons. *Journal of Neurophysiology, 76,* 3823-3833.

Fitzsimmons, N. A., Drake, W., Hanson, T. L., Lebedev, M. A., & Nicolelis, M. A. L. (2007). Primate reaching cued by multichannel spatiotemporal cortical microstimulation. *Journal of Neuroscience, 27,* 5593-5602.

Fraisse, P. (1963). *Psychology of time*. New York: Harper & Row.

Fuentes, R., Petersson, P., Siesser, W. B., Caron, M. G., & Nicolelis, M. A. L. (2009). Spinal cord stimulation restores locomotion in animal models of Parkinson's disease. *Science, 323,* 1578-359.

Gibbon, J., & Church, R. M. (1992). Comparison of variance and covariance patterns in parallel and serial theories of timing. *Journal of the Experimental Analysis of Behavior, 57,* 393-406.

Gold, C., Henze, D. A., & Koch, C. (2007). Using extracellular action potential recordings to constrain compartmental models. *Journal of Computational Neuroscience, 23,* 39-58.

Gold, C., Henze, D. A., Koch, C., & Buzsaki, G. (2006). On the origin of the extracellular action potential waveform: A modeling study. *Journal of Neurophysiology, 95,* 3113-3128.

Gradinaru, V., Mogri, M., Thompson, K. R., Henderson, J. M., & Deisseroth, K. (2009). Optical deconstruction of Parkinsonian neural circuitry. *Science, 324,* 354-359.

Harrington, D. L., Zimbelman, J. L., Hinton, S. C., & Rao, S. M. (2010). Neural modulation of temporal encoding, maintenance, and decision processes. *Cerebral Cortex.* DOI: 10.1093/cercor/bhp194.

Henderson, J., Hurly, T. A., Bateson, M., & Healy, S. D. (2006). Timing in free-living rufous hummingbirds, Selasphorus rufus. *Current Biology, 16,* 512-515.

Hills, T. (2003). Towards a unified theory of animal event timing. In W.H. Meck (Ed.) Functional and Neural Mechanisms of Interval Timing. pp. 77-111. Boca Raton, FL: CRC Press.

Izzo, P. N., & Bolam, J. P. (1988). Cholinergic synaptic input to different parts of spiny striatonigral neurons in the rat. *Journal of Comparative Neurology, 269,* 219–234.

James, W. (1890). *The principles of psychology*. Chapter 15: The perception of time.

Jesuthasan, S. J., & Mathuru, A. S. (2008). The alarm response in zebrafish: Innate fear in a vertebrate genetic model. *Journal of Neurogenetics, 22,* 211-228.

Jin, D. Z., Fujui, N., & Graybiel, A. M. (2009). Neural representation of time in cortico-basal ganglia circuits. *PNAS, 106,* 19156-19161.

Jinno, S., Klausberger, T., Marton, L. F., Dalezios, Y., Roberts, J. D., Fuentealba, P., . . . Somogyi, P. (2007). Neuronal diversity in GABAergic long-range projections from the hippocampus. *Journal of Neuroscience, 27,* 8790-8804.

Joshua, M., Adler, A., Mitelman, R., Vaadia, E., & Bergman, H. (2008). Midbrain dopaminergic neurons and striatal cholinergic interneurons encode the difference between reward and aversive events at different epochs of probabilistic classical conditioning trials. *Journal of Neuroscience, 28,* 11673-11684.

Kawaguchi, Y. (1993). Physiological, morphological, and histochemical characterization of three classes of interneurons in rat neostriatum. *Journal of Neuroscience, 13,* 4908-4923.

Kita, H., Kosaka, T., & Heizmann, C. W. (1990). Parvalbumin-immunoreactive neurons in the rat neostriatum: A light and electron microscopic study. *Brain Research, 536,* 1-15.

Klausberger, T. (2009). GABAergic interneurons targeting dendrites of pyramidal cells in the CA1 area of the hippocampus. *European Journal of Neuroscience, 30,* 947-957.

Klausberger, T., Magill, P. J., Marton, L. F., Roberts, J. D. B., Cobden, P. M., Buzsaki, G., & Somogyi, P. (2003). Brain-state and cell-type-specific firing of hippocampal interneurons *in vivo*. *Nature, 421,* 844-848.

Koos, T., & Tepper, J. M. (1999). Inhibitory control of neostriatal projection neurons by GABAergic interneurons. *Nature Neuroscience, 2,* 467-472.

Koos, T., & Tepper, J. M. (2002). Dual cholinergic control of fast-spiking interneurons in the neostriatum. *Journal of Neuroscience,* 22, 529-535.

Kreitzer, A. C. (2009). Physiology and pharmacology of striatal neurons. *Annual Review of Neuroscience, 32,* 127-147.

Kreitzer, A. C., & Malenka, R. C. (2008). Striatal plasticity and basal ganglia circuit function. *Neuron, 60,* 543-554.

Kubikova, L., Turner, E. A., Jarvis, E. D. (2007). The pallidal basal ganglia pathway modulates the behaviorally driven gene expression of the motor pathway. *European Journal of Neuroscience, 25,* 2145-2160

Kubota, Y., Liu, J., Hu, D., DeCoteau, W. E., Eden, U. T., Smith, A. C., & Graybiel, A. M. (2009). Stable encoding of task structure coexists with flexible coding of task events in sensorimotor striatum. *Journal of Neurophysiology, 102,* 2142-2160.

Levey, A. I., Hersch, S. M., Rye, D. B., Sunahara, R. K., Niznik, H. B., Kitt, C. A., . . . Ciliax, B. J. (1993). Localization of D1 and D2 dopamine receptors in brain with subtype-specific antibodies. *PNAS, 90,* 8861-8865.

Likhtik, E., Pelletier, J. G., Popescu, A. T., & Pare, D. (2006). Identification of basolateral amygdala projection cells and interneurons using extracellular recordings. *Journal of Neurophysiology, 96,* 3257-3265.

Long, M. A., & Fee, M. S. (2008). Using temperature to analyse temporal dynamics in the songbird motor pathway. *Nature, 456,* 189-194.

Lustig, C., & Meck, W. H. (2001). Paying attention to time as one gets older. *Psychological Science, 12,* 478-484.

Lustig, C., Matell, M. S., & Meck, W. H. (2005). Not "just" a coincidence: Frontal-striatal synchronization in working memory and interval timing. *Memory, 13,* 441-448.

MacDonald, C. J., Cheng, R. K., Clore, E. L., Crawford, E., Laino, A., & Meck, W. H. (2010). Interval-timing decision thresholds require de novo protein synthesis in dorsal and ventral striatum. Submitted.

Malapani, C., Rakitin, B., Levy, R., Meck, W. H., Deweer, B., Dubois, B., & Gibbon, J. (1998). Coupled temporal memories in Parkinson's disease: A dopamine-related dysfunction. *Journal of Cognitive Neuroscience, 10,* 316-331.

Mallet, N., Ballion, B., Le Moine, C., & Gonon, F. (2006). Cortical inputs and GABA interneurons imbalance projection neurons in the striatum of parkinsonian rats. *Journal of Neuroscience, 26,* 3875-3884.

Matell, M. S., & Meck, W. H. (2004). Corticostriatal circuits and interval timing: coincidence detection of oscillatory processes. *Cognitive Brain Research, 21,* 139-170.

Matell, M. S., Bateson, M., & Meck, W. H. (2006). Single-trials analyses demonstrate that increases in clock speed contribute to the methamphetamine-induced horizontal shifts in peak-interval timing functions. *Psychopharmacology, 188,* 201-212.

Matell, M. S., Meck, W. H., & Nicolelis, M. A. L. (2003a). Integration of behavior and timing: Anatomically separate systems or distributed processing? In W.H. Meck (Ed.), *Functional and neural mechanisms of interval timing*. (pp. 371-391). Boca Raton, FL: CRC Press.

Matell, M. S., Meck, W. H., & Nicolelis, M. A. L. (2003b). Interval timing and the encoding of signal duration by ensembles of cortical and striatal neurons. *Behavioral Neuroscience, 117,* 760-773.

Meck, W. H. (1983). Selective adjustment of the speed of internal clock and memory processes. *Journal of Experimental Psychology: Animal Behavioral Process, 9,* 171-201.

Meck, W. H. (1986). Affinity for the dopamine D2 receptor predicts neuroleptic potency in decreasing the speed of an internal clock. *Pharmacology, Biochemistry, and Behavior, 25,* 1185-1189.

Meck, W. H. (1991). Modality-specific circadian rhythmicities influence mechanisms of attention and memory for interval timing. *Learning & Motivation, 22,* 153-179.

Meck, W. H. (1996). Neuropharmacology of timing and time perception. *Cognitive Brain Research, 3,* 227-242.

Meck, W. H. (2006a). Frontal cortex lesions eliminate the clock speed effect of dopaminergic drugs on interval timing. *Brain Research, 1108,* 157-167.

Meck, W. H. (2006b). Neuroanatomical localization of an internal clock: a functional link between mesolimbic, nigrostriatal, and mesocortical dopaminergic systems. *Brain Research, 1109,* 93-107.

Meck, W. H., & Church, R. M. (1984). Simultaneous temporal processing. *Journal of Experimental Psychology: Animal Behavior Processes, 10,* 1-29.

Meck, W. H., & Williams, C. L. (1997a). Characterization of the facilitative effects of perinatal choline supplementation on timing and temporal memory. *Neuroreport, 8,* 2831-2835.

Meck, W. H., Penney, T. B., & Pouthas, V. (2008). Cortico-striatal representation of time in animals and humans. *Current Opinion in Neurobiology, 18,* 145-152.

Mita, A., Mushiake, H., Shima, K., Matsuzaka, Y., & Tanji, J. (2009). Interval time coding by neurons in the presupplementary and supplementary motor areas. *Nature Neuroscience, 12,* 502-507.

Moore, T., & Armstrong, K. M. (2003). Selective gating of visual signals by microstimulation of frontal cortex. *Nature, 421,* 370-373.

Morris, G., Arkadir, D., Nevet, A., Vaadia, E., & Bergman, H. (2004). Coincident but distinct messages of midbrain dopamine and striatal tonically active neurons. *Neuron, 43,* 133-143.

Murasugi, C. M., Salzman, C. D., & Newsome, W. T. (1993). Microstimulation in visual area MT: Effects of varying pulse amplitude and frequency. *Journal of Neuroscience, 13,* 1719-1729.

Numano, R., Szobota, S., Lai, A. Y., Gorostiza, P., Volgraf, M., Roux, B.,…Isacoff, E. Y. (2009). Nanosculpting reversed wavelength sensitivity into a photoswitchable iGluR. *PNAS, 106,* 6814-6819.

Paule, M. G., Meck, W. H., McMillan, D. E., Bateson, M., Popke, E. J., Chelonis, J. J., & Hinton, S. C. (1999). The use of timing behaviors in animals and humans to detect drug and/or toxicant effects. *Neurotoxicology and Teratology, 21,* 491-502.

Paxinos, G., Watson, C., 1998. *The rat brain in stereotaxic coordinates*. Academic Press, New York.

Penney, T. B., Gibbon, J., & Meck, W. H. (2000). Differential effects of auditory and visual signals on clock speed and temporal memory. *Journal of Experimental Psychology: Human Perception and Performance, 26,* 1770-1787.

Quiroga, R. Q., & Panzeri, S. (2009). Extracting information from neuronal populations: Information theory and decoding approaches. *Nature Reviews of Neuroscience, 10,* 173-185.

Rakitin, B. C., Gibbon, J., Penney, T. B., Malapani, C., Hinton, S. C., & Meck, W. H. (1998). Scalar expectancy theory and peak-interval timing in humans. *Journal of Experimental Psychology: Animal Behavior Processes, 24,* 15-33.

Reynolds, J. N. J., & Wickens, J. R. (2004). The corticostriatal inputs to giant aspiny interneurons in the rat: A candidate pathway for synchronizing the response to reward-related cues. *Brain Research, 1011,* 115-128.

Roberts, S. (1981). Isolation of an internal clock. *Journal of Experimental Psychology: Animal Behavioral Processes, 7,* 242-268.

Scanziani, M., & Hausser, M. (2009). Electrophysiology in the age of light. *Nature, 461,* 930-939.

Sharrot, A., Moll, C. K. E., Engler, G., Denker, M., Grun, S., & Engel, A. K. (2009). Different subtypes of striatal neurons are selectively modulated by cortical oscillations. *Journal of Neuroscience, 29,* 4571-4585.

Skinner, B. F. (1938).*The behavior of organisms*, Appleton-Century-Crofts, New York.

Stuber, G. D. (2010). Dissecting the neural circuitry of addiction and psychiatric disease with optogenetics. *Neuropsychopharmacology, 35,* 341-342.

Tehovnik, E. J. (1996). Electrical stimulation of neural tissue to evoke behavioral responses. *Journal of Neuroscience Methods, 65,* 1-17.

Tolias, A. S., Sultan, F., Augath, M., Oeltermann, A., Tehovnik E. J., Schiller, P. H., & Logothetis, N. K.(2006). Mapping cortical activity elicited with electrical microstimulation using FMRI in the macaque. *Neuron, 48,* 901-911.

Viskontas, I. V., Ekstrom, A. D., Wilson, C. L., & Fried, I. (2007). Characterizing interneuron and pyramidal cells in the human medial temporal lobe *in vivo* using extracellular recordings. *Hippocampus, 17,* 49-57.

Wallace, D. G., Wallace, P. S., Field, E., & Whishaw, I. Q. (2006). Pharmacological manipulations of food protection behavior in rats: Evidence for dopaminergic contributions to time perception during a natural behavior. *Brain Research, 1112,* 213–221.

Wickersham, I., & Groh, J. M. (1998). Neurophysiology: Electrically evoking sensory experience. *Current Biology, 8,* R412-414.

Williams, Z. M., & Eskandar, E. N. (2006). Selective enhancement of associative learning by microstimulation of the anterior caudate. *Nature Neuroscience, 9,* 562-568.

Wilson, C. J. (1995). The contribution of cortical neurons to the firing pattern of striatal spiny neurons, in: J.C. Houk, J.L. Davis, D.G. Beiser (Eds.), *Models of information processing in the basal ganglia. (*pp.29-50). MIT Press, Cambridge.

Wiltschko, A. B., Pettibone, J. R., & Berke, J. D. (2010). Opposite effects of stimulant and antipsychotic drugs on striatal fask-spiking interneurons. *Neuropsychopharmacology, 35,* 1261-1270.

Yin, H. H., & Knowlton, B. J. (2006). The role of basal ganglia in habit formation. *Nature Reviews of Neuroscience, 7,* 464-476.

Yin, H. H., Knowlton, B. J., & Balleine, B. W. (2006). Inactivation of dorsolateral striatum enhances sensitivity to changes in the action-outcome contingency in instrumental conditioning. *Behavioural Brain Research, 166,* 189-196.

Yin, H. H., Mulcare, S. P., Hilario, M. R., Clouse, E., Holloway, T., Davis, M. I., . . . Costa, R. M. (2009). Dynamic reorganization of striatal circuits during the acquisition and consolidation of a skill. *Nature Neuroscience, 12,* 333-341.

Zhou, F. M., Wilson, C. J., & Dani, J. A. (2002). Cholinergic interneuron characteristics and nicotinic properties in the striatum. *Journal of Neurobiology, 53,* 590-605.

Biography

Birth

Tao-Yuan, Taiwan, R.O.C., February 24, 1977

Education

Undergraduate Institute
National Cheng-Chi University, Taipei, Taiwan
Degree: B.S. in Psychology 6/1999
Graduate Institute
National Cheng-Chi University, Taipei, Taiwan
Degree: M.S. in Psychology 6/2002

Selected Published Work

1. Cheng, R. K., MacDonald, C. J., & Meck, W. H. (2006). Differential effects of cocaine and ketamine on time estimation: Implications for neurobiological models of interval timing. *Pharmacology, Biochemistry and Behavior*, *85*, 114-122.

2. Cheng, R. K., Ali, Y. M., & Meck, W. H. (2007). Ketamine "unlocks" the reduced clock-speed effect of cocaine following extended training: Evidence for dopamine-glutamate interactions in timing and time perception. *Neurobiology of Learning and Memory, 88,* 149-159.

3. Cheng, R. K., MacDonald, C. J., Williams, C. L., & Meck, W. H. (2008). Prenatal choline availability alters timing, emotion, and memory performance (TEMP) of adult male and female rats as indexed by the differential reinforcement of low-rate schedule behavior. *Learning & Memory, 15,* 153-162.

4. Cheng, R. K., Williams, C. L., & Meck, W. H. (2009). Neurophysiological mechanisms of sleep-dependent memory consolidation and its facilitation by prenatal choline supplementation. *Chinese Journal of Physiology, 52,* 223-235. (invited review article)

5. Coull, J. T., Cheng, R. K., & Meck, W. H. (2010). Neuroanatomical and neurochemical substrates of timing. Neuropsychopharmacology Reviews, under review. (invited review article)

Awards

1. Aiken Foundation Neuroscience Fellowship (2006)